

**Experimental Investigation of  
the In-plane Cyclic Response of Infilled Reinforced Concrete Frames  
and Their Possible Retrofit Measures**

Arifa Iffat Zerin



Department of Civil Engineering

BANGLADESH UNIVERSITY OF ENGINEERING AND TECHNOLOGY

2018

**Experimental Investigation of  
the In-plane Cyclic Response of Infilled Reinforced Concrete Frames  
and Their Possible Retrofit Measures**

by

Arifa Iffat Zerin  
(Student No. 040504326 P)

MASTER OF SCIENCE IN CIVIL ENGINEERING (STRUCTURAL)



Department of Civil Engineering

BANGLADESH UNIVERSITY OF ENGINEERING AND TECHNOLOGY

September 2018

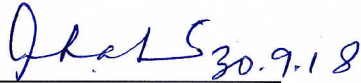
The Thesis titled “Experimental Investigation of the In-plane Cyclic Response of Infilled Reinforced Concrete Frames and Their Possible Retrofit Measures”, submitted by Arifa Iffat Zerine, Roll No: 040504326P, Session: April/2005; has been accepted as satisfactory in partial fulfillment of the requirement for the degree of Master of Science in Civil Engineering (Structural) on 30th September 2018.

### BOARD OF EXAMINERS



Dr. Khan Mahmud Amanat  
Professor  
Department of Civil Engineering, BUET

Chairman  
(Supervisor)



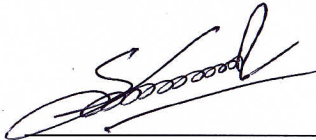
Dr. Ahsanul Kabir  
Professor and Head  
Department of Civil Engineering, BUET

Member (Ex-Officio)



Dr. Ishtiaque Ahmed  
Professor  
Department of Civil Engineering, BUET

Member



Dr. Shameem Ahmed  
Assistant Professor  
Department of Civil Engineering, BUET

Member



Dr. Md. Mahmudur Rahman  
Professor  
Department of Civil Engineering,  
Ahsanullah University of Science and Technology,  
141 & 142, Love Road, Tejgaon Industrial Area,  
Dhaka-1208.


Member (External)

## DECLARATION

---

It is hereby declared that except for the contents where specific reference have been made to the work of others, the studies contained in this thesis is the result of investigation carried out by the author. No part of this thesis has been submitted to any other University or other educational establishment for a Degree, Diploma or other qualification (except for publication).

Signature of the Candidate

  
30-09-2018

(Arifa Iffat Zerine)

## ACKNOWLEDGEMENT

---

Thanks to Almighty Allah for His graciousness and unlimited kindness.

The author wishes to express her deepest gratitude to her supervisor Dr. Khan Mahmud Amanat, for his continuous guidance, invaluable suggestions, affectionate encouragement, generous help and unfailing enthusiasm at every stage of this study. His active interest in this topic and valuable advice was the source of author's inspiration.

The author extends her gratitude to her former colleagues Engr. Mainuddin Ahmed, Director, HBRI, Engr. Md. Reaz Uddin Sarker, the former Head of the Department, Structural Engineering and Construction Division, HBRI, Engr. Abdus Salam, the Head of the Department and Senior Research Engineer, HBRI, Engr. Md. Akhtaruzzaman, Project Officer, HBRI for their consistent support in continuing the study with suggestions and advice in research.

The author would like to convey her heartfelt thanks to Sadia Sharmin Tonny, ex-teaching assistant, BUET and Md. Shahinul Islam, M. Engineering. Graduate, Dept. of Civil Engineering., BUET for their painstaking cooperation in conducting the laboratory investigations corresponding to the present research.

The author would like to extend her sincerest thanks to the technical staffs of the concrete laboratory, welding shop and machine shop and the construction workers who had supported consistently during the experimental work.

The author would like to convey her thanks to all her fellow colleagues of HBRI who were always supportive in the present study.

A very special debt of deepest gratitude is offered to her husband Md. Taskin Alam, her daughter Ayaan Ereshva, her parents, mother-in-law, her brother and sister who are always the constant sources of inspiration and support throughout her life.

In the present study, an extensive experimental laboratory investigation has been carried out to study the comparative in-plane cyclic behavior of brick infilled, isolated brick infilled and bare reinforced concrete (RC) frames and to find an appropriate retrofit measure for those frames against earthquakes.

Bangladesh is recognized to be an earthquake prone region where multistoried masonry infilled reinforced concrete framed buildings are commonly seen. Burnt clay bricks are the most common infill materials used as partition walls in those RC framed structures. Lack of knowledge on the mechanical properties of the clay brick infills prevents the local structural engineers from idealizing the seismic performances of such buildings in Bangladesh. In this context, present study focuses on the experimental investigation of the comparative in-plane cyclic response of the bare RC frames and the locally available brick infilled RC frames. Moreover, in-plane cyclic behavior of a newly proposed construction method of brick infilled RC frames where the infill is isolated from the surrounding RC frames have also been evaluated and compared with the bare and the conventional brick infilled RC frames.

In the present research, the increasing in-plane reverse cyclic loads in increasing magnitude have been applied on six single bays, single story  $\frac{1}{2}$  scale models comprising two bare RC frames; two brick infilled RC frames and two isolated brick infilled RC frames till their ultimate capacities were reached accompanied by substantial deformation and propagation of cracks. Behaviors of these frames were evaluated through the observed strength and deformation characteristics along with hysteretic energy dissipation capacity and ductility. Later, the damaged specimens were repaired with FC laminates and tested following the same procedures as for the original frames.

The experimental results proved three times larger shear capacity as well as lower ductility of brick infilled RC frames in comparison to bare RC frames. While, the isolated brick infilled RC frames exhibited 40% lower shear capacity and comparatively large energy dissipation capacity as compared to the brick infilled RC frame. Furthermore, repair or retrofitting with ferrocement laminates confirmed improved performances of all the damaged frames regarding shear capacity, stiffness degradation and energy dissipations. Eventually more than the original strengths were achieved by repairing the damaged frames with ferrocement laminates.

## CONTENTS

---

ACKNOWLEDGEMENT	iii
ABSTRACT	iv
CONTENTS	v
LIST OF FIGURES	ix
LIST OF TABLES	xvi
Chapter 1: INTRODUCTION	1
1.1 General	1
1.2 Historical Background of the Study	1
1.3 Present State of Art of the Research Topic	4
1.4 Objective of the Study	7
1.5 Justification of the Study	7
1.6 Methodology of the Study	9
1.7 Organization of the Thesis	10
Chapter 2: REVIEW OF LITERATURE	11
2.1 Introduction	11
2.2 Behavior of Infilled RC Frames against lateral Load	11
2.3 Effect of Soft Ground Story on Infill Frames during Earthquake	14
2.4 Historical Review of Works on the Seismic Behavior of Infilled Frames	16
2.4.1 Previous Studies on the Lateral Responses of Infilled Frames	16
2.4.2 Building Codes	17
2.4.3 Experimental Research on the Seismic Behavior of Infilled Frames	20
2.4.4 Analytical Studies on Infilled Frames	24
2.5 Ductility Requirements for RC Frames against Lateral Loads	28
2.5.1 Indian Standard Code Requirements	28
2.5.2 Requirements Specified in BNBC	32
2.6 Existing Seismic Retrofit and Repair Techniques for Masonry and RC Frame Structures	32
2.6.1 Grouting, Sealing, Bonding with Epoxies and Internal Reinforcing	33
2.6.2 Surface Coatings	35
2.7 An Overview for Ferrocement- As a Repair and Retrofit Material	43
	v

2.7.1	Constituents of Ferrocement	43
2.7.2	Parameters Characterizing the Reinforcement in Ferrocement	45
2.7.3	Properties of Ferrocement	47
2.7.4	General Repair Procedures with Ferrocement for RC Frames with Infills	51
2.7.5	Rehabilitation of Distress RC Frame	53
2.7.6	Rehabilitation of Distress RC Frame Infill	53
2.8	Remarks	53
 Chapter 3: EXPERIMENTAL PROGRAM		55
3.1	Introduction	55
3.2	Experimental Setup	55
3.2.1	Strong Base	55
3.2.2	Anchor Bolts	58
3.2.3	Reaction Frames and Hydraulic Jacks	58
3.2.4	Tripod Stands for Mounting Sensors	58
3.2.5	Displacement Transducers (Dial Gauges)	58
3.3	Model Specimens	64
3.3.1	Dimensions and Reinforcement Details of the Model Specimen Frames	65
3.3.2	Construction of RC Frames for All the Model Specimen Frames	65
3.3.3	Construction of Brick Infills	66
3.3.4	Gap Provisions for Isolated Infilled Frames	67
3.3.5	Surface Finishing and Painting	74
3.4	Laboratory Investigation	74
3.4.1	Test Phase-I: In-plane Cyclic Loading Test of Specimen Frames A1, A2, B1, B2, C1 and C2	74
3.4.2	Test Phase- II: In-plane Cyclic Loading Test of Specimen Frames A1, A2, B1, B2, C1 and C2	76
 Chapter 4: EXPERIMENTAL RESULTS AND DISCUSSIONS		87
4.1	Introduction	87
4.2	Experimental Results for Brick Infilled RC Frames	87
4.2.1	Crack Patterns of the Original Frames A1 and A2	88
4.2.2	Crack Patterns of the Repaired Frames AR1 and AR2	88



4.2.3	Shear Capacity of the Original and the Repaired Brick Infilled RC Frames	92
4.2.4	Comparative Hysteretic Behavior of the Original and the Repaired Brick Infilled RC Frames	96
4.2.5	Comparative Lateral Stiffness of the Original and the Repaired Brick Infilled RC Frames	98
4.2.6	Comparative Energy Dissipation of the Original and the Repaired Brick Infilled RC Frames	99
4.2.7	Displacement Ductility Ratio of the Original and the Repaired Brick Infilled RC Frames	99
4.3	Experimental Results for Bare RC Frames	100
4.3.1	Crack Patterns of the Original Frames B1 and B2	100
4.3.2	Crack Patterns of the Repaired Frames AR1 and AR2	103
4.3.3	Shear Capacity at Yield for the Original and the Repaired Brick Infilled RC Frames	103
4.3.4	Comparative Hysteretic Behavior of the Original and the Repaired Bare RC Frames	107
4.3.5	Comparative Lateral Stiffness of the Original and the Repaired Bare RC Frames	107
4.3.6	Comparative Energy Dissipation of the Original and the Repaired Bare RC Frames	107
4.3.7	Displacement Ductility Ratio of the Original and the Repaired Bare RC Frames	110
4.4	Experimental Results for Isolated Brick Infilled RC Frames	110
4.4.1	Crack Patterns of the Original Frames C1 and C2	111
4.4.2	Crack Patterns of the Repaired Frames CR1 and CR2	112
4.4.3	Shear Capacity of the Original and the Repaired Isolated Infilled RC Frames	115
4.4.4	Comparative Hysteretic Behavior of the Original and the Repaired Isolated Infilled RC Frames	115
4.4.5	Comparative Lateral Stiffness of the Original and the Repaired Isolated Infilled RC Frames	119
4.4.6	Comparative Energy Dissipation of the Original and	

the Repaired Isolated Infilled RC Frames	119
4.4.7 Displacement Ductility Ratio of the Original and the Repaired Isolated Infilled RC Frames	122
4.5 Comparative Cyclic Behaviors of Brick Infilled RC Frames, Bare RC Frames and Isolated Brick Infilled RC Frame	123
4.5.1 Later Forces versus Story Drift	123
4.5.2 Energy Dissipation versus Story Drift	123
4.5.3 Stiffness versus Story Drift	123
4.6 Overall Comparative Behaviors of Infilled, Bare and Isolated Brick Infilled RC Frames	127
4.7 Effectiveness of FC Laminates as a Repair or Retrofitting Material	132
 Chapter 5: CONCLUSIONS	135
5.1 General	135
5.2 Findings in Brief	136
5.2.1 Comparative In-plane Cyclic Behavior of Brick Infilled, Bare and Isolated Brick Infilled RC Frames	136
5.2.2 Effectiveness of FC Overlay as Repair and Retrofitting Techniques for the Damaged Brick Infilled, Bare and Isolated Brick Infilled RC Frames	137
5.3 Recommendations for Safeguarding Brick Infilled RC Frame Buildings with Soft Ground Floor	139
5.4 Scope for Future Study	140
 REFERENCES	141
Appendix-A: Compressive Strength of Concrete Cylinders	148
Appendix-B: Properties of Steel Embedded in the RC Specimen Frames	151
Appendix-C: Compressive Strength of Mortar Cubes	152
Appendix-D: Compressive Strength Test of Brick Prism	153
Appendix-E: Calculations	165

## LIST OF FIGURES

---

### Chapter 1: INTRODUCTION

Figure 1.1	Seismic zoning map of Bangladesh	5
Figure 1.2	Izmit earthquake in 1999 (Turkey)	6
Figure 1.3	Bhuj earthquake in 2001 (India)	6
Figure 1.4	Nepal earthquake in 2015 (Nepal)	6

### Chapter 2: REVIEW OF LITERATURE

Figure 2.1	Change in lateral load transfer mechanism due to masonry infills	12
Figure 2.2	(a) Interactive behavior of frame and infill, (b) Analogous braced frame	12
Figure 2.3	Modes of infill failure	14
Figure 2.4	Modes of frame failure	14
Figure 2.5	Effects of masonry infills on the first mode shape of a typical frame of a ten story RC building a) Displacement profile b) Fully infilled frame, c) Frame with open ground floor	15
Figure 2.6	Buildings with open ground story a) actual building b) building being assumed in current design practice	16
Figure 2.7	Different arrangements of masonry infill walls in RC frame	20
Figure 2.8	End bent of ties	30
Figure 2.9	Required extra links to keep the concrete in place	30
Figure 2.10	Placing vertical bars and closed ties in columns	31
Figure 2.11	Different types of wire mesh used in ferrocement	44

### Chapter 3: EXPERIMENTAL PROGRAM

Figure 3.1	Outline of in-plane cyclic loading test setup	56
Figure 3.2	In-plane cyclic loading test setup in BUET, Bangladesh	57
Figure 3.3	Pre-tensioning of anchor bolts using hydraulic jack to ensure the fixity of the specimen along the strong base	59
Figure 3.4	Anchor bolts ensuring the fixity of the specimen	59
Figure 3.5	Reaction frame and the position of hydraulic jack	60
Figure 3.6	Dial gauge and pumper attached with the hydraulic jack	60

Figure 3.7 (a) and (b) Positions of hydraulic jacks fixed with the reaction frame	61
Figure 3.8 Position of tripod stands for mounting displacement transducers	62
Figure 3.9 Mounting of displacement transducers to measure the top deflections	62
Figure 3.10 Position of hydraulic jack and displacement transducer	63
Figure 3.11 Location of displacement transducer to measure the base movement of the specimens	63
Figure 3.12 Geometry and reinforcement details of test model specimen	66
Figure 3.13 Steel casing for the specimen base	68
Figure 3.14 Seismic detailing of the reinforcing steel	68
Figure 3.15 Casting of the specimens' bases in first step	69
Figure 3.16 Casting of columns for the specimens	69
Figure 3.17 Construction of brick infills in specimens C1, C2 and A1 (from front)	70
Figure 3.18 Application of cork sheets into gaps between the infill and the surrounding RC frame for the isolated infilled RC frame	70
Figure 3.19 Placement of the single layer cork sheet at the infill-RC beam interface and tetra layer cork sheet at the infill-RC column interface and application of wire mesh along the interfaces	71
Figure 3.20 Application of wire mesh with GI wire and nails along the surface area of the infill-RC column interface	71
Figure 3.21 Application of sand cement mortars on the specimen surface and the wire mesh fastened along the infill-RC column interface	72
Figure 3.22 Surface finishing of the isolated brick infilled RC frame specimen	72
Figure 3.23 Finished Specimens C1, C2 and A1 (from front)	73
Figure 3.24 Finished Specimens B1, B2, A2 (right column) and C1, C2 and A1 (left column)	73
Figure 3.25 In-plane cyclic load test of the model specimens in Test Phase-I	
(a) In-plane cyclic load test of brick infilled RC frame	
(b) In-plane cyclic load test of bare RC frame	
(c) In-plane cyclic load test of isolated infilled RC frame	75

Figure 3.26	Surface cleaning of damaged specimens after by chipping of the plasters	80
Figure 3.27	Shear sliding, mortar bed joint failure and corner crushing of the isolated infill have been identified clearly after chipping of the plasters	80
Figure 3.28(a)	Wiremesh wrapped around the RC frame and the infill	81
Figure 3.28(b)	Closed up view of Wiremesh wrapped around the RC frame (two layers of wire mesh) and the infill (one layer of wiremesh)	81
Figure 3.29(a)	Wrapping of wiremesh on isolated infilled RC frame to repair the bed joint failures of isolated infill wall	82
Figure 3.29(b)	Gouting along the wrapped wiremesh around the RC frame and the infill RC frame interface	82
Figure 3.30	Close up view of wire mesh wrapping around the RC frame and infill-RC frame interface for the isolated infilled RC frames	83
Figure 3.31	Wiremesh wrapped specimens were plastered with rich mortars	83
Figure 3.32	Test specimen AR1 after applying cyclic load in Test Phase-II	84
Figure 3.33	Test specimen AR2 after applying cyclic load in Test Phase-II	84
Figure 3.34	Test specimen BR1 after applying cyclic load in Test Phase-II	85
Figure 3.35	Test specimen BR2 after applying cyclic load in Test Phase-II	85
Figure 3.36	Test specimen CR1 after applying cyclic load in Test Phase-II	86
Figure 3.37	Test specimen CR1 after applying cyclic load in Test Phase-II	86
<b>Chapter 4: EXPERIMENTAL RESULTS AND DISCUSSIONS</b>		
Figure 4.1(a)	Crack patterns at maximum lateral load in brick infilled RC frame model specimen A1	90
Figure 4.1(b)	Crack patterns at maximum lateral load in brick infilled RC frame model specimen A2	90
Figure 4.2(a)	Crack patterns at peak load in repaired brick infilled RC frame model specimen AR1	91
Figure 4.2(b)	Crack patterns at peak load in repaired brick infilled RC frame model specimen AR2	91

Figure 4.3(a) Lateral load versus story drift in original brick infilled RC frames (A1, A2)	93
Figure 4.3(b) Lateral load versus story drift in FC laminated repaired brick infilled RC frames (AR1, AR2)	93
Figure 4.4(a) Hysteretic load-displacement curves in Test Model A1	94
Figure 4.4(b) Hysteretic load-displacement curves in Test Model AR1	94
Figure 4.4(c) Hysteretic load-displacement curves in Test Model A2	95
Figure 4.4(d) Hysteretic load-displacement curves in Test Model AR2	95
Figure 4.5(a) Comparison of stiffness degradation in each loading cycle with respect to story drift in original specimen A1 and AR1	97
Figure 4.5(b) Comparison of stiffness degradation in each loading cycle with respect to story drift in repaired specimens A2 and AR2	97
Figure 4.6(a) Comparison of cumulative energy dissipation in each loading cycle with respect to story drift in original specimen A1 and AR1	98
Figure 4.6(b) Comparison of cumulative energy dissipation in each loading cycle with respect to story drift in repaired specimens A2 and AR2	98
Figure 4.7(a) Crack patterns at maximum lateral load in RC Bare frame model specimen B1	101
Figure 4.7(b) Crack patterns at maximum lateral load in RC Bare frame in specimen B2	101
Figure 4.8(a) Crack patterns at peak load in Repaired RC Bare frame model specimen BR1	102
Figure 4.8(b) Crack patterns at peak load in repaired RC Bare frame specimen BR2	102
Figure 4.9(a) Lateral Load versus Story Drift in Original and Repaired Bare RC Frames (B1, BR1)	104
Figure 4.9(b) Lateral Load versus Story Drift in in Original and Repaired Bare RC Frames (B2, BR2)	104
Figure 4.10(a) Hysteretic load-displacement curves in Test Model B1	105
Figure 4.10(b) Hysteretic load-displacement curves in Test Model BR1	105

Figure 4.10(c) Hysteretic load-displacement curves in Test Model B2	106
Figure 4.10(d) Hysteretic load-displacement curves in Test Model BR2	106
Figure 4.11(a) Comparison of stiffness degradation in each loading cycle with respect to story drift in original specimen B1 and BR1	108
Figure 4.11(b) Comparison of stiffness degradation in each loading cycle with respect to story drift in repaired specimens B2 and BR2	108
Figure 4.12(a) Comparison of cumulative energy dissipation with respect to story drift in original specimen B1 and BR1	109
Figure 4.12(b) Comparison of cumulative energy dissipation with respect to story drift in repaired specimens B2 and BR2	109
Figure 4.13(a) Crack patterns at maximum lateral load in isolated infilled RC frame model specimen C1	113
Figure 4.13(b) Crack patterns at maximum lateral load in isolated infilled RC frame specimen C 2	113
Figure 4.14(a) Crack patterns at peak load in repaired isolated infilled RC frame model specimen CR1	113
Figure 4.14(b) Crack patterns at peak load in repaired isolated infilled RC frame model specimen CR2	114
Figure 4.15(a) Comparative lateral forces versus story drift in each loading cycle in original isolated infilled RC frames (C1, C2)	116
Figure 4.16(a) Hysteretic Load-Displacement Curves for Test Model C1 and C2	117
Figure 4.16(b) Comparison of Hysteretic Load-Displacement Curves between C1 and CR1 and between C2 and CR2	118
Figure 4.17(a) Comparison of stiffness degradation in each loading cycle with respect to story drift in original specimen C1	120
Figure 4.17(b) Comparison of stiffness degradation in each loading cycle with respect to story drift in repaired specimens C2 and CR2	120
Figure 4.18(a) Comparison of cumulative energy dissipation in each loading cycle with respect to story drift in original specimen C1 and CR1	121
Figure 4.18(b) Comparison of cumulative energy dissipation in each	

	loading cycle with respect to story drift in repaired specimens C2 and CR2	121
Figure 4.19	Comparison of story drift with respect to maximum lateral forces in each cycle for brick infilled RC frames (A1 and A2), Bare RC frame (B1 and B2) and isolated brick infilled RC frames (C1 and C2)	124
Figure 4.20	Comparison of story drift with respect to cumulative energy dissipation in each cycle for brick infilled RC frames (A1 and A2), Bare RC frame (B1 and B2) and isolated brick infilled RC frames (C1 and C2)	125
Figure 4.21	Comparison of story drift with respect to stiffness in each cycle for brick infilled RC frames (A1 and A2), Bare RC frame (B1 and B2) and isolated brick infilled RC frames (C1 and C2)	126
Figure 4.22	Comparative Crack Patterns and Failure Mechanisms of Original Brick Infilled, Bare and Isolated Brick Infilled RC Frames	128
Figure 4.23	Comparative Crack Patterns and Failure Mechanisms of Repaired Brick Infilled, Bare and Isolated Brick Infilled RC Frames	129
Figure 4.24	Comparative Hysteretic Behavior of Original and Repaired Brick Infilled, Bare and Isolated Brick Infilled RC Frames	130
Figure 4.25(a)	Comparative shear capacity	131
Figure 4.25(b)	Comparative cumulative energy dissipation	131
Figure 4.25(c)	Comparative stiffness degradation	131
Figure 4.26	Comparative shear capacities of original and FC laminated repaired frames	132
Figure 4.27	Comparative Stiffness Degradation of Original and FC Laminated Repaired Frames	133
Figure 4.28	Comparative Energy Dissipation of Original and FC Laminated Repaired Frames	134
<b>Appendix-D: COMPRESSIVE STRENGTH TEST OF BRICK PRISM</b>		
Figure D.1	Specimen-1: Maximum Load=19.74 Ton	154
Figure D.2	Specimen-2: Maximum Load=21.55 Ton	154



Figure D.3(a) Specimen-3: Maximum Load=12.18 Ton	155
Figure D.3(b) Specimen-3: Maximum Load=12.18 Ton	155
Figure D.4(a) Specimen-4: Maximum Load=17.39Ton	156
Figure D.4(b) Specimen-4: Maximum Load=17.39Ton	156
Figure D.5(a) Specimen-5: Maximum Load=12.18 Ton	157
Figure D.5(b) Specimen-5: Maximum Load=12.18 Ton	157
Figure D.5(c) Specimen-5: Maximum Load=12.18 Ton	157
Figure D.6(a) Specimen-6: Maximum Load=20.51Ton	158
Figure D.6(b) Specimen-6: Maximum Load=20.51Ton	158
Figure D.7(a) Specimen-7: Maximum Load=14.26Ton	159
Figure D.7(b) Specimen-7: Maximum Load=14.26Ton	159
Figure D.8(a) Specimen-8: Maximum Load=10.10 Ton	160
Figure D.8(b) Specimen-8: Maximum Load=10.10 Ton	160
Figure D.9(a) Specimen-9: Maximum Load= 8.02 Ton	161
Figure D.9(b) Specimen-9: Maximum Load= 8.02 Ton	161
Figure D.9(c) Specimen-9: Maximum Load= 8.02 Ton	161
Figure D.10(a) Specimen-10: Maximum Load= 17.41 Ton	162
Figure D.10(b) Specimen-10: Maximum Load= 17.41 Ton	162
Figure D.10(c) Specimen-10: Maximum Load= 17.41 Ton	162
Figure D.11(a) Specimen-11: Maximum Load= 18.95 Ton	163
Figure D.11(b) Specimen-11: Maximum Load= 18.95 Ton	163
Figure D.12(a) Specimen-12: Maximum Load= 10.10 Ton	164
Figure D.12(b) Specimen-12: Maximum Load= 10.10 Ton	164
Figure D.12(c) Specimen-12: Maximum Load= 10.10 Ton	164

## LIST OF TABLES

---

Chapter 1: INTRODUCTION	
Table 1.1 Model Specimens	9
Chapter 3: EXPERIMENTAL PROGRAM	
Table 3.1 Model Specimens in Test Phase-I	64
Table 3.2 Model Specimens in Test Phase-II	65
Table 3.3 (a) Average Material Properties of the Construction Materials of the Model Specimens	76
Table 3.3 (b) Materials Used in FC Laminating for Repair of Damaged Specimens	76
Table 3.4 Reinforcement Parameters for FC Laminated Specimens AR1 and AR2	77
Table 3.5 Reinforcement Parameters for FC Laminated Specimens BR1 and BR2	78
Table 3.6 Reinforcement Parameters for FC Laminated Specimens CR1 and CR2	79
Chapter 4: EXPERIMENTAL RESULTS AND DISCUSSIONS	
Table 4.1 Summary of Experimental Results for A1, A2, AR1 and AR2	87
Table 4.2 Failure Mechanism of Original and Repaired Frames	88
Table 4.3 Ductility Ratio of Test Model Specimens	99
Table 4.4 Summary of Experimental Results for B1, B2, BR1 and BR2	100
Table 4.5 Failure Mechanism of Original and Repaired Bare RC Frames	100
Table 4.6 Ductility Ratio of Bare RC Frame Specimens	110
Table 4.7 Summary of Experimental Results for C1, C2, CR1 and CR2	111
Table 4.8 Failure Mechanism of Original and Repaired Isolated Infilled Frames	111
Table 4.9 Ductility Ratio of Test Model Specimens	122
Table 4.10 Brief Summary of Experimental Results	127

Appendix-A: COMPRESSIVE STRENGTH OF CONCRETE CYLINDERS	
Table A.1	28 days Compressive Strength of Concrete Cylinder 148
Table A.2	Compressive Strength of Concrete Cylinders of Respective Frames at the date of Testing 149
Appendix-B: PROPERTIES OF STEEL EMBEDDED IN THE RC SPECIMEN FRAMES	
Table B.1	Properties of Steel 151
Appendix-C: COMPRESSIVE STRENGTH OF MORTAR CUBES	
Table C.1	Compressive Strength of Mortar Cubes 152
Appendix-D: COMPRESSIVE STRENGTH TEST OF BRICK PRISM	
Table D.1	Load Parallel to Bed Joint 153
Table D.2	Load Perpendicular to Bed Joint 153
Appendix-E: LOAD-DEFLECTION HISTORY	
Table E.1	Story Drift, stiffness and cumulative energy dissipation regarding infilled frame A1 167

#### 1.1 General

Multistoried masonry infilled reinforced concrete (MIRC) buildings are the popular construction practice in Bangladesh. Generally, in all framed structures in Bangladesh, bricks made from burned clay are used in partition walls serving as infills to the frames. Lack of knowledge on local masonry properties discourages local structural engineers to consider infill walls as structural components. Consequently, it has become a common practice to exclude the contribution of stiffness and strength of infills in structural analysis of MIRC buildings even under seismic loads.

Asteris, P. G. et al. (2013) demonstrated that presence of infills provides local as well as global increase of strength and stiffness according to their extent and position in the frames affecting the distribution and intensity of the inertia forces generated in seismic excitation. This may initiate stress concentrations in certain regions of structures causing localized cracking or unexpected brittle failures detrimental to overall performance of MIRC frames. Hence, it is essential for the professional structural engineers to understand the effect of local masonry infills on seismic performances of MIRC buildings in Bangladesh.

In this context, present study focuses on the experimental investigation of the comparative in-plane cyclic response of the bare RC frames and the locally available brick infilled RC frames. Moreover, in-plane cyclic behavior of a newly proposed construction method of brick infilled RC frames where the infill is isolated from the surrounding RC frames have also been evaluated and compared with the bare and conventional brick infilled RC frames.

#### 1.2 Historical Background of the Study

Even though infill walls have usually been ignored (except as dead weight) in the engineering design of reinforced concrete frames, for many years, they have been the focus of concern in engineering research and code development. Research has shown that the infill masonry walls behave as a “diagonal strut” resisting the deflection of the frame when lateral forces are applied (Stafford Smith, 1966). If the masonry infill is

strong enough, the diagonal strut that is formed when the frame is forced to sway in an earthquake can cause the shear failure of the column, precipitating collapse. In addition, the stiffness of the walls causes the buildings to be subject to greater forces than the walls or the frames are capable of resisting. Moreover, when there is insufficient stiffness in the frame, the non-load bearing partitions participate as shear walls as they become loaded by the deformation of the frame. If the ground floor is diaphanous, undivided and has higher columns, a classic “soft-story” results with stiffer than expected mass over a very weak (soft) ground floor. In such buildings, the upper floors drift over the ground floor causing plastic hinges and permanent deformations.

In fact, the behavior of infill walls has been an area of active research since the 1950s. Polyakov (1956) is amongst the earliest to discuss the structural importance of infill. Research in the 1950s to 1960s (Holmes 1961, Smith 1966) on unreinforced masonry (brick) infills had shown that the walls could be modeled as a strut formulation. Stafford Smith (1966) related the width of the equivalent diagonal strut to the infill frame stiffness parameters. A number of researchers like Liauw and Kwan (1985), Mander et al.(1993), Saneinejad and Hobbs (1995), Negro et al. (1996), Lourenco et al. (1997), Madan et al.(1997) and Papia (1998) etc. addressed the problem of frame-panel interaction and suggest a number of methods to take into account the effect of infill in the analysis and design. Mehrabi et al. (1996) contributed towards our understanding of the beneficial effect of infill. Bunapane and White (1999), clearly stated that the available methods for estimating shear strength that neglect infill-frame interaction were found to largely underestimate measured shear strength. After conducting a large- and small-scale unreinforced masonry infill test program, Henderson (2003) demonstrated that unreinforced masonry infills are more ductile and resist lateral loads more efficiently than anticipated by conventional code procedures.

The concept of modular infilled frames specifically developed for retrofit applications has been investigated by Frosch et al. (1996). Silva et al. (2001) developed a new technique to retrofit infill unreinforced masonry wall using fiber reinforced polymer composites. Langenbach (2003) investigated the possibility of using armature cross walls for vulnerable reinforced concrete masonry infilled framed buildings. Again,

after performing some laboratory tests, Alam (2003) showed that capacities of such infilled frames can be further enhanced by retrofitting with ferrocement. Shing et al. (2006) conducted experimental investigation on retrofit of non-ductile reinforced concrete frames with infill walls. El-Gawady et al. (2007) investigated the behavior of framed masonry wall subjected to in-plane monotonic loading by a full-scale test and a method of discontinuous deformation analysis.

A comparative study of the non-linear behavior of infilled reinforced concrete multistory structures is carried out by Lu (2002). Ms. Haque (2007) compared conventional 'Equivalent Static Force Method (ESFM)' and 'Response Spectrum Methods' for cyclic analysis of several 'soft-story' buildings and found different cyclic behavior for the different two methods applied on same structural models. For preventive measures for seismic damage, she has suggested two alternatives for those infilled 'soft-story' buildings – i) base shear amplification in 'soft-story' column design and ii) isolation of infill from frame element at construction stage.

Although previous researches help in understanding the fundamental behavior of infill as a lateral load resisting structural system; it is necessary to understand the characteristics of locally available brick infilled RC frames in Bangladesh in order to establish their effect on the expected seismic performances. Besides, efficient, reliable and cost-effective repair and retrofitting techniques are indispensable to prevent the casualties in future earthquakes. Therefore, the importance of carrying out experimental research on seismic performance evaluation of locally available brick infilled RC frames and establishing their possible repair and retrofit measures has never been lost.

### **1.3 Present State of Art the Research in Context of Bangladesh**

Bangladesh is situated in an earthquake prone region (Fig.1.1). The cities of this county are densely populated because of unplanned urbanization. Moderate to severe earthquakes may result in devastation in Bangladesh especially in the cities where multistoried clay brick masonry infill buildings with soft ground stories are commonly seen.

Conventionally, the ground floors of such buildings are reserved for car parking leaving it open without any infill. Recent earthquakes (San Fernando in 1971, El Centro in 1940, Los Angeles in 1994, Japan (Kobe) in 1995, Turkey and Taiwan in 1999, India (Bhuj) in 2001, Morocco and Algeria in 2003, Iran in 2004, Nepal in 2015 and Indonesia (Palu) in 2018) have proved that those are the most vulnerable structures. Typical examples of such collapses are shown in Figs. 1.2-1.4.

Brick made from burning clay is a unique construction material available in the Indian subcontinent. Clay solid bricks are used widely in Bangladesh as one of the principle construction materials due to the unavailability of stones. Lack of knowledge on mechanical properties prevents structural engineers to consider brick partition walls as structural elements in analyses. However, it is apparent that infill can have substantial in-plane stiffness which can enhance the lateral strength and stiffness of RC frames. Due to lack of knowledge on the seismic performances of brick infilled RC frames, the actual behavior of the structures cannot be impeccably predicted through the conventional analysis procedures. This also obliterates any scope to incorporate the effects of infill positioned in the upper stories though buildings with open ground floor are very common in this country. This is a serious drawback of the entire system and endangers the structures from seismic point of view.

Therefore, it is important to understand the seismic performance of existing infilled reinforced concrete frames constructed in Bangladesh. Simultaneously, it is necessary to find out the appropriate preventive and retrofit measures for the vulnerable constructions like infill RC frames and “soft-story” buildings.

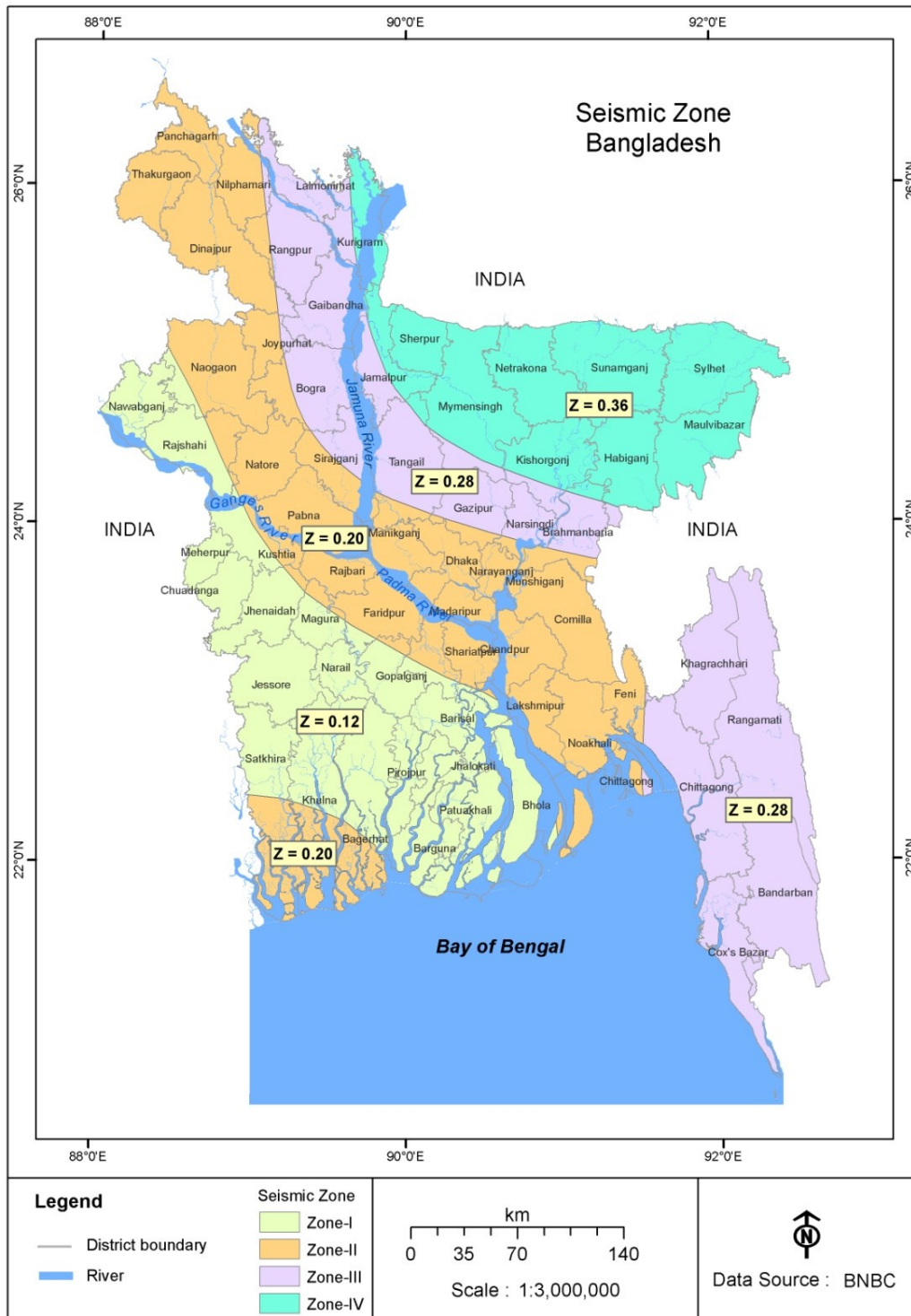


Figure 1.1 Seismic zoning map of Bangladesh (Source: BNBC 2014, HBRI)





Figure 1.2 Izmit earthquake in 1999 (Turkey) (Source: Yolalmis)



Figure 1.3 Bhuj earthquake in 2001 (India) (Source: NICEE)



Figure 1.4 Nepal earthquake in 2015 (Nepal) (Source: <http://www.wired.com>)

## 1.4 Objective of the Study

The basic objectives of this research are:

- 1) to investigate the in-plane cyclic behavior of the locally constructed clay brick infilled RC frames in Bangladesh
- 2) to investigate a preventive or retrofit measure considering isolated infills from surrounding RC frames to protect “soft-story” or “weak-story” mechanism in open ground floor infilled RC framed buildings
- 3) to suggest appropriate cost-effective repair and retrofit measures utilizing ferrocement laminates to minimize the damage due to collapse of infill walls and RC frames

## 1.5 Justification of the Study

In recent past, severe earthquakes have caused substantial physical losses and casualties in this sub-continent. The 2001 Gujrat Earthquake in India and 2005 Kashmir Earthquake in Pakistan and India, and 2015 Nepal Earthquake revealed the vulnerability of “non-earthquake-proof” cities and villages in the Indian sub-continent. In 1897, an earthquake of magnitude 8.7 (recently modified to be 8.0) caused serious damages to buildings and lives in the northeastern part of India including Bangladesh. Historical records have revealed that there are areas of high seismic activity over north and east of Bangladesh and some of major earthquakes originating in these areas affect adjacent part of Bangladesh. According to long-term historical records, occurrence of earthquake in Bangladesh is quite frequent with the magnitude averaging around 5 in Richter scale. During these earthquakes, damage such as collapse of reinforced concrete buildings killing several people in the port city Chittagong (November 1997), serious structural damage on the cyclone shelters in Moheshkhali of Chittagong (July, 1999), considerable cracking in masonry buildings and electric transformer damage in Chittagong city (July, 2003) and considerable cracks approximately in twenty five numbers of buildings in Chittagong Division (November, 2007) along with frequent shaking have raised alarm and growing concern among the people. If a major earthquake happens, the damage in urban areas is expected to be severe. This is because most of the buildings constructed are not designed to resist earthquake.

In Bangladesh, unreinforced masonry walls used for façade and interior partition walls which fit tightly in between the structural columns and beams/slabs, are considered non-structural though they do interact with the structural members confining it. Again, here infill is eliminated almost all cases at the lower levels of the commonly used non-ductile frame creating “soft-story” which is the most common cause of collapse of mid-rise and high-rise non-ductile concrete buildings in prior major earthquake. Thousands have died in such type of buildings in earthquakes in different countries around the world, including recently in Los Angeles in 1994, Japan (Kobe) in 1995, Turkey and Taiwan in 1999, India (Bhuj) in 2001, Morocco in 2003, Iran in 2004 and Nepal in 2015.

In Bangladesh no serious thought is being given to potential impact of such construction practice on the expected seismic performance of these buildings. Therefore, it is important to understand the seismic performance of infilled reinforced concrete frames constructed in Bangladesh and to find out the appropriate preventive and retrofit measures for vulnerable constructions like infill frame structures and “soft-story” buildings. Present experimental research has focused on the assessment of the existing lateral load resistance capacities of the infill reinforced concrete plane frames and proved the applicability of ferrocement (FC) as a repair or retrofitting material and technique. Ferrocement Laminate was chosen because of its enhanced strength and energy dissipation capacity, crack arrest mechanism and cost effectiveness. Further, isolated infilled RC frames were also explored where infill is uncoupled from the surrounding frame by keeping structural gaps. In this case, initial stiffness is anticipated to reduce so that the overall structure can remain flexible which will be governed by predominant frame action.

Consequently, findings of the present experimental investigation are applicable to utilize in the following areas of national interest,

- 1) to determine constituent material properties and the constitutive models for masonry infills to utilize in the numerical analysis of full scale brick infilled RC framed buildings
- 2) to assess the earthquake load resisting capacity of existing older buildings
- 3) to utilize the infill as a low-cost alternative to costly shear wall system for medium-rise buildings

- 4) to formulate a repair or retrofitting scheme for vulnerable buildings to minimize earthquake damage due to collapse of infill walls as well as frames
- 5) to formulate a justified and cost effective retrofit measure to protect “soft-story” or “weak-story” mechanism in infilled reinforced concrete framed structures

## 1.6 Methodology of the Study

In the present research, the increasing reverse cyclic in-plane loads were applied on six single bay, single story ½ scale models comprising two bare RC frames; two brick infilled RC frames and two isolated brick infilled RC frames till their ultimate capacities were reached accompanied by substantial deformation and propagation of cracks. Behaviors of the frames were evaluated through the observed strength and deformation characteristics along with hysteretic energy dissipation capacity and ductility. Later, the damaged specimens were repaired with FC laminates and tested following the same procedures as for the original frames. Table 1.1 lists the number and types of frames those were tested,

**Table 1.1 Model Specimens**

Sl. No.	Description of specimen frame type	Number of specimens
1	Bare reinforced concrete portal frame	2
2	Reinforced concrete portal frame having brick infill	2
3	Reinforced concrete portal frame having brick infill isolated from frame elements	2
4	Retrofitted damaged infilled frames of Sl. No. 1, 2 and 3	2+2+2 = 6

The experimental research scheme involved use of a test rig existing in Civil Engineering Laboratory, BUET. The rig has different components like the base, reaction block, the specimen frame with infill, anchor bolts etc. In 1st phase, tests were performed on bare frames as well as on infill frames. At first all the frames were tested for cyclic load. Then those damaged specimens were retrofitted with ferrocement laminates for observing their behavior under cyclic load. Here the model reinforced concrete frames with infill were attached to the base by means of anchor bolts. Cyclic load was applied by means of two loading jacks (hydraulic) mounted on

two opposite reaction frames and operating the jacks alternately. Displacement transducers were fitted at selected locations of the frame to measure the deflections.

### **1.7 Organization of the Thesis**

Chapter 1: Introduction - introduces the reader with the thesis work.

Chapter 2: Literature Review - reviews previous experimental and analytical researches on masonry infilled RC structures and various repair and retrofitting techniques for infilled RC frames including Ferrocement overlay are described.

Chapter 3: Experimental Program - describes the test setup, test models and test procedures.

Chapter 4: Experimental Results and Discussion – presents all the experimental results with intensive discussion and analysis.

Chapter 5: Conclusions and Recommendations – depicts the overall findings and future recommendations.

Appendices: Appendix-A, Appendix-B, Appendix-C, Appendix-D describe material properties obtained from the laboratory investigations whereas Appendix-E presents load-deflection history and Appendix-F includes sample calculations regarding analysis of results.

## **2.1 Introduction**

Masonry infilled reinforced concrete (MIRC) frames are the commonly used structural systems in developing countries. These masonry infill walls are considered as non-load bearing components of the frames. Therefore, it is a common practice to exclude the infill walls in the numerical models for structural analysis of MIRC frame under seismic load. As a consequence, the stiffness and strength contribution of infill walls are neglected in structural design and analysis. In this context, present chapter summarizes previous studies on the characteristics of infilled RC frame structures. Along with previous researches, theories and formulas for determining material properties of masonry constituents within infills are also have been summarized in the present chapter.

## **2.2 Behavior of Infilled RC Frames Against Lateral Load**

Previous researches have shown the beneficial effects of the interaction between masonry infills and structural elements for seismic performance of existing frame buildings. Proper use of infills in frames could result in significant increases in the strength and stiffness of structures subjected to seismic excitations (Klingner and Bertero 1978, Mehrabi et al. 1996, Bertero and Brokken, 1983). However, the locations of infill in a building must be carefully selected to avoid or minimize torsional effect as well as soft story effect. Architectural restrictions have to be considered when assigning these locations.

Masonry infill walls confined by reinforced concrete (RC) frames on all four sides play a vital role in resisting the lateral seismic loads on buildings. The behavior of masonry infilled frames has been extensively studied (Smith and Coull, 1991; Murty and Jain 2000; Moghaddam and Dowling 1987 etc) to develop a rational approach for design of such frames. It has been shown experimentally that masonry infill walls possess a high initial lateral stiffness and low deformability (Moghaddam and Dowling 1987). Thus, introduction of masonry infills in RC frames changes the lateral-load transfer mechanism of the structure from predominant frame action to

predominant truss action (Murty and Jain 2000), as shown in Figure. 2.1, responsible for reduction in bending moments and increase in axial forces in the frame members.

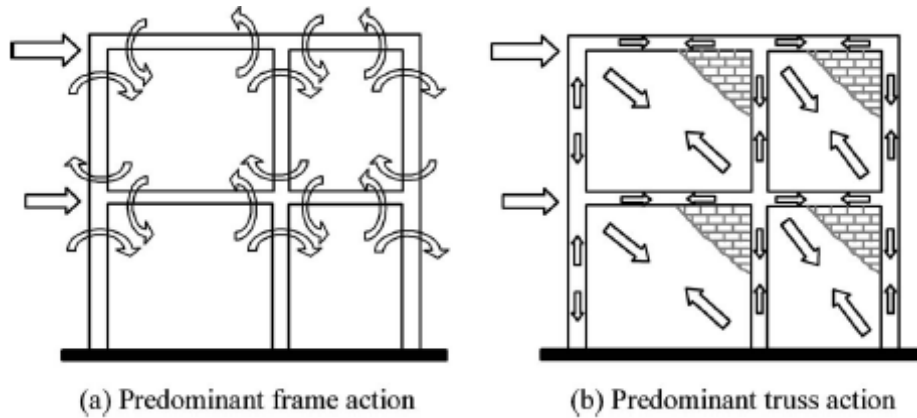


Figure 2.1 Change in lateral load transfer mechanism due to masonry infills (Murty and Jain 2000)

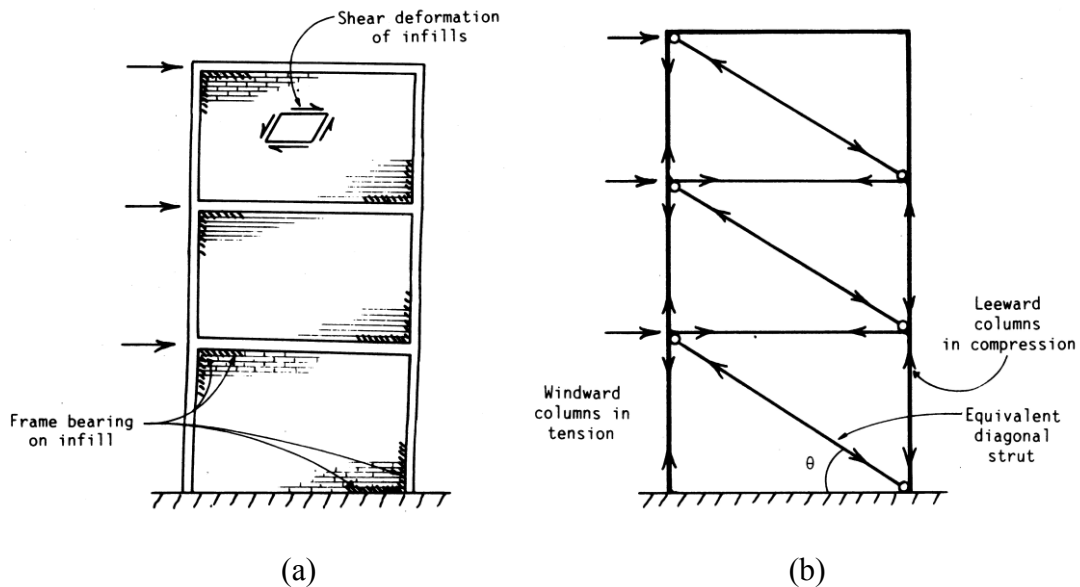


Figure 2.2 (a) Interactive behavior of frame and infill, (b) Analogous braced frame (Smith and Coull, 1991)

The high in-plane rigidity of the masonry wall significantly stiffens the relatively flexible frame. The result is, therefore, a relatively stiff and tough bracing system. The wall braces the frame partly by its in-plane shear resistance and partly by its behavior as a diagonal bracing strut as shown in Figure 2.2(a). When the frame is subjected to horizontal loading, it deforms with double-curvature bending of the columns and beams. The translation of the upper part of the column in each story

and the shortening of the leading diagonal of the frame cause the column to lean against the wall as well as to compress the wall along its diagonal. It is roughly analogous to a diagonally braced frame, shown in Figure 2.2(b).

The potential modes of failure of the wall arise as results of its interaction with the frame are given below:

- 1) Tension failure of the tension column due to overturning moments
- 2) Flexure or shear failure of the columns
- 3) Compression failure of the diagonal strut
- 4) Diagonal tension cracking of the panel and
- 5) Sliding shear failure of the masonry along horizontal mortar beds

The failure modes are shown in Figure 2.3-2.4. The "perpendicular" tensile stresses are caused by the divergence of the compressive stress trajectories on opposite sides of the leading diagonal as they approach the middle region of the infill. The diagonal cracking is initiated at and spreads from the middle of the infill, where the tensile stresses are a maximum, tending to stop near the compression corners, where the tension is suppressed. The nature of the forces in the frame can be understood by referring to the analogous braced frame shown in Figure 2.2(b). The windward column or the column facing earthquake load, is in tension and the leeward column or the other side of the building facing earthquake load is in compression. Since the infill bears on the frame not as a concentrated force exactly at the corners, but over short lengths of the beam and column adjacent to each compression corner, the frame members are subjected also to transverse shear and a small amount of bending. Consequently, the frame members or their connections are liable to fail by axial force or shear, and especially by tension at the base of the windward column.



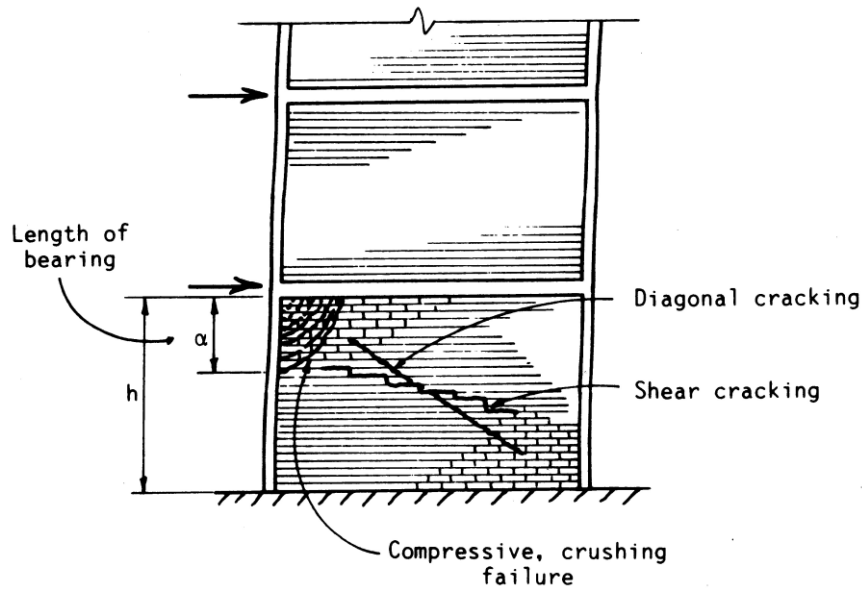


Figure 2.3 Modes of infill failure (Smith and Coull, 1991)

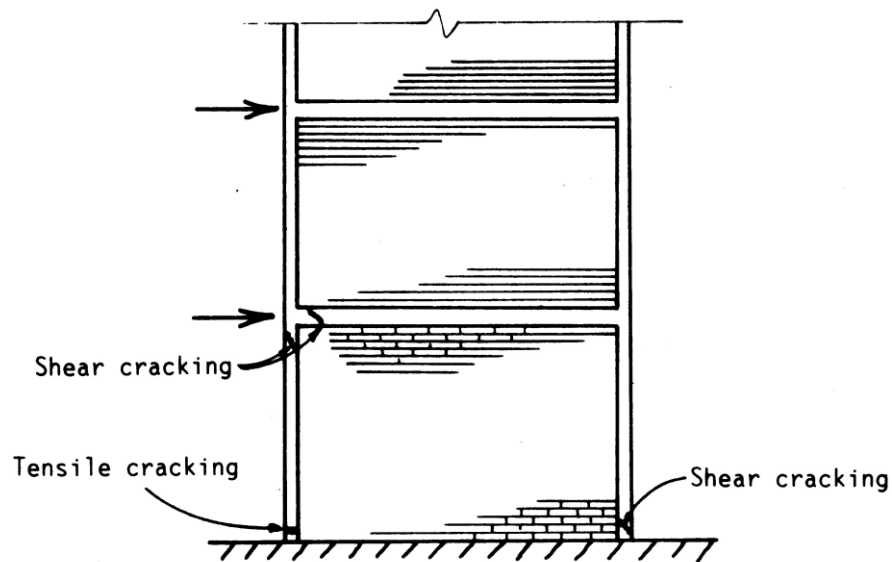


Figure 2.4 Modes of frame failure (Smith and Coull, 1991)

### 2.3 Effect of Soft Ground Story on Infill Frames During Earthquake

When a sudden change in stiffness takes place along the building height, the story at which this significant change of stiffness occurs is called a soft story. According to BNBC (1993) and UBC (1997) a soft story is the one in which the lateral stiffness is less than 70% of that in the story above or less than 80% of the average stiffness of the three stories above. IBC (2000) defines an extreme soft story as the one in which the lateral stiffness is less than 60 percent of that in the story above or less than 70

percent of the three stories above. The vertical geometric irregularity shall be considered to exist where the horizontal dimensions of the lateral-force-resisting system in any story is more than 130 percent of that in an adjacent story.

The most common form of vertical discontinuity arises due to the unintended effect of infill component in the upper stories. For open ground story building, presence of walls in upper stories makes them much stiffer than the ground story. Thus, upper stories move almost together as a single block and most of the horizontal displacement of the building occurs in the soft ground story itself. In common language, this type of buildings can be explained as a building on chopsticks. Thus, such buildings swing back-and-forth like inverted pendulums during earthquake shaking, and the columns in the open ground story are severely stressed. If the columns are weak (do not have the required strength to resist these high stresses) so that they do not have adequate ductility, they may be severely damaged which may even lead the collapse of such buildings.

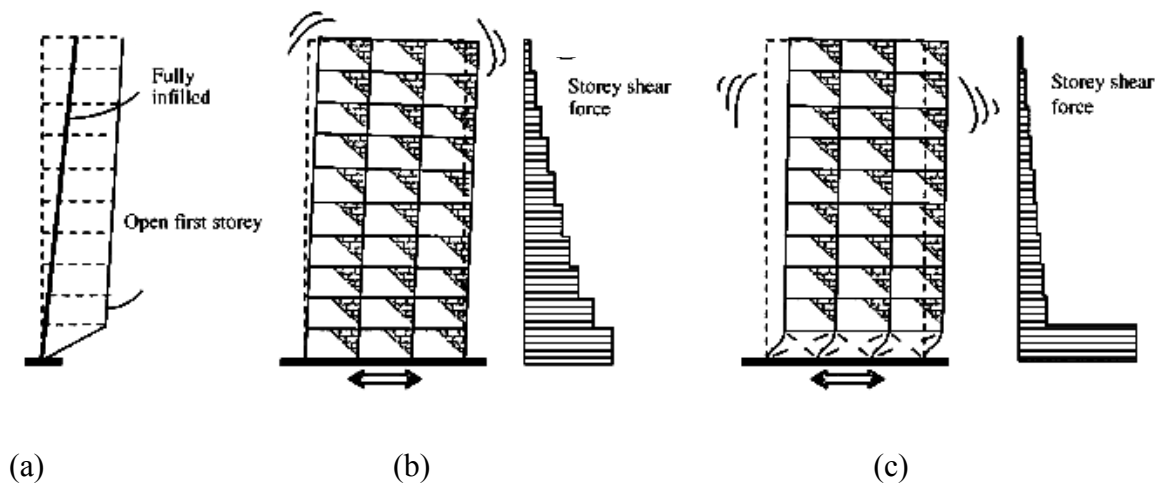


Figure 2.5 Effects of masonry infills on the first mode shape of a typical frame of a ten-story RC building a) Displacement profile b) Fully infilled frame c) Frame with open ground floor (EERI, 2001)

For infilled RC framed structures, the mode shapes and the corresponding contribution of different modes depend upon the amount and location of infills in the frame because of their high initial stiffness, as shown in Figure 2.5, where a single frame of the ten-story building is shown.

In case of a fully infilled frame, lateral displacements are uniformly distributed throughout the height as shown in Figure 2.5(b). On the other hand, in case of open

ground floor buildings, most of the lateral displacement is accumulated at the ground level itself because this floor is the most flexible due to absence of infills (Fig. 2.6(c)). Similarly, the seismic story shear forces and subsequently the bending moments concentrate in the open ground story (Figure 2.5(c)); instead of gradually varying as in fully infilled frame (Figure. 2.6(b)).

Although, in the current design practice, stiff masonry walls (Figure. 2.6(a)) are neglected and only bare frames are considered in design calculations (Figure. 2.6(b)).

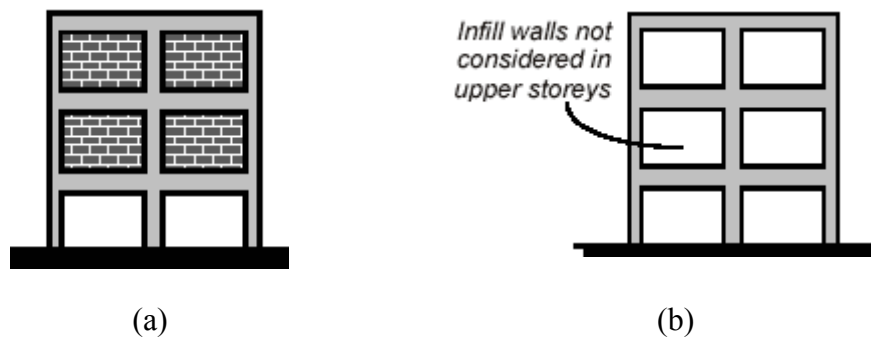


Figure 2.6 Buildings with open ground story (a) actual building (b) building being assumed in current design practice

## 2.4 Historical Review of Works on the Seismic Behavior of Infilled Frames

### 2.4.1 Previous studies on the lateral responses of infilled frames

The study on interaction of infill walls with frames has been started since 1950s. Polyakov (1956) was the first who identify the structural importance of infill. Researches from 1950s to 1960s on masonry infills had revealed that the walls could be modeled as a strut formulation (Holmes, 1961, 1963, and Smith, 1962, 1966). In this context Smith (1966) related the width of the equivalent diagonal strut to the infill frame stiffness parameters.

According to (Asteris, 2003), the assumed ‘diagonal strut’ bears a part of applied seismic loads and transmit them to other regions of the structure providing relief to certain structural elements of the RC frames. This action results in a significant redeployment of the internal actions developing within the structural elements of the frame. Although this redistribution increases overall stiffness and load carrying capacity of the frame, it may develop stress concentrations in specific areas of

joints, beams and columns. Such stress concentration may result in localized cracking even unpredictable modes of failure (Asteris, et al., 2013).

Except for in-plane response, out-of-plane behavior of infill walls must be considered in structural assessment of infilled RC frames. Out-of-plane motion can potentially cause an infill wall to sustain major damage or even collapse. Consequently, after sustaining a certain degree of damage, infill walls can no longer support in enhancing in-plane stiffness of RC frames. The experimental and analytical investigations explain that infill walls have substantial out-of-plane displacement capacity. Hence, it shows more ductile behavior than conventionally accepted (Asteris et al., 2013). Furthermore, several studies explain that the confined infill panel with its' arching effect, can possess significant out-of-plane resistance depending on its slenderness.

Furthermore, a number of researchers have addressed the problem of frame-panel interaction and suggest a number of methods to take into account the effect of infill in the analysis and design (Liau and Kwan, 1985; Mander et al., 1993; Saneinejad and Hobbs, 1995; Louréncço et al., 1997; Madan et al., 1997 and Papia, 1988).

On the contrary, Mehrabi et al., (1996) contributed towards the understanding of the beneficial effect of infill.

#### **2.4.2 Building codes**

Building codes specify design and construction requirements, which are intended to protect buildings from major structural damages and the public from loss of life and injury. These requirements are based on past earthquake experience and judgment. Because of differences in the magnitude of earthquakes, geological formations, types of construction, and other factors, the philosophy of seismic design among different countries of engineers varied in different aspects. Various national codes can be broadly grouped in two categories of those that consider or do not consider the role of masonry infill walls while designing RC frames.

A very few codes specifically recommend isolating the masonry infills from the RC frames such that the stiffness of the infills does not play any role in the overall stiffness of the frame (NZS-3101 1995, SNIP-II-7-81 1996). As a result, masonry

infill walls are not considered in the analysis and design procedure. The isolation helps to prevent the problems associated with the brittle behavior and asymmetric placement of masonry infills.

Another group of national codes prefers to take advantage of certain characteristics of masonry infill walls such as high initial lateral stiffness, cost-effectiveness, and ease in construction. These codes require that the beneficial effects of masonry infill are appropriately included in the analysis and design procedure and that the detrimental effects are mitigated. In other words, these codes tend to maximize the role of masonry infills as a first line of defense against seismic actions, and to minimize their potential detrimental effects through proper selection of their layout and quality control.

Most national codes recognize that structures with simple and regular geometry perform well during earthquakes, and unsymmetrical placement of masonry infill walls may introduce irregularities into them. These codes permit static analysis methods for regular short buildings located in regions of low seismicity. However, for other buildings, dynamic analyses are recommended, in which it is generally expected but not specifically required that all components imparting mass and stiffness to the structure are adequately modeled. Most codes restrict the use of seismic design force obtained from dynamic analysis such that it does not differ greatly from a minimum value that is based on the code-prescribed empirical estimate of natural period. This restriction prevents the design of buildings for unreasonably low forces that may result from various uncertainties involved in a dynamic analysis.

Natural period of vibration is an important parameter in the building code equations for determining the design earthquake force by any kind of equivalent static force method. Natural periods of buildings depend upon their mass and lateral stiffness. Presence of non-isolated masonry infill walls in buildings increases both the mass and stiffness of buildings; however, the contribution of stiffness is more significant. Consequently, the natural period of a masonry infilled reinforced concrete (MIRC) frame is normally lower than that of the corresponding bare frame. Therefore, the seismic design forces for masonry infilled frames are generally higher than those for the bare frames. Although, all national codes explicitly specify empirical formulae

for the fundamental natural period calculations of bare RC frames, only a few specify the formulae for MIRC frames.

Several codes—IS-1893 (2002); NBC-105 (1995); NSR-98 (1998); Egyptian code (1988); Venezuelan code (1988); Algerian code (1988) suggest using an empirical formula given by Eqn. 2.1 to calculate the natural period of MIRC frames,  $T_a$  in sec.

$$T_a = \frac{0.09h}{\sqrt{d}} \quad 2.1$$

where  $h$  is the height of the building (in meter) and  $d$  the base dimension of building (meter) at the plinth level along the considered direction of the lateral force.

For  $T_a$  estimation, French code (AFPS-90 1990) recommends Eqn. 2.1 as the most unfavorable and the following equation that specified for masonry buildings is:

$$T = 0.06 \frac{h}{\sqrt{d}} \sqrt{\frac{h}{2d+h}} \quad 2.2$$

In Eqn. 2.1 and 2.2, total base width of buildings is used to calculate the natural period of MIRC frames which may not be appropriate. For example,  $d$  will be equal to the total base dimension for all the frames in Figure 2.7 irrespective of the distribution of masonry infill in the frame. However, for frame in Figure 2.7(c), it is more appropriate to consider  $d'$  as the effective base width, rather than total width  $d$  of the building. Therefore, Eqn. 2.1 and 2.2 may not estimate correct the natural periods for different frames shown in Figure 2.7.

A few national codes penalize beams and/or columns of the irregular stories, as they are required to be designed for higher seismic forces to compensate for the reduction in the strength due to absence of infills in the irregular stories. The Indian seismic code (IS-1893 2002) requires members of the soft story (story stiffness less than 70% of that in the story above or less than 80% of the average lateral stiffness of the three stories above) to be designed for 2.5 times the seismic story shears and moments, obtained without considering the effects of masonry infills in any story. The factor of 2.5 is specified for all the buildings with soft stories irrespective of the extent of irregularities; and the method is quite empirical. The other option is to

provide symmetric RC shear walls, designed for 1.5 times the design story shear force in both directions of the building as far away from the center of the building as feasible.

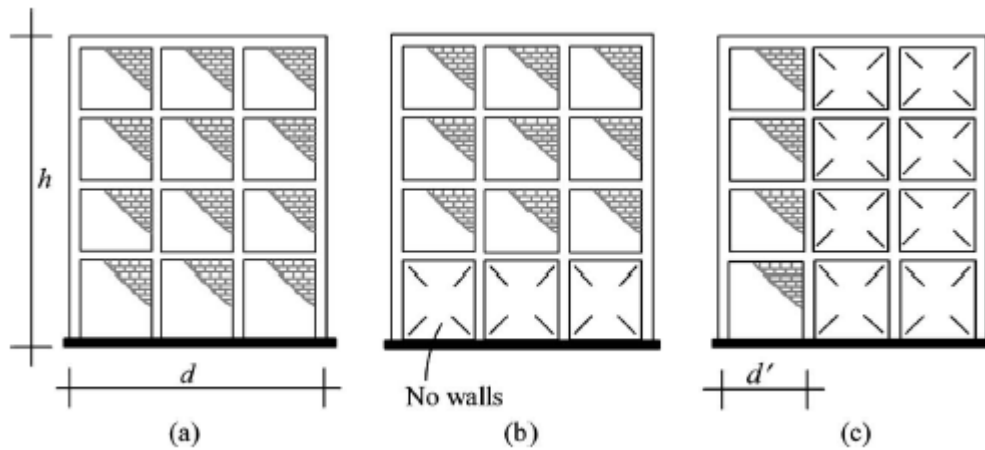


Figure 2.7 Different arrangements of masonry infill walls in RC frame

Costa Rican Code (1986) requires that all structural-resisting systems must be continuous from the foundation to the top of buildings, and stiffness of a story must not be less than 50% of that of the story below.

### 2.4.3 Experimental research on the seismic behavior of infilled frames

Reliable laboratory test results are indispensable in order to formulate and verify the respective constitutive models denoting the material behavior and response (Asteris et al., 2013). Regarding the seismic performance of masonry infilled RC frames, many laboratory investigations have been carried out to identify:

- 1) The responses of different materials concerned in the infilled frames, i.e. concrete, steel, masonry etc.
- 2) The differential behavior of the structural elements, i.e. beams, columns, walls, slabs, joints, infill walls embracing infilled frames
- 3) The overall response of frames considering the contribution of the infill walls on their structural performance

Historically, five different types of infill have been considered in the study of the behavior of infilled frames: brick, clay tile, concrete block, plain concrete, and

reinforced concrete. The surrounding framing in these studies comprised either reinforced concrete or steel members. The following literature review focuses on the reinforced concrete frame-masonry infill wall system due to its distinctive behavior, with a summary of other infilled frames. According to Liauw et al. (1983), infilled frames may be divided into two categories: (1) those with connectors along the interfaces between the frames and the infill walls are called integral infilled frames; and (2) those without are called non-integral infilled frames.

Research on infilled frames started with the investigation of their static behavior under monotonic lateral loading (e.g. Holmes, 1961) with the intention of developing an effective method to predict their ultimate lateral strength. With the recognition that the lateral loading imposed on infilled frames is induced by dynamic phenomena producing reversing load histories, such as earthquakes, wind, or explosions, researchers began to focus their efforts on the cyclic load behavior of infilled frames. During the last three decades, experiments with three different types of loading have been carried out to simulate dynamic phenomena, especially seismic forces: cyclic static and dynamic load tests, pseudo-dynamic tests, and shake-table tests.

Mallick and Severn (1968) performed half-cyclic dynamic load tests on small scale, two-story infilled steel frames, where the cyclic load was applied to the infilled frame in one direction only. The steel frames comprised 0.75 inch x 0.75 inch square steel bars and the story dimension was 24 inch x 24 inch. The dynamic characteristics, such as the damping ratio and the energy dissipation capacity, were compared between infilled steel frames with and without interface shear connectors. It was found that using a small number of shear connectors in loaded corners could prevent the rotation of the infill walls inside the steel frames and increase the stiffness of the system. However, they failed to see any strength increase with the use of shear connectors. The frequencies and mode shapes of multi-story infilled steel frames were obtained analytically using two models: a shear model in which the axial deformation of the steel components was ignored, and a cantilever model in which the bending deformation of the steel frame members was ignored. Test results showed that the cantilever model was better than the shear model for analysis



of multi-story infilled steel frames, particularly for those with a height/span ratio greater than 2.

Liauw (1983, 1985 and 1988) conducted both static and dynamic cyclic load tests on both integral and non-integral steel frames with RC infill walls. The four-story steel frame models comprised 22 mm x 22 mm square steel bars, with the size of infill being 305 mm x 610 mm x 22 mm (height x width x thickness). The reinforcement ratio for the infill wall was 0.56%. In contrast to the conclusion drawn by Mallick and Severn (1968), the presence of the interface connectors was shown to increase both frame stiffness and strength significantly. Furthermore, failure of the integral infilled steel frames was induced largely by shear between the steel frames and the infill walls, instead of by the diagonal compression failure of the infill walls in the non-integral infilled steel frames. The dynamic characteristics of these systems were studied further in another series of cyclic tests (Liauw and Kwan, 1985) on similar infilled steel frames having three different interface configurations: (1) no connectors; (2) connectors welded only along the infill wall/steel girder interface; and (3) connectors welded along the entire infill wall/steel frame interface. The tests showed that the infilled steel frames with the Type 3 interface configurations were the most reliable type of construction because they possessed the highest energy dissipation capacity, the greatest damping ratio in the nonlinear range of deformation and the slowest stiffness degradation.

Shake-table tests are believed to be the best approach for simulating the behavior of a structure during an earthquake. However, shake-table tests are expensive, especially for large scale models. Kwan and Xia (1995) reported a shake-table test on steel frames infilled with light reinforced concrete walls (non-integral). In their tests, the specimen comprised a pair of one-third scale infilled steel frames, connected through reinforced concrete floor slabs at each story, representing a one-bay, four-story structure. The steel frame comprised 40 mm x 40 mm x 2.5 mm high-yield tubes and story dimension is 1125 mm x 1500 mm (height x width). Accelerograms from the El Centro earthquake were used to excite the shake-table, with progressively increasing magnitudes of acceleration being applied until failure of the specimen occurred. It was observed that the infill walls separated from the steel frames during early loading stages and acted as a diagonal compressive strut.

The specimen reached its maximum strength when the corners of the infill walls in the first story were crushed. The specimen did not fail even when the applied peak acceleration was increased to 1.50g, although the frames were badly damaged. However, it was concluded that the RC infill walls would have collapsed out-of-plane, had there not been steel plates attached to the outside of the RC walls to keep them in place. It was also found that the natural frequency of the specimen decreased rapidly as the applied peak acceleration of the simulated earthquake was increased, while the damping increased from 1.7% to 11.0%.

Masonry is a traditional infill material for both steel and RC frame structures. Several experimental studies have been carried out to evaluate the effect of masonry infill on the seismic behavior of the surrounding frames. Although it was found that masonry infill can also significantly increase the stiffness and strength of frame structures (Klinger and Bertero, 1978; Mehrabi et al., 1996; Negro and Verzelett, 1996), designers in the United States are reluctant to treat unreinforced masonry infill as a structural element in seismic regions due to several unfavorable characteristics of the masonry infill. For example, Mander and Nair (1994) found that the shear strength of brick infill walls was greatly affected by cyclic loading. Furthermore, shake-table tests indicated that it is often unavoidable for the masonry infill to collapse out-of-plane because of increased acceleration of ground motion (Dawe et al., 1989; Kwan and Xia, 1995).

Mehrabi et al. (1997) performed a comprehensive research, more relevant to the current study. They studied the influence of masonry infill panels on the seismic performance of reinforced concrete frames. Two types of frames were considered. One was designed for wind load and the other for strong earthquake forces. Twelve ½ -scale, single story, single span frame specimens were tested. The parameters investigated included the strength of infill panels with respect to that of the bounding frame, the panel aspect ratio, the distribution of vertical loads and the lateral load history. The experimental results indicated that the infill panels could significantly improve the performance of RC frames. However, specimens with strong frames and strong panels exhibited a better performance than those with weak frames and weak panels in terms of the load resistance and energy dissipation

capability. The lateral loads developed by the infilled frame specimens were always higher than that of bare frame.

Huang (2005) studied the structural behaviors of low-to-midrise concrete buildings of various configurations with emphases on dynamic properties, internal energy, and the magnitude and distribution of seismic load. Several idealized models were made to represent different structural configurations including pure frame, frames with fully or partially infilled panels, and frames with a soft story at the bottom level, and comparisons were made on the fundamental periods, base shear, and strain energy absorbed by the bottom level between these structures.

Mezzi (2004) illustrated soft story is very dangerous from a seismic point of view, because the lateral response of these buildings is characterized by a large rotation ductility demand concentrated at the extreme sections of the columns of the ground floor, while the superstructure behaves like a quasi-rigid body. A solution was proposed for the preservation of an architectonic double soft-story configuration.

Santhi and Knight (2005) studied two single-bay, three-story space frames, one with brick masonry infill in the second and third floors representing a soft-story frame and the other without infill were designed and their 1:3 scale models were constructed according to non-seismic detailing and the similitude law.

#### **2.4.4 Analytical studies on infilled frames**

During the last three decades, different approaches have been proposed for the prediction of the ultimate strength of infilled steel frames subjected to monotonic lateral load. Holmes (1961) proposed that the infill wall be replaced by an equivalent diagonal strut having a width equal to one-third of the diagonal length of the infill wall. In his elastic model, no axial deformation was included in the steel members and the infilled steel frame achieved its maximum lateral strength when the equivalent strut reached a limiting value of compressive strain. The corresponding deflection was calculated based on the shortening of the equivalent strut. Smith (1966) proposed an expression relating the width of the equivalent strut to the properties of the frame and infill wall. The width of the equivalent strut varied with the value of the following non-dimensional factor:

$$\lambda h = \frac{E_c t h^3 \sin 2\theta}{4E_s I}^{1/4} \quad 2.3$$

where

$E_c$  = elastic modulus of the infill material, ksi

$E_s$  = elastic modulus of the frame material, ksi

$t$  = thickness of the infill wall, inches

$h$  = height of a single story, inches

$I$  = moment of inertia of the frame columns, inch<sup>4</sup>

$\theta$  = slope of the infill diagonal relative to horizontal

Smith and Carter (1969) further related the width of the equivalent strut not only to factor  $\lambda h$ , but also to the variation of the elastic modulus of the infill material at different stress levels.

Liau and Kwan (1983) expressed the equivalent strut width as a fraction of  $h \cos \theta$ :

$$b = \frac{0.86}{\sqrt{\lambda h}} (h \cos \theta) \leq 0.45 (h \cos \theta) \quad 2.4$$

where, the non-dimensional factor parameter  $\lambda h$  is defined in Eq. (2.3). This relation was obtained by parametric study using the finite element method. Despite the controversy on the determination of a reasonable width of the equivalent strut, the equivalent strut concept was applied in the elastic design of multi-story infilled frames by different researchers (Smith and Carter, 1969; Smith and Coull, 1991; Saneinejad and Hobbs, 1995). It should be noted that all the previous equivalent strut methods were established for the analysis of non-integral infilled frames.

A concept of the behavior of infilled frames has been developed by Smith and Coull (1991) from a combination tests results and finite element analyses. Shear failure of the infill is related to the combination of shear and normal stresses induced at points in the infill when the frame bears on it as the structure is subjected to the external lateral shear. An extensive series of plane-stress membrane finite-element analyses has shown that the critical values of this combination of stresses occur at the center of the infill and that they were expressed empirically by

$$\text{Shear stress } \tau_{xy} = \frac{1.43Q}{Lt} \quad 2.5$$

$$\text{Vertical compressive stress } \sigma_y = \frac{(0.8 h/L - 0.2)Q}{Lt}$$

Where Q is the horizontal shear load applied by the frame to the infill of length L, height h, and thickness t.

Similarly, diagonal cracking of the infill is related to the maximum value of diagonal tensile stress in the infill. This also occurs at the center of the infill and, based on the results of the analyses, expressed empirically as

$$\text{Diagonal tensile stress } \sigma_d = \frac{0.58Q}{Lt} \quad 2.6$$

The diagonal tensile strength of masonry is somewhat uncertain in value. However, according to Smith and Coull (1991), it can be estimated conservatively as approximately equal to one-tenth of the mortar compressive strength. Codes of Practice give an allowable flexural tensile stress in masonry equal to approximately one-fortieth of the compressive strength of the weakest allowable mortar. Assuming a typical factor of safety of 4 for brickwork, it is reasonable to take the allowable diagonal tensile stress in masonry as equal to its allowable flexural tensile stress, that is  $f_d = f_t$ . Then, equating the maximum diagonal tensile stress (Eq. (8.3)) to the permissible diagonal tensile stress

$$\frac{0.58Q}{Lt} = f_t \quad 2.7$$

from which the allowable horizontal shear Q, based on the diagonal tensile failure criterion, is given by

$$Q = 1.7Ltf_t \quad 2.8$$

Several researchers have proposed analytical methods based on plastic analysis theory, because the equivalent strut method neglects the contribution of the steel frame and cannot fully represent the behavior of composite infilled steel frames up to their ultimate strength levels. Wood (1978) applied plastic analysis to non-integral steel frames, in which the collapse modes and loads depended on the bending strength of the steel frames and the crushing stress of the infill wall. However, an unrealistic assumption was made in his models that the whole infill wall would behave in a perfectly plastic manner. Therefore, an empirical penalty factor,  $\gamma_p$ , was needed to reduce the effective crushing stress of the infill wall and to

account for the discrepancy between the theoretical predictions and experimental results. Four different failure modes were identified in Wood's work: a composite shear mode, a shear rotation mode, a diagonal compression mode, and a corner crushing mode.

Based on the results of a nonlinear finite element analysis and experimental observations, Liauw and Kwan (1983) proposed plastic analysis models for both integral and non-integral infilled steel frames, in which the infill wall always failed through crushing in the corner regions. Furthermore, the formation of plastic hinges in the steel frames was determined based on the distribution of the compressive crushing stress in the corner regions of the infill walls. The contribution of interface friction was neglected in these models.

Based on nonlinear finite element analysis and model tests, Saneinejad and Hobbs (1995) developed an inelastic method to calculate the ultimate lateral load and cracking load of non-integral infilled steel frames. Three distinct failure modes were categorized: corner crushing mode (CC), which is crushing of infill in at least one of its loaded corners; diagonal compression mode (DC), which is crushing of infill within its central region; and shear mode (S), which is horizontal shear failure through bed joints of a masonry infill. Diagonal cracking of the infill is regarded as only a serviceability limit state and not necessarily as a sign of failure. Ductility Requirement for RC Frames against Lateral Loads

Earthquake forces the building frames to swing and hinges are formed at the beam-column connection due to the lateral movement. Rotation takes place at joints and some work is done as moment develops. Energy dissipation takes place as heat, through material crushing, and so on. Hence, the frame should possess not only enough strength, but proper detailing is essential to absorb the energy. Different codes specify special ductility requirement detailing for earthquake resistant design. Therefore, proper detailing of column reinforcement in accordance with standard code is essential to ensure ductile column behavior.

## **2.5 Ductility Requirements for RC Frames against Lateral Loads**

### **2.5.1 Indian standard code requirements**

Columns contain two types of steel reinforcement, namely: (a) long straight bars (called longitudinal bars) placed vertically along the length, and (b) closed loops of smaller diameter steel bars (called transverse ties) placed horizontally at regular intervals along its full length. Columns can sustain two types of damage, namely axial-flexural (or combined compression-bending) failure and shear failure. Shear damage is brittle and must be avoided in columns by providing transverse ties at close spacing. Closely spaced horizontal closed ties help in three ways, namely (i) they carry the horizontal shear forces induced by earthquakes, and thereby resist diagonal shear cracks, (ii) they hold together the vertical bars and prevent them from excessively bending outwards (in technical terms, this bending phenomenon is called buckling), and (iii) they contain the concrete in the column within the closed loops. The ends of the ties must be bent as  $135^\circ$  hooks (Figure 2.8-2.9). Such hook ends prevent opening of loops and consequently buckling of concrete and buckling of vertical bars. Designing a column involves selection of materials to be used (i.e. grades of concrete and steel bars), choosing shape and size of the cross-section, and calculating amount and distribution of steel reinforcement. The first two aspects are part of the overall design strategy of the whole building.

The Indian Ductile Detailing Code IS 1893-2002 requires columns to be at least 300mm wide. A column width of up to 200mm is allowed if unsupported length is less than 4m and beam length is less than 5m. Columns that are required to resist earthquake forces must be designed to prevent shear failure by a skillful selection of reinforcement.

The Indian Standard IS 1893-2002 prescribes following details for earthquake-resistant columns:

- 1) Closely spaced ties must be provided at the two ends of the column over a length not less than larger dimension of the column, one-sixth the column height or 450mm.

2) Over the distance specified above and below a beam-column junction, the vertical spacing of ties in columns should not exceed  $D/4$  for where  $D$  is the smallest dimension of the column (e.g., in a rectangular column,  $D$  is the length of the small side). This spacing need not be less than 75mm nor more than 100mm. At other locations, ties are spaced as per calculations but not more than  $D/2$ .

3) The length of tie beyond the  $135^\circ$  bends must be at least 10 times diameter of steel bar used to make the closed tie; this extension beyond the bend should not be less than 75mm.

Construction drawings with clear details of closed ties are helpful in the effective implementation at construction site. In columns where the spacing between the corner bars exceeds 300mm, the Indian Standard prescribes additional links with  $180^\circ$  hook ends for ties to be effective in holding the concrete in its place and to prevent the buckling of vertical bars. These links need to go around both vertical bars and horizontal closed ties; special care is required to implement this properly at site.

In the construction of RC buildings, due to the limitations in available length of bars and due to constraints in construction, there are numerous occasions when column bars have to be joined. A simple way of achieving this is by overlapping the two bars over at least a minimum specified length, called lap length. The lap length depends on types of reinforcement and concrete. For ordinary situations, it is about 50 times bar diameter.

Further, IS 1893-2002 prescribes that the lap length be provided only in the middle half of column and not near its top or bottom ends (Figure 2.10). Also, only half the vertical bars in the column are to be lapped at a time in any storey. Further, when laps are provided, ties must be provided along the length of the lap at a spacing not more than 150mm.



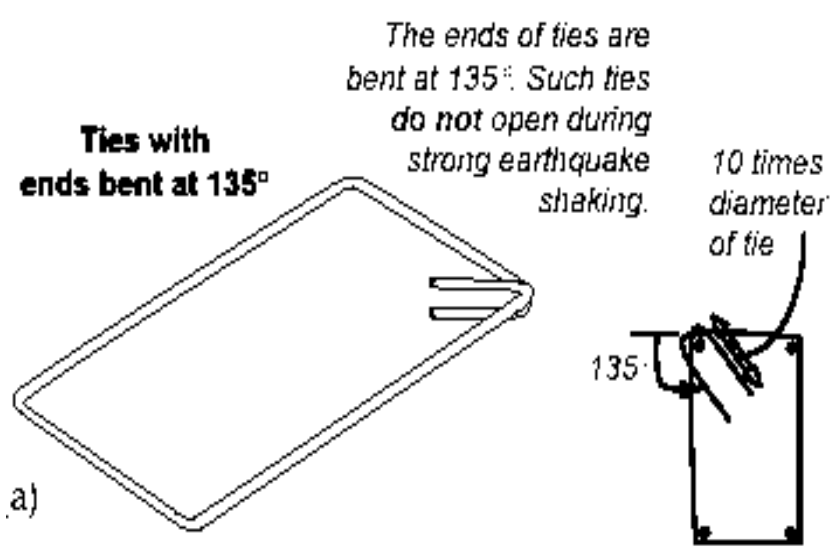


Figure 2.8 End bent of ties (Murty 2005)

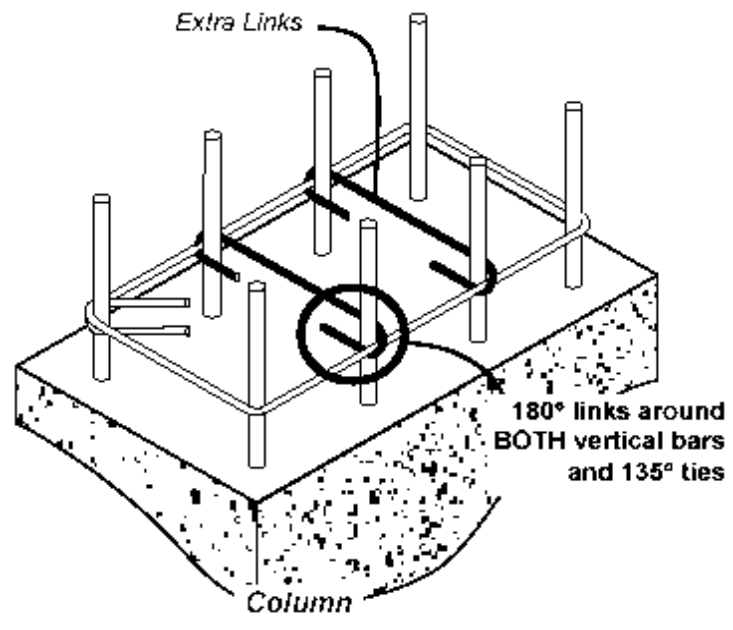


Figure 2.9 Required extra links to keep the concrete in place (Murty, 2005)

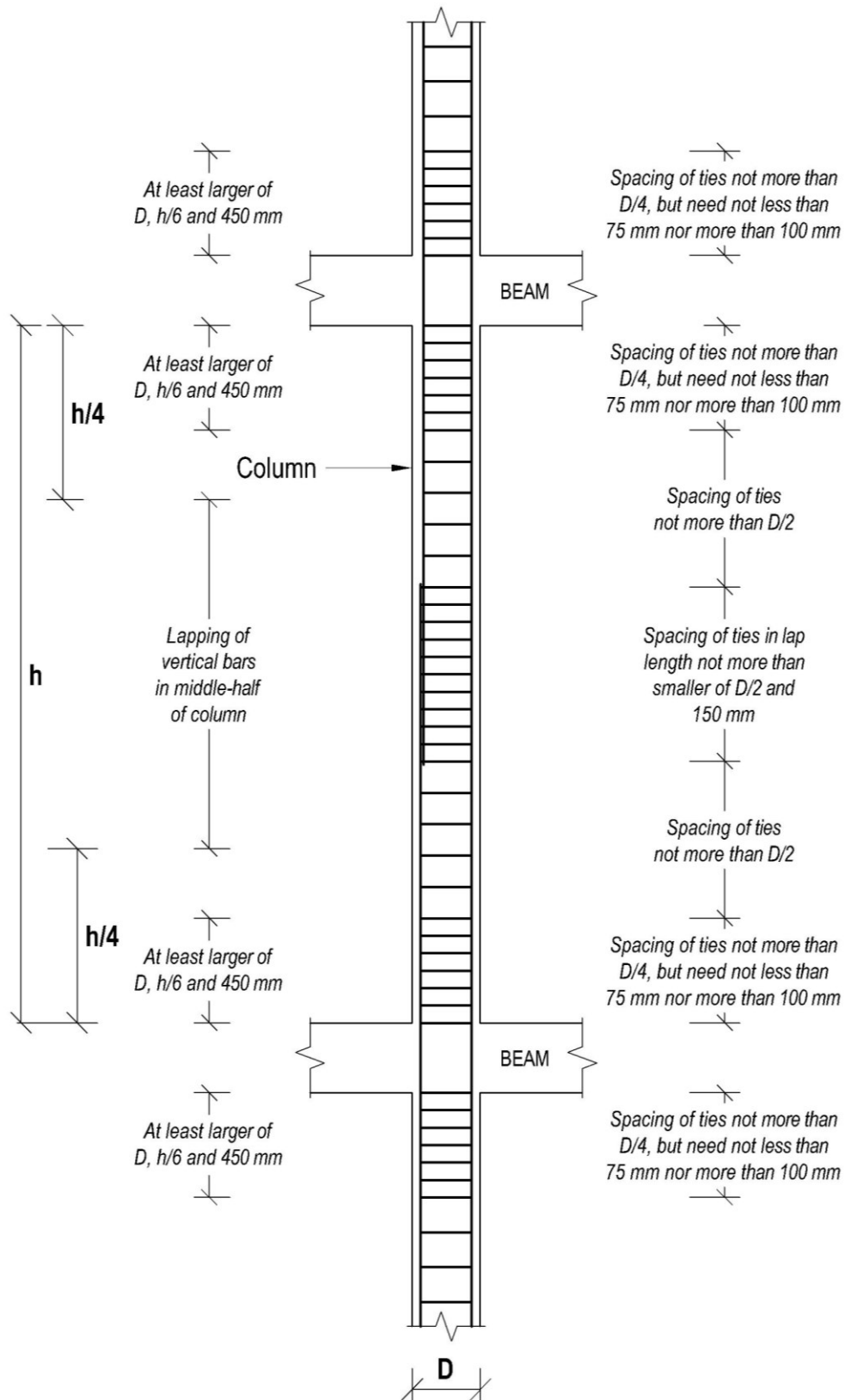


Figure 2.10 Placing vertical bars and closed ties in columns (Murty, 2005)

### **2.5.2 Requirements specified in BNBC**

Bangladesh National Building Code (BNBC, 1993, 2014) specifies special requirements for design and construction of reinforced concrete members of a structure subjected to earthquake motions. The interaction of all structural and nonstructural members shall be considered in the analysis. Compressive strength of the concrete shall be not less than  $20 \text{ N/mm}^2$ . Reinforcement used shall comply with ASTM A706, ASTM A615 and BDS 1313. Special requirements for such columns are listed below.

- 1) Maximum tie spacing shall not exceed  $s_0$  over a length  $l_0$  measured from the joint face. The spacing  $s_0$  shall not exceed (a) 8 times the diameter of the smallest longitudinal bar enclosed, (b) 24 times the diameter of the tie bar, (c) one-half of the smallest cross-sectional dimensions of the frame member, and (d) 300 mm. The length  $l_0$  shall not be less than (a) one-sixth of the clear span of the member, (b) maximum cross-sectional dimension of the member, and (c) 450 mm.
- 2) The first tie shall be located not more than  $s_0/2$  from the joint face.
- 3) Tie spacing shall not exceed  $2 \times s_0$  throughout the length of the member.

### **2.6 Existing Seismic Retrofit and Repair Techniques for Masonry and RC Frame Structures**

The existence in earthquake prone region of many older masonry and RC buildings, built before any provision for earthquake loading was required, presents one of the most serious problems facing the earthquake engineers today. This problem has generated a wide range of research directed to both the retrofit and repair of such structures. Several types of retrofitting techniques have been developed which can be categorized in:

- 1) Grouting, Sealing, Bonding with Epoxies and internal reinforcing
- 2) Surface coatings
- 3) Reinforced or post-tensioned cores
- 4) Addition of structural elements

### **2.6.1 Grouting, sealing, bonding with epoxies and internal reinforcing**

#### 1) Grouting

Grouting, Sealing, Bonding with Epoxies are useful to improve the strength, stiffness and durability of decayed concrete and masonry. These are useful when the predominant stresses are in compression. However, if the structure is subjected to tensile stresses, some type of reinforcement needs to be included. Rahman (2002) reported that cracks wider than about 1 mm in the upper surfaces of beams, slabs etc. can often be sealed by brushing in dry cement followed by light spraying with water. This treatment will seal the upper part of a crack against ingress of moisture and carbon dioxide. It will not hide the cracks completely. For cracks wider than about 2 mm it may be preferable to use a cement water grout.

#### 2) Sealing

According to ACI Committee 224, (2007), sealing involves enlarging the crack along its exposed face and filling and sealing it with a suitable material. This is the simplest and most common technique for sealing cracks and is applicable for sealing both fine pattern cracks and larger isolated defects. The operation consists of following along the crack with a concrete saw or hand or pneumatic tools. A minimum surface width of 6.35mm is desirable smaller opening are difficult to work on. The surface of the routed joint should be clean and permitted to dry before placing the sealant. The methods used for placing the sealant depend on the material to be used and follows standard techniques.

#### 3) Bonding with Epoxies and Internal Reinforcing

The injection of epoxies into cracks in concrete as a mean of for bonding the broken surface represents an application for which there is no real alternate procedure. However, unless the crack is dormant (or the cause of cracking is removed there by making the crack dormant) it will probably recur, possibly somewhere else in the structure. Also, the technique is applicable if the defects are actively leaking to the extent that they cannot be dried out or where the cracks are numerous (ACI Committee 224, 2007).

Cracks in concrete may be bonded by the injection of epoxy bonding compounds under pressure. Usual Practice is to drill in to the crack from face of the concrete at several locations, inject water or a solvent to flush out the defect, allow the surface to dry (using a hot air, if needed). The epoxy is injected through the holes about 19mm diameter and 19mm at 152mm to 152mm; centers (The smaller spacing are used for fine cracks). Injection is made through five-valve stems fastened in the drilled holes with an epoxy bonding. Compound and injection process proceeds from point to point, all valves in the circuit being capped except the one being injected the injection pressure should be maintained for several minutes to the epoxy back in to the firer parts of the cracks.

Binda et al (1999) conducted tests to investigate the influence and effectiveness of epoxy formulated resin injection for improving strength and durability of decayed brick masonry. The procedure consists on inserting steel bars in previously grooved bed mortar joints and then refilled by a repointing material. This technique is particularly suitable for brick walls having regular mortar courses. The way in which the joints have to be prepared, the type of reinforcement and repointing material greatly influence the mechanical behavior of the masonry. Five 1100×500×250 wassettes were subjected to compression loads up to 80% of their capacity, strengthened and then tested again until failure. The specimens were reinforced with 2 steel bars ( $\phi=6\text{mm}$ ) every three bed joints (10-15mm) on one side only. A hydraulic lime mortar with expansive additives and two types of synthetic resins were considered as repointing material. The experimental results showed that although the technique did not improve the material strength, significant results could be obtained in terms of deformation. The panels showed reduced cracking on the reinforced side while the cracks on the other side (without reinforcement) increased in size and depth. Manzouri et al (1996) evaluated the efficiency of injecting grout for repairing unreinforced clay-unit masonry walls as well as the effect of vertical and horizontal reinforcement. The rehabilitation procedure consisted in repairing the damaged test walls by first replacing cracked units and mortar joints with new materials and subsequently filling cracks, internal voids and collar joints with grout. Fine grout was injected to cracks with widths ranging from 0.2 to 1.5mm whereas coarse grout was used for the remaining cases. In this experimental program, four unreinforced masonry walls were constructed, tested,

repaired and re-tested. Each test wall was laid in three-wythe running bond. The test walls were subjected to repeated and reversed in-plane lateral forces until substantial damage occurred. The test showed that both strength and stiffness of the damaged walls could be restored with grout injections. Furthermore, the strength and ductility of the test walls could be enhanced with the introduction of steel reinforcement. Grout injection proved to be a reliable means for bonding the new reinforcement to the masonry.

### **2.6.2 Surface coatings**

The second of these retrofit procedures involves a thin bonded coat of reinforced cement to one or both sides of the masonry unit. These overlay procedures have been found to be very effective with the resulting composite wall developing at least the original in-plane shear strength of a damaged unit. When used with undamaged masonry the shear strength is usually doubled. The out-of-plane resistance is also substantially improved as is the composite ductility (Reinhorn et al., 1985). Surface coating procedures are also attractive from a construction standpoint requiring very little surface preparation, very little forming and little highly skilled labor. For the reasons cited, surface treatment procedures for masonry retrofit and repair are considered by many to be among the most promising of all. They have been the subject of a considerable amount of research activity.

Information on the behavior of externally coated masonry can be drawn from static and dynamic tests performed on regular reinforced masonry walls. Such tests have been conducted by Pristley et al. (1974), Meli et al. (1980) and Gulkan et al. (1979) who showed that the shear failure mechanism is more brittle than the flexural mechanism. The reinforcement contributes to the control of a flexural failure but not as much to the shear strength. The shear ductility however, is somewhat improved by the spacing of reinforcing bars (Hidalgo et al., 1979). One additional procedure for retrofit involves the use of external bracing and/or prestressed tendons or infilled walls.

Experiments on the behavior of plastered walls carrying in-plane shear forces were carried out by Schneider and Dickey (1980), Sheppard and Terceli (1980), Meli et al. (1980), Jabarov et al. (1980) applied monotonic cyclic loads and simulated

earthquakes on masonry walls coated with either reinforced plaster or fiberglass strengthened mortar. In most cases, the strength of the wall was doubled by the coating process and the ductility increased.

The Surface Coatings covers a wide variety of techniques including the direct lamination of composite overlays on the structural members using organic resins and the application of mortar layers reinforced by steel mats or meshes, steel reinforcement, or short fibers. Shotcrete is sometimes sprayed onto the unreinforced masonry wall surface.

#### 1) FRP composites

Recently, the use of fiber reinforced polymers (FRP) for rehabilitation of different types of structures has become popular. This material is used in the form of sheets and rods. Three basic component materials are commonly used of the installation of the FRP sheets: primer, putty and impregnating resin. The combination of the latter and the fibers form the FRP laminate. The use of a Carbon Fiber Cement Matrix (CFCM) Overlay System for masonry strengthening has being investigated by Kolsch (1998). This procedure combines advanced composite fibers (carbon) in the form of woven fabrics with a polymer-modified cement matrix to form structural overlays for structural components. The surfaces of the relevant structural members are cleaned in order to remove old paint and weak or weathered surfaces. The first layer of polymer-modified cement – the matrix – is applied to the surface of the member. Subsequently, a textile fabric of carbon, the reinforcement is pressed into the fresh cement. If necessary, the last two steps are repeated until the required stiffness and strength of the overlay is reached. Finally, a covering sheet of polymer-modified cement is applied. In this way a laminated composite is produced on the surface of the structural member. In this experimental program  $3 \times 3 \times 0.24\text{m}^3$  and  $2 \times 2 \times 0.24\text{m}^3$  walls with a reinforcing overlay of three layers of unidirectional carbon fabric and a polymer-modified mortar were tested out-of-plane. Load perpendicular to the wall plane was applied with a pressure bag while no vertical load other than the self-weight acted. The walls were loaded and unloaded quasi-statically in increasing load steps. The wall was able to sustain a horizontal load of 120kN for a wall mass of 3,900kg. This capacity is much larger than the required by any seismic code.

## 2) Poly-propylene Band:

Sathiparan et al. (2011) conducted shaking table tests that were carried out using non-retrofitted and retrofitted two story masonry houses by PP-band meshes. From the tests it was found that a structure retrofitted with PP-band meshes would be able to resist against strong aftershocks. Moreover, it proves that even though houses retrofitted with PP-band were cracked due to strong earthquake, it could be repaired and be expected to withstand subsequent strong shakes. From the experimental results, it was found that PP-band retrofitting technique proposed can enhance safety of both existing and new masonry buildings even in the worst-case scenario of earthquake ground motion like JMA 7 intensity. Therefore, proposed method can be one of the optimum solutions for promoting safer building construction in developing countries and can contribute earthquake disaster in the future.

## 3) Ferrocement Laminates

Among the available coating procedures, a thin ferrocement overlay has been suggested as one having considerable promise for use with unreinforced masonry walls that need enhanced in-plane and out-of-plane strength and ductility. Research and development work on ferrocement has progressed at a tremendous pace during recent years and a variety of structures using innovative design and construction techniques have been built worldwide. As a result, a large volume of technical information is now available on various aspects of ferrocement design, construction, maintenance and repair. Increasing popularity and growing public acceptance have made it necessary to formulate design and working guidelines by collecting the available information. Efforts have also been made in recent years to improve the performance of reinforced concrete elements by applying ferrocement overlay. The concept has been intuitively applied for repair and strengthening of distressed elements.

Reinhorn and Prawel (1985) carried out an experimental program to study the effect of a thin ferrocement overlay with a steel square embedded mesh. Two uncoated and five coated specimens (648mm square and 200mm width) having a different spacing of the reinforcing wires were tested in diagonal compression. The wire spacing in the mesh varied from 3.2mm to 50.8mm and the coating thickness varied



to maintain a constant reinforcement volume ratio. The meshes were kept in place by tie wires passing through the masonry. The mortar was then passed between the meshes aided by a high-speed surface vibrator. The bare masonry specimens showed a distinctly nonlinear load deformation curve over almost the entire load range while the coated specimens maintained an almost proportional pattern up to the yielding. The coated wall strength was more than twice the corresponding to the control walls. The coated specimens with more closely spaced reinforcement developed cracks within the same wide band that were difficult to identify. After substantial cracking of the outside surface, separation between the masonry and ferrocement developed leading to a complete dislocation of the ferrocement plates. At this point the separated plates failed in compression by a local crushing at the loaded corners. Ultimately, the wire mesh was unable to develop its maximum strength. The effect of the bolt spacing was studied to determine the optimum arrangement of connectors. In another set of experiments, Prawel et al (1988) found the optimum spacing for a configuration of testing walls and used it for evaluating the effectiveness of ferrocement strengthening. The test results showed that, if the ferrocement can fully develop its strength, the coated specimens could develop three times the strength of the uncoated walls.

Alcocer et al (1996) reported on the jacketing of masonry walls with a concrete mortar cover reinforced with steel welded wire meshes. In this experimental program four full-scale confined masonry specimens were rehabilitated and tested under alternated cyclic lateral loads. The rehabilitation process started by cleaning the walls and removing and replacing cracked and crushed concrete at the ends of interior tie-columns. Inclined masonry cracks were further cleaned with water jet to remove the dust and crushed particles. All cracks were filled with cement mortar and brick pieces. A welded wire mesh ( $150 \times 150 \text{mm}^2$ ,  $\phi=3.43 \text{mm}$  wire) was placed and covered with 25-mm thick cement mortar. The meshes were anchored to the wall by 50-mm long nails for wood driven by hand next to the wire intersection. Metal bottle caps were left between the wall surface and the mesh to ease the placement of mortar behind the mesh and to improve the mortar-masonry bond. Prior to placement of mortar, wall surfaces were saturated. The mortar was placed manually using masonry trowels. The test showed a more uniform inclined crack pattern and a remarkably higher strength in all specimens rehabilitated by jacketing

as compared to the control masonry specimens. The energy dissipated by the jacketed specimens was also higher. The contribution of welded steel wire meshes to strength was depended on the amount of horizontal reinforcement, deformation applied, and type of anchor as well as on mortar quality.

Zegarra et al (1997) investigated the reinforcement of adobe houses with galvanized welded wire steel meshes and cement mortar overlay. Two house modules with and without strengthening were tested on a shaking table. The wire diameter was 1.0mm and the mesh pitch, 20mm. The mesh was attached to the house walls with 64mm long nails placed at 250mm pitch. Additionally, holes were drilled through the walls at 500mm pitch and the meshes on both sides of the wall were connected through wires. The wall holes were later filled with cement mortar. In this method, the steel mesh is not placed on all the house wall surfaces but only at the intersections between walls and at the walls with long unsupported length. After the mesh is set, a 20mm thick cement mortar is laid over the walls. The results of the shaking table tests showed that the reinforced house performed well and could withstand the imposed excitation whereas the unreinforced specimen failed. This technique was applied in some houses in Peru. During the last 2001 Atico Earthquake, one of the houses that belonged to this program was located in the region subjected to strong shaking. The house showed very little damage, which was within the limits of repairing.

Anwar *et al.* (1991) investigated the rehabilitation technique for reinforced concrete structural beam elements using ferrocement. The technique involved strengthening of reinforced concrete beams by application of hexagonal chicken wire mesh and skeletal steel combined with ordinary plaster. The test result is in good compliance with the original design capacity of the beams. From the test result obtained, a design chart has been developed to determine the parameters for rehabilitation of the beam elements.

Lub and Wanroji (1988) reported that strengthening of existing beams in reinforced concrete building structures by means of shotcrete ferrocement. It was found that the mesh is fully effective and a monolithic condition of shotcrete layer and original concrete beam attained. The wire mesh was found to act as excellent shear reinforcement.

Rosenthal and Bljoger (1985) studied the flexural behavior of ferrocement reinforced concrete composite beams in the serviceability and ultimate limit states. The flexural behavior of four rectangular composite beams made of low strength ferrocement, was compared with four reference beams in the serviceability and ultimate limit states. In doing so, special deformational and crack formation properties of the encasing elements (reinforced with wire meshes) were exploited, resulting in hair cracks which appear in the beams under service load, rather than regular width cracks. Cracking moments of the composite beams were 11% and 13% higher than those of reference beams due to additional flexural tensile strength contributed by the elements. Crack in the composite beams have only reached, at failure, a width of 0.4 mm to 0.5 mm, as compared to twice as much in the reference beams. Composite action between the skin and core components was fully obtained until crack appearance. Beyond that stage and up to failure, a partial separation might have happened, according to somewhat different crack patterns of the reference and composite beams.

Kaushik and Dubey (1994) studied the performance of RC ferrocement composite beams through experimental investigation on RC beam cast on ferrocement and distressed beams rehabilitated by ferrocement jacketing. They reported that the increase in ultimate strength compared to RC beams was 44% for composite beams and 39% for rehabilitated beams. This showed that composite beams and rehabilitated beams are capable of performing equally well. Moreover, the ultimate strength and stiffness of RC beam can be significantly increased by strengthening with precast ferrocement plates in the shear failure zone. Therefore, ferrocement can satisfactorily be used as the precast part of the composite in which RC beam is cast.

An experimental investigation was carried by Kadir *et al.* (1997) to study the ultimate load, flexural behavior and mode of failure at collapse of reinforced concrete beams using ferrocement permanent formwork (composite beams). The linkage between the two materials was achieved by placing shear connectors along the length of the beam. Test result showed that the reinforced concrete beams with ferrocement permanent formwork failed by flexure. The composite beam with shear connectors carried about 12% higher load and 10% reserved flexural strength and showed lower deflection when subjected to reinforced concrete beam without shear

connectors. The ferrocement formwork with and without shear connectors contributed about 21%-75% and 16%-50% to the flexural strength respectively.

Afsaruddin and Hoque (1998) performed an experimental research work on reinforced concrete beams with ferrocement overlay in the concrete laboratory, BUET. They investigated the possibility of using ferrocement as a permanent formwork for reinforced concrete beams. A total of twelve beams were constructed and tested in the investigation. Eight ferrocement beam formworks were made having different sizes. All of them were filled with reinforced concrete. Four reinforced concrete beams and eight number of reinforced concrete coated with ferrocement formwork containing single layer wire mesh were cast to compare the behavior of ferrocement formwork reinforced concrete beam with the normal concrete beam. The study demonstrates that the use of ferrocement as a permanent formwork increase the cracking load and ultimate load of the composite system compared to normal RC beams. The number of cracks and width of cracks have been found to have reduced considerably due to the provision of ferrocement layer used as formwork. From the study it appears that permanent precast ferrocement formwork could become a reliable alternative to wooden formwork in the construction of reinforced concrete beams.

The ability of ferrocement to fit snugly into curved surface make it an ideal material for the rehabilitation of dome and shells. An example of such rehabilitation is the restoration of domes in the Widmill theatre in UK (1988) (Rahman, 2002).

Sharma *et al.* (1984) rehabilitated an overhead circular water tank of 210000-litre capacity using ferrocement. The superior crack resistance properties made it suitable for water retaining satisfactorily. The tank was put out of service due to heavy leakage soon after its construction. The inspection of tank revealed the presence of a large cracked and honeycombed area in the center of tank wall which was all along the wall periphery. At some point only, coarse aggregate was deposited with no fine aggregate making it the major source of water leakage through the voids in such an area. After repairing by using ferrocement no leakage was observed, and the tank seemed to be performing with full efficiency. The rehabilitated tank is currently under service.

Reinhorn and Prawel (1988) successfully used a thin ferrocement coating on the sides of the unreinforced masonry wall that need enhanced in plane and out of plane strength and ductility. Ferrocement coating was mounted on the two sides of the wall with tension ties provided through the masonry. The result of the test showed the suitability of ferrocement as a retrofit (strengthening) material with a doubling of the wall.

Singh *et al.* (1976) suggest a simple procedure for the strengthening of brick masonry columns using ferrocement. Brick masonry column in old structure and are usually used for low-rise structures. Although the performance of masonry columns under axial loads may be satisfactory, they possess a limited moment carrying capacity. Improving a moment carrying capacity become vital if structure is subjected to modifications resulting in eccentric loads to be transferred to the columns. Ferrocement encasement of masonry column can considerably increase its capacity to resist axial loads and moments. Applying the ferrocement encasement, (Singh *et al.* 1988) report the failure loads to be double that of uncased columns. Failure is due to failure in casing under combined bending and tension under lateral loads.

Moreover, Amanat et al. (2007) revealed that lateral capacities of damaged brick infilled RC frames can be further enhanced by strengthening them with ferrocement (FC).

For many repair and renovation programs of civil engineering structures, Chowdhury and Robles-Austriaco (1986) cited the suitability of ferrocement because of

- a) Better cracking behavior.
- b) Capacity of improving some of the mechanical properties of the treated structures.
- c) Further modification or repair of ferrocement treatment is not difficult.
- d) Imposition of little additional dead load requiring no adjustment of the supporting structures.
- e) Ability to withstand thermal changes very efficiently.

- f) Ability of achieving waterproofing property without providing any surface treatment.
- g) Readily available constituent materials.
- h) No need for special equipment.
- i) Ability to be used in repair program with no distortion or down grading of architectural concept of the structures.
- j) Flexibility of further modification.

## **2.7 An Overview for Ferrocement as A Repair or Retrofit Material**

To study the effect of ferrocement overlay on reinforced concrete elements, first it is necessary to understand the behaviour of ferrocement under different conditions. In this regard, it is necessary to identify the parameters affecting the properties of ferrocement and review relevant literature in this field. This chapter presents a brief literature review on the properties of ferrocement and review relevant literature in this field. Experimental investigations carried out by several researchers on the behaviour of a reinforced concrete beam with ferrocement overlay are also included.

### **2.7.1 Constituents of ferrocement**

The constituent materials of ferrocement are cement, sand, water and reinforcing mesh.

#### **1) Cement**

The cement is to be an ordinary Portland cement of type 1 and shall be conforming to ASTM standard.

#### **2) Sand**

Sand should be obtained from a reliable source and should comply with ASTM C33 for aggregates. It should be clean, hard, strong, and free of organic impurities and deleterious substances. The fineness of sand should be such that 100% of it passes through standard sieve no. 4(2.36mm)

#### **3) Water**

Water used in the mixing should be free from any organic and harmful solution, which leads to be the deterioration of the properties of mortar. In any cases saline

water should not be used. Any water with a pH (degree of acidity) of 6.0 to 8.0 that does not taste saline is suitable for use.

#### 4) Reinforcing Mesh

In 1993 ACI Committee 549 reported that one of the essential components of ferrocement is wire mesh. Wire mesh generally consists of thin wires either woven or welded in to mesh. Different types of wire mesh are available everywhere.

Common wire meshes have hexagonal or square openings. Meshes with hexagonal openings are sometimes referred to as chicken wire mesh or aviary mesh. They are not structurally as efficient as meshes with square openings because the wires are not always oriented in the directions of the principal (maximum) stresses. However, they are very flexible and can be used in doubly curved elements.

Meshes with square openings are available in welded or woven form. Welded wire mesh is made of straight wires in both the longitudinal and transverse direction. Thus, welded mesh thickness is equal to two wire diameters. Woven mesh is made of longitudinal wires woven around straight transverse wires.

Depending on the tightness of the weave, woven mesh thickness may be up to three wire diameters. Welded wire meshes have a higher modulus and hence higher stiffness than woven meshes; they lead to smaller crack width in the initial portion of the load- deformation curve. Woven wire meshes are more flexible and easier to work with than welded meshes. Again, welding anneals the wire and reduces its tensile strength, (ACI Committee 549, 1993).

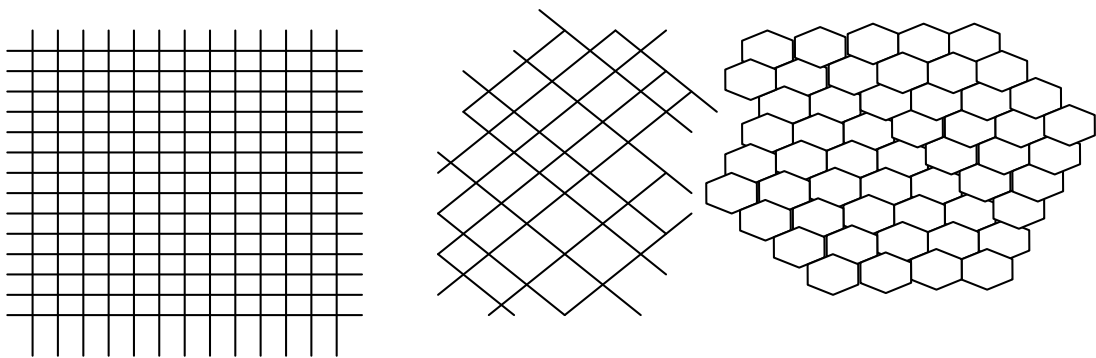


Fig.2.11 Different types of wire mesh used in ferrocement (ACI Committee 549, 1993)

## 2.7.2 Parameters used for characterizing the reinforcement in ferrocement

The recognition of parameters defining the subdivision and distribution of the reinforcement is fundamental in understanding many of the properties of ferrocement. Three parameters, commonly used in characterizing the reinforcement in ferrocement applications are as follows:

- 1) Volume fraction
- 2) Specific surface of reinforcement and
- 3) Effective modulus of the reinforcement
- 4) Effective Area of Reinforcement

### 1) Volume fraction of reinforcement

Volume fraction ( $V_f$ ) is the total volume of reinforcement divided by the volume of composite (reinforcement and matrix). For a composite reinforced with meshes with square opening,  $V_f$  is equally divided into  $V_{fl}$  and  $V_{ft}$  for the longitudinal and transverse directions, respectively. For other types of reinforcement  $V_{fl}$  and  $V_{ft}$  may be unequal. For ferrocement reinforced with square or rectangular mesh, the volume fraction of mesh reinforcement can be calculated from the following relation.

$$V_f = \frac{N\pi d_b^2}{4h} \left( \frac{1}{D_l} + \frac{1}{D_t} \right) \quad 2.5$$

Where,  $N$  = number of layer of mesh reinforcement

$d_b$  = diameter of wire mesh

$h$  = thickness of ferrocement

$D_l$  = center to center spacing of wires aligned longitudinally in reinforcing mesh

$D_t$  = center to center spacing of wires aligned transversely in reinforcing mesh

### 2) Specific surface of reinforcement

Specific surface,  $S_r$  is the total bonded area of reinforcement (interface area or area of the steel that comes in contact with the mortar) divided by the volume of composite.  $S_r$  is not to be confused with the surface area of reinforcement divided by



the volume of reinforcement. For a composite using square meshes,  $S_r$  is divided equally into  $S_{rl}$  and  $S_{rt}$  in the longitudinal and transverse directions, respectively.

For a ferrocement plate of width  $b$  and depth  $h$ , the specific surface of reinforcement can be computed from (Rahman, 2002).

$$S_r = \frac{\sum o}{bh} \quad 2.6$$

In which  $\sum o$  is the total surface area of bonded reinforcement per unit length.

For square and rectangular mesh, the expression for  $S_r$  will become

$$S_r = \frac{\pi d_b (D_l + D_t)}{D_l D_t h} \quad 2.7$$

The relation between  $S_r$  and  $V_f$  when square grid wire meshes are used is

$$S_r = \frac{4V_f}{d_b} \quad 2.8$$

Where,  $d_b$  is the diameter of the wire. For other types of wire meshes,  $S_{rl}$  and  $S_{rt}$  may be unequal (Rahman, 2002).

### 3) Effective modulus of reinforcement

Rahman (2002) describes that although most ferrocement properties have similar definition as those of reinforced concrete, one property is defined differently. It is the effective modulus of the reinforcing system  $E_r$ . This is because the elastic modulus of the mesh (steel or other) is not necessary the same as the elastic modulus of the filament (wire or other) from which it is made. In a woven steel mesh, weaving imparts an undulating profile to the wires. Hence, the woven mesh behaves as if it has a lower elastic modulus than that of the steel wires from which it is made.

### 4) Effective area of reinforcement

The area of reinforcement per layer of mesh considered effective to resist tensile stresses in cracked ferrocement section can be determined as follows (Rahman, 2002)

$$A_{si} = \eta V_{fi} A_c \quad 2.9$$

Where,  $A_{si}$  = effective area of reinforcement for mesh layer  $i$

$\eta$  = global efficiency factor of mesh reinforcement in the loading direction considered.

$V_{fi}$  = volume fraction of reinforcement for mesh layer  $i$

$A_c$  = gross cross-sectional area of mortar (concrete) section.

The global efficiency factor when multiplied by the volume fraction of reinforcement, gives the equivalent volume fraction (or equivalent reinforcement ratio) in the loading direction considered. In effect, it leads to an equivalent (effective) area of the reinforcement per layer of mesh in that loading direction. For square mesh,  $\eta$  is equal to 0.5 when loading is applied in one of the principal directions. For a reinforcing bar loaded along its axis ( $\eta = 1$ ), (Rahman, 2002).

### 2.7.3 Properties of ferrocement

Ferrocement, considered to be an extension of reinforced concrete technology, has relatively better mechanical properties and durability than ordinary reinforced concrete. Within certain loading limits, it behaves like as a homogeneous elastic material and these limits are wider than for normal concrete. The uniform distribution and better crack arrest mechanism arrests propagation of cracks and results in high tensile strength of materials. Many of the properties unique to ferrocement derive from the relatively large amount of two-way reinforcement made up of relatively small elements with much higher surface area than conventional reinforcement. In the words of Nervi, who first used the term ferrocement, its most notable characteristic is "greater elasticity and resistance to the cement mortar by the extreme subdivision and distribution of reinforcement".

#### 1) The strength property of ferrocement

The strength of ferrocement, as in ordinary concrete, is commonly considered as the most valuable property, although in many practical cases other characteristics, such as durability and permeability may in fact be more important. Nevertheless, strength

always gives an overall picture of the quality of ferrocement, as strength is directly related to the properties of the hardness of cement paste and reinforcement.

## 2) Tensile strength of ferrocement

The basis of the structural design is the knowledge of the material properties. The tensile characteristics of ferrocement have not yet been fully defined and standardized. In tension the load is essentially independent of specimen thickness because the matrix cracks well before failure and does not contribute directly to composite strength. Naaman and Shah (1971) have studied the influence of types, sizes and volumes of wire meshes on elastic cracking and ultimate behaviour of ferrocement in uniaxial tension. They observed that the ultimate tensile strength of ferrocement is the same as that of mesh alone while its modulus of elasticity can be predicted from those of mortar and mesh, (Naaman and Shah, 1971, Johnston and Mattar, 1976 and Pama *et al.* 1974). The specific surface of the reinforcement strongly influenced the cracking behaviour of ferrocement. In general, the optimal choice of reinforcement for ferrocement strength in tension depends on whether the loading is essentially uniaxial or significantly biaxial. Expanded metal in its normal orientation is more suitable than other reinforcing meshes for uniaxial loading because a higher proportion of the total steel is effective in the direction of applied stresses, (Johnston and Mattar, 1976). For biaxial loading, square mesh is more effective because the steel is equally distributed in the two perpendicular directions, although the weakness in the 45-degree direction may govern in this case.

## 3) Compressive strength of ferrocement

In this mode, unlike tension, the matrix contributes directly to ferrocement strength in proportion to its cross-sectional area. Compressive strength of ferrocement (regardless of the amount of mesh reinforcement) seems to be much the same as that of mortar alone. The experimental results (Pama *et al.* 1974) showed that under compression the ultimate strength is lower than that of equivalent pure mortar. The compressive strength at ultimate condition is assumed to be  $0.85 f'_c$  where  $f'_c$  is the ultimate compression strength of the mortar. An investigation in to the behaviour of ferrocement specimen in direct compression has been discussed by Rao (1969). Conclusions were drawn with respect to the effect of percentage of reinforcement

and the size of reinforcement on the behaviour of ferrocement. Provision of reinforcement in excess of about 2 to 2.5% is uneconomical in ferrocement as the proportional increase in strength is not achieved (ACI committee 549). Smaller diameter wire mesh would be preferable to use as this gives higher elasticity and higher ultimate compressive strength for the same percentage of reinforcement, all other factors remaining essentially the same. When mesh reinforcement is arranged parallel to the applied in one plane only (as opposite to closed peripheral arrangement), no improvement in strength is observed, (Pama *et al.* 1974). The only forms of reinforcement likely to result in significant strength gains in compression are square mesh reinforcement (ACI Committee Report 549) fabricated in closed box or cylindrical arrangements which results in the matrix, thus forcing it to adopt the triaxial stress condition associate with higher strength.

#### 4) First cracking strength of ferrocement

The term first cracking strength or its equivalent appears frequently in literature on the behaviour of ferrocement under tension and flexure, but its use without qualification is unfortunate because it can be defined in various ways and therefore can mean different things to different people. In a comprehensive discussion of this problem by Walkus (1975), it is noted that micro cracks are inherent in the mortar matrix even before it is loaded, and that as the micro cracks widen, propagate and progressively join together under load, they are detected by some means, visual or otherwise, and termed "first crack". However, in the various Polish and Russian studies, by Walkus (1975) "first cracking is defined by a crack width ranging from  $2 \times 10^{-4}$  in. to a value visible to the naked eye,  $1.2 - 3.3 \times 10^{-3}$  in. (0.03 - 0.1 mm). In other studies, first cracking is defined as the first deviation from linearity of the load elongation function in tension (900-1500 micro strain) or the corresponding deviation of the load-deflection curve in flexure, also as a crack width under flexural loading of 0.003 in (0.075 mm), as the point at which the matrix at the tension face of flexural specimen reaches a strain equal to the cracking strain of the unreinforced matrix, or simply as the first visible crack (Johnston *et al.* 1976). Therefore, it is necessary to perform experimental investigations for accurate prediction of the first cracking stress of ferrocement in direct tension and in flexure.

Research studies have showed that crack width in reinforced concrete structure can be reduced by increasing the bond between the reinforcement and the concrete, by increasing the distribution of the reinforcement and by reducing the thickness of the cover. All these factors are favorable for ferrocement. Crack width is nearly zero at the interface between the steel and the mortar and increases from the interface towards the surface. Therefore, the smaller the distance between the interface and the surface of the structure, the smaller will be the crack width. Specific surface and volume of the reinforcement and their influences are studied by several researchers and empirical relationships between these parameters and the first cracking stress is proposed.

#### 5) Deformation characteristics of ferrocement

Following the consideration given to ultimate and cracking strength, it is appropriate to examine the overall loading deformation behavior of ferrocement under various form of loading, in particular its modulus of elasticity, which historically has been identified as one of its major attributes.

#### 6) Load deformation behavior in tension

For square mesh reinforcements, the load-elongation behavior of reinforcement has been characterized in three stages, (Naaman and Shah, 1971, Pama, *et al.* 1974). In the initial stages the matrix and reinforcement act as a continuum having a composite elastic modulus about equal to that predicted from the volumetric law of mixtures of the longitudinal reinforcement and the matrix, (Naaman and Shah, 1971). The second stage associated with a fully cracked matrix, is also linear. Its modulus is somewhat greater than the product of the volume fraction and the modulus of the longitudinal reinforcement, (Naaman and Shah, 1971 and Pama, *et al.* 1974) thus supporting the view that the, mortar and the lateral reinforcement continue to play an active role after first cracking, either individually or in combination. In the third stage, the matrix ceases to play role. Failure corresponds to the yielding of the reinforcement.

## 7) Load deformation behavior in compression

When the reinforcement is in one plane only, it has a minimal effect on the load deformation relationship, and the associated elastic modulus remains virtually the same as that for mortar matrix, (Pama, *et al.* 1974). When present in closed peripheral form, the load-deformation relationship is curvilinear with the initial tangent modulus increasing gradually with the amount of reinforcement. The initial elastic modulus can be predicted quite accurately and conservatively on the basis of the volumetric influence of the two material components acting together. The values of the elastic modulus are slightly higher for specimens reinforced with welded mesh than for their equivalents with expanded metal, (Johnston and Mattar, 1976). The experimental results obtained by various investigators, (Lee and Pama, 1972 and Rao, 1969) show that the modulus of elasticity in direct compression increases proportionately with the increase in steel content.

Studies on mechanical properties of ferrocement have been made since the last decade but studies of formulation of these properties based on fundamental material properties has begun only recently. Some of its mechanical properties have not been sufficiently investigated yet and not enough technical information are available to suggest acceptable formula for design. In some other cases enough research information are available that can be used as assumption to set up a tentative design approach.

### **2.7.4 General repair procedure with ferrocement for rc frames with infill**

Rehabilitation or repair of RC frames with infill structure by application of ferrocement layers will consist of choosing proper materials, preparation of affected surface, providing bonding medium and application of ferrocement. The general procedures are detailed below-

#### 1) Preparation of surface

Rahman (2002) reported that the execution of the repair works the most essential requirement is to remove all deteriorated or damaged concrete from the structures. The affected area should be thoroughly scrubbed and cleaned from all grease, dirt and grit, roughened by chiseling or wire brush, washed with water and air blown to

remove any loose materials. The preparation for the repair of the structural elements showing spalling of concrete, all unsound damaged, fouled, porous or otherwise undesirable concrete should be removed, where.

It is not deemed necessary encase the bars fully, more than half the circumference of the bars shall be exposed. But the corner bars should be fully exposed. In case of exposing the bars of the beams and columns of any structure for the repair works temporary propping should always be provided beforehand. For that the propping system should be designed accordingly.

#### 2) Cleaning the surface

The surface of the existing concrete, which is to be bonded to the new work, should be cleaned and moistened just prior to the placement of ferrocement.

Following a preliminary rinsing, cleaning by use of some blasting in preference to wire brushing should be made. The cleaning operation should be performed just prior to placing the fibrocement intruder to avoid fouling of the surface by windblown dust or debris.

#### 3) Moistening the surface

After clearing the surface should be saturated with water and then allowed to approach dryness just before placing the ferrocement. The surfaces should keep moist for several hours to assure saturation.

#### 4) Bonding layer

To ensure sufficient bonding layer should be provided. It consists of cement slurry with 0.5 parts and 1 part by weight of cement by weight of water. Cement slurry should be applied on exposed surfaces and the cement sand mortar in the ratio of 1:2 by volume should be trowel led into the groves and surfaces, so that a flat rough surface is obtained. This bonding level should be thin film usually 4 – 6 mm thick.

### **2.7.5 Rehabilitation of distress RC frame**

Rahman (2002) reported for the spalled concrete over the column surfaces, partly or totally or around the cross section a procedure similar to the state above should be followed. The procedure for placing the fibrocement is stated below:

Step -1: The exposed sides of the main reinforcement and ties towards the core section should be filled micro concrete to rebuild column section up to the ties.

Step -2: The first wire mesh should be laid all around the column section. After fixing the wire mesh with galvanized wires to the nails the wire mesh should be covered with 6-8 mm thick cement sand mortar of proportion 1:2.5 by volume.

Step -3: After about 12 hours of mortar application as in step 2, the surface should be roughened the second layer of wire mesh should be laid and covered with 6-8 mm thick mortar as in step 2.

Step -4: After finishing the surface to the desired level curing should be done by covering the rehabilitated areas with hessian and keeping it constantly wet for about 14 days.

### **2.7.6 Rehabilitation of distress RC frame infill**

Step -1: The plaster of the exposed wall is to be removed. The existing surface should be cleaned and moistened.

Step -2: A single layer wire mesh should be laid all around the infill. After fixing the wire mesh with galvanized wire to the nails. The wire mesh should be covered with 19 mm thick cement sand mortar of proportion 1:2.5 by volume.

Step -3: After finishing the surface to the desired level curing should be done by covering the rehabilitated areas with hessian and keeping it constantly wet for about 14 days.

## **2.8 Remarks**

All the discussed previous experimental and analytical studies contributed to development and verification of the mathematical models as well as retrofitting



techniques for infilled RC frames. However, most of the researches corresponded to stone masonry, RC blocks and RC panels. Enough work has not been done on solid clay brick infills and the constitutive laws regarding constituent material for modeling of local MIRC buildings in Bangladesh. There is a scope for study both in experimental and analytical parts to develop models incorporating contribution of infill wall in RC infilled frames and conferring structural engineers the assurance to exploit them confidently in structural design and analysis. Moreover, the properties of ferrocement discussed in this chapter were utilized in the process of repairing the distressed reinforced concrete infilled frame by using ferrocement laminates. This methodology provides an alternative in repairing or retrofitting of structural elements using ferrocement.

### **3.1 Introduction**

Present experimental research is focused on the comparative study on in-plane cyclic performance of bare RC frames, brick infilled RC frames and RC frame with brick infilled isolated from surrounding frames. In addition, the effectiveness of Ferrocement (FC) laminates as a repair or retrofit measure for the aforesaid model frames were also investigated under in-plane cyclic loads. For each test initial cracking load, failure load, crack patterns and lateral displacements were observed.

### **3.2 Experimental Setup**

The corresponding laboratory investigation involved use of an in-plane cyclic loading test setup comprised of strong base, reaction frames convenient for reverse loading, model specimen frames, anchor bolts for fixing the specimens, displacement transducers (dial gauges) for measuring lateral deflection of the specimens etc. (Figure 3.1). The setup is existing in the Civil Engineering Laboratory, Bangladesh University of Engineering and Technology (BUET) (Figure 3.2).

Cyclic load was applied by means of hydraulic jacks (capacity 600 kN) mounted on the reaction frames. At the time of applying cyclic load the lateral displacements of the test model specimens were noted by means of three displacement transducers fitted at the selected locations of the specimen frames.

#### **3.2.1 Strong base**

The strong base is the sub-structure of the test setup. Anchor bolts are fitted into the strong base. The model specimen frames were attached to the strong base by means of four pairs of anchor bolts. Anchor bolt sockets are placed all along the strong beam to ensure that infill frame of different spans can be tested (Figure 3.3).

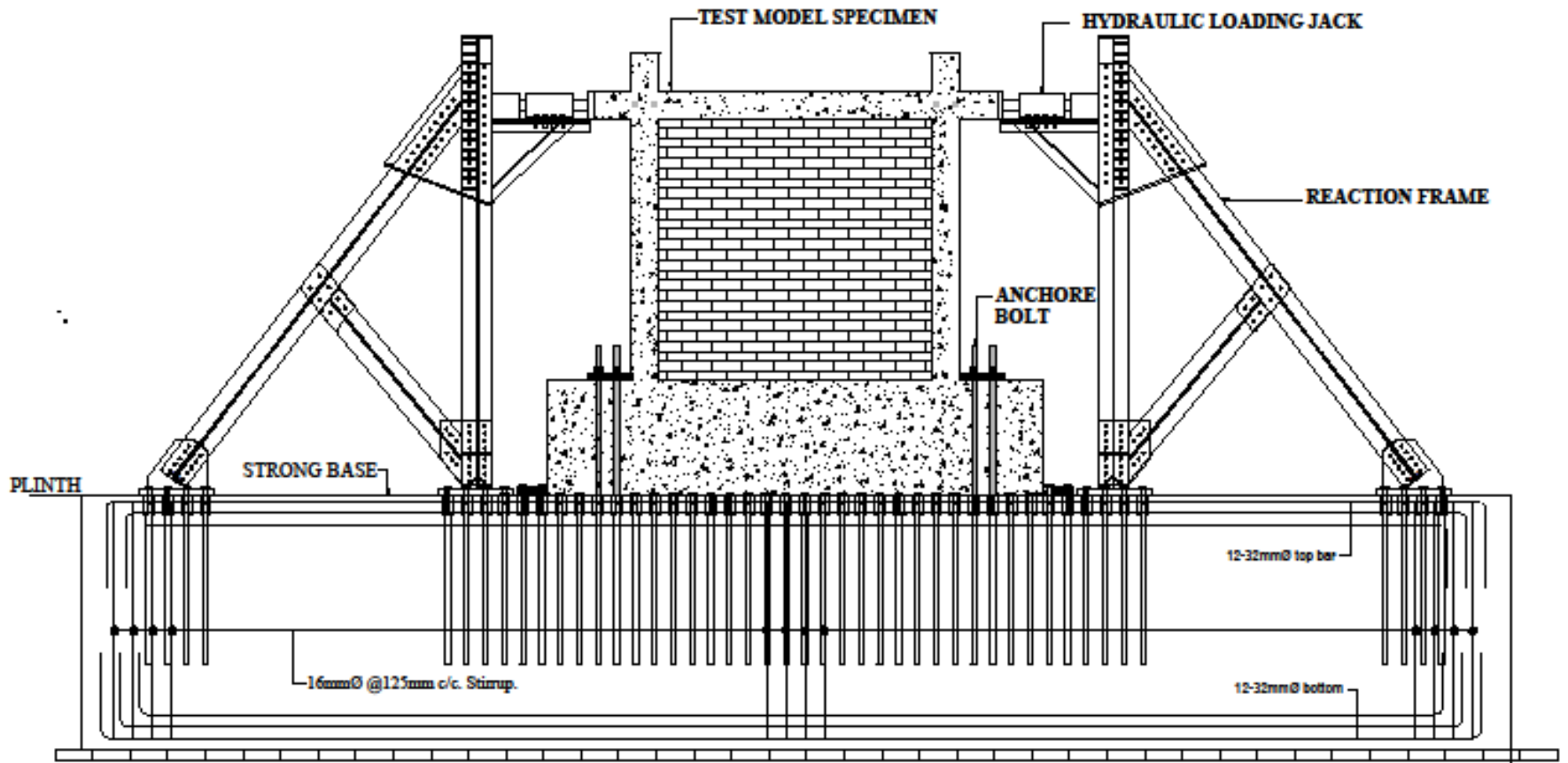


Figure 3.1. Outline of in-plane cyclic loading test setup



Figure 3.2 In-plane cyclic loading test setup in BUET, Bangladesh

### **3.2.2 Anchor bolts**

There were four pairs of anchor bolts for fixing of the specimen frames. Each pair of anchor bolts were pre-tensioned with 178 kN tension forces by a hydraulic jack for fixing of the test models with the strong base producing the same amount of compression forces along the bases of specimen frames (Figure 3.3-3.4).

### **3.2.3 Reaction frames and hydraulic jacks**

The super-structure of the test setup is the two reaction frames which are steel truss structures bolted with the strong base. Cyclic loads were applied to the specimen frames by means of two loading jacks (Hydraulic) of capacity 600 kN mounted on the two opposite reaction frames and operating the jacks alternately (Figure 3.5-3.7).

### **3.2.4 Tripod stands for mounting sensors**

To record the lateral displacement of the test specimen frames displacement transducers (dial gauge) were mounted at appropriate position by means of two independent tripod stand support systems (Figure 3.8).

### **3.2.5 Displacement transducers (dial gauges)**

Three displacement transducers (DT) were used to measure the lateral displacement of the model specimen frames. Two displacement transducers were positioned at top-north and top-south of specimen frames to measure the corresponding deflections while another DT was fitted to monitor in case of base movement of the specimens (Figure 3.9-3.11).



Figure 3.3 Pre-tensioning of anchor bolts using hydraulic jack to ensure the fixity of the specimen along the strong base

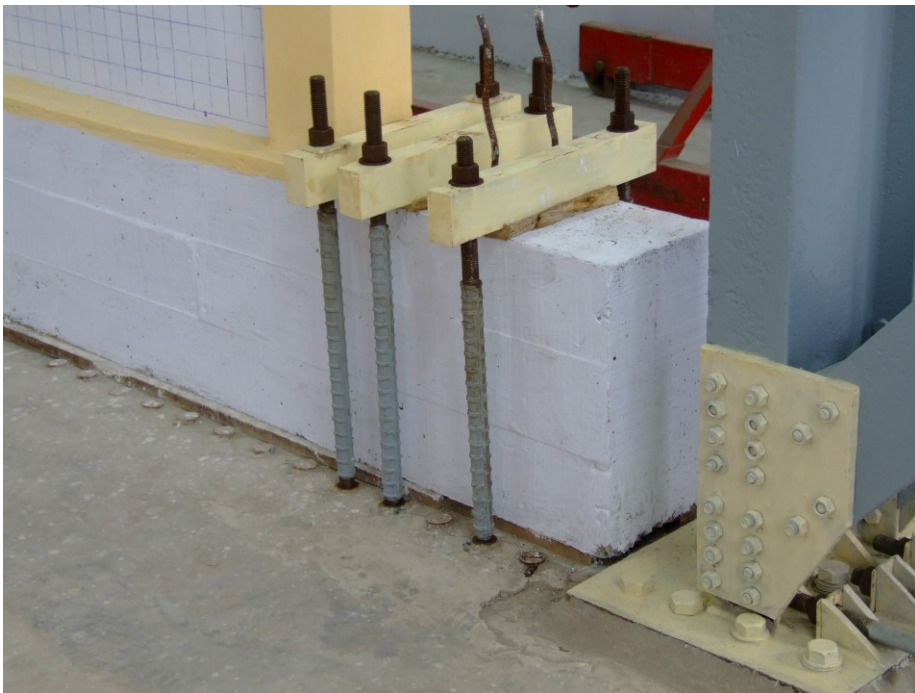


Figure 3.4 Anchor bolts ensuring the fixity of the specimen



Figure 3.5 Reaction frame and the position of hydraulic jack



Figure 3.6 Dial gauge and pumper attached with the hydraulic jack



(a)



(b)

Figure 3.7(a) and (b) Positions of hydraulic jacks fixed with the reaction frame



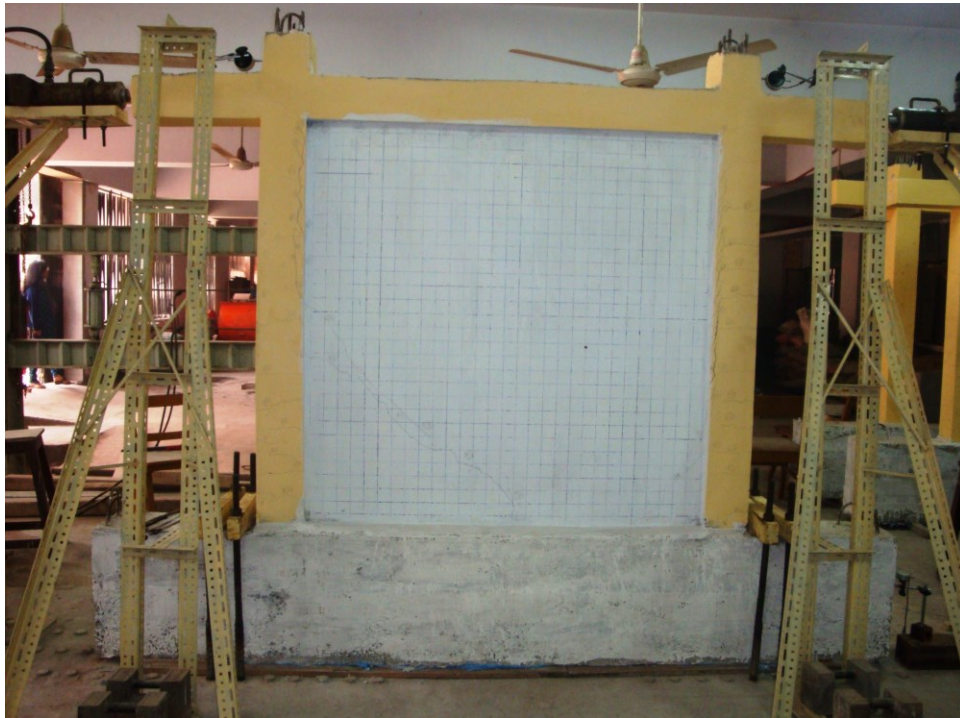


Figure 3.8 Positions of tripod stands for mounting displacement transducers



Figure 3.9 Mounting of displacement transducers to measure the top deflections

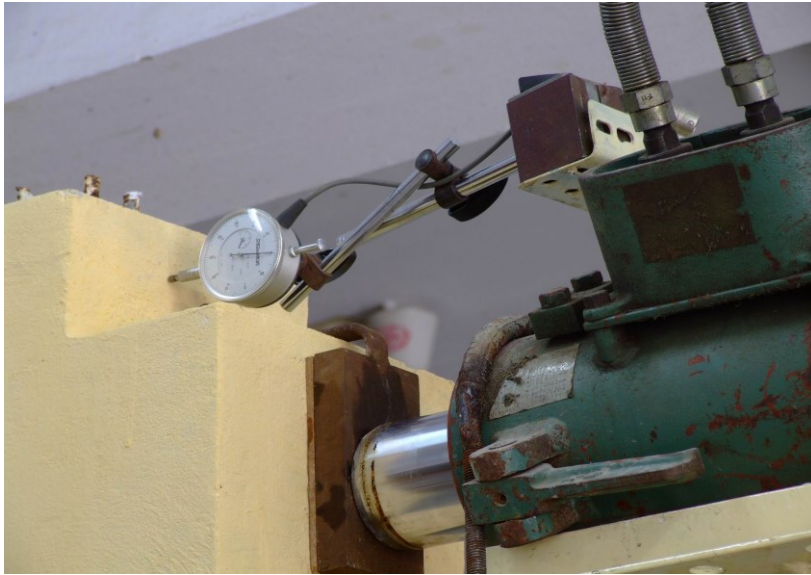


Figure 3.10 Position of hydraulic jack and displacement transducer



Figure 3.11 Location of displacement transducer to measure the base movement of the specimens

### 3.3 Model Specimens

The experiment was conducted by constructing single bay single story half scaled six numbers of model RC frame specimens subjected to in-plane cyclic load to establish their corresponding behavior and to study the behavior of these distressed frames repaired by Ferrocement (FC) laminates.

Table 3.1 and Table 3.2 list the number and the designation of the three types of frames those were tested in two phases, i.e., Phase-I and Phase-II.

**Table 3.1 Model Specimens in Test Phase-I**

Sl. No.	Description of specimen frame type	Number of specimens	Designation
1	Brick infilled RC frames	2	A1, A2
2	Bare RC frames	2	B1, B2
3	RC frames having brick infill isolated from frame elements	2	C1, C2

In six specimen frames there were two brick infilled reinforced concrete frames are designated as A1 and A2, two bare reinforced concrete frames without infill walls designated as B1 and B2 representing soft-storey frame; and other two reinforced concrete frames with brick infills isolated from frame elements are designated as C1 and C2.

In six specimen frames the two bare reinforced concrete frames without infill walls representing soft-storey frame, two brick infilled reinforced concrete frames and other two reinforced concrete isolated brick infilled frames. For last two specimens, the non-structural infill wall was uncoupled from the surrounding frame by providing some structural gap between the infill wall and the surrounding frame elements. However, some sort of lateral support was provided by single layer of FC laminate along the wall-frame interface to prevent the wall from falling in the out of plane direction. The clearance distance between the wall and the frame was considered as  $50 \text{ mm} \geq 0.025h$ , the possible maximum drift of the RC frame (2.5% of storey height,  $h=1600 \text{ mm}$ ) and the gaps were filled with compressible filler materials (cork sheet). The most important philosophical underpinning of such investigation with gap provision is that the initial stiffness of reinforced concrete

frame with infill wall building be deliberately reduced from the current conditions so that the overall structure can remain flexible within the limits of the integrity of the surrounding reinforced concrete frame.

In Phase-I, the model specimens A1, A2, B1, B2, C1 and C2 were damaged after application of reverse cyclic loads and further designated as AR1, AR2, BR1, BR2, CR1 and CR2 respectively when repaired with FC laminates described in Table 3.2.

**Table 3.2 Model Specimens in Test Phase-II**

Sl. No.	Description of specimen frame type	Number of specimens	Designation
1	FC laminated brick infilled RC frames previously damaged in test phase-I	2	AR1, AR2
2	FC laminated Bare RC frames previously damaged in test phase-I	2	BR1, BR2
3	FC laminated RC frames having brick infills isolated from frame elements previously damaged in test phase-I	2	CR1, CR2

### 3.3.1 Dimensions and reinforcement details of the model specimen frames

The reinforcement details of the ½ scale RC frame models were designed to meet the requirement of the Bangladesh National Building Code (BNBC 1993) as described previously in Section 2.5.2 of Chapter 2. Each model (A1, A2, B1, B2, C1 and C2) has typical height of 1600 mm and typical width of 1675 mm center to center of columns. The RC frames consist of 150 mm square columns and loading beam. The dimensions with the reinforcement details of model specimens are illustrated in Figure 3.12.

### 3.3.2 Construction of RC frames for all the model specimen frames

The concrete used in the construction of the RC frames for the six model specimens A1, A2, B1, B2, C1 and C2 was made with ordinary Portland cement (C) conforming to the ACI code, 12 mm downgraded stone chips as coarse aggregate (CA) and Sylhet sand (F.M.> 2.0) as fine aggregate (FA) according to the mix proportion=C:FA:CA=1:1.5:3 along with the water cement ratio as 0.45. The wooden formworks were made up of as per the size of beam and columns. The frames were cast in the Civil Engineering Laboratory in BUET. Curing of the RC frame was done by covering with hessians keeping them moist for 28 days. Figures 3.13-3.24 illustrate the construction stages of the six specimen frames.

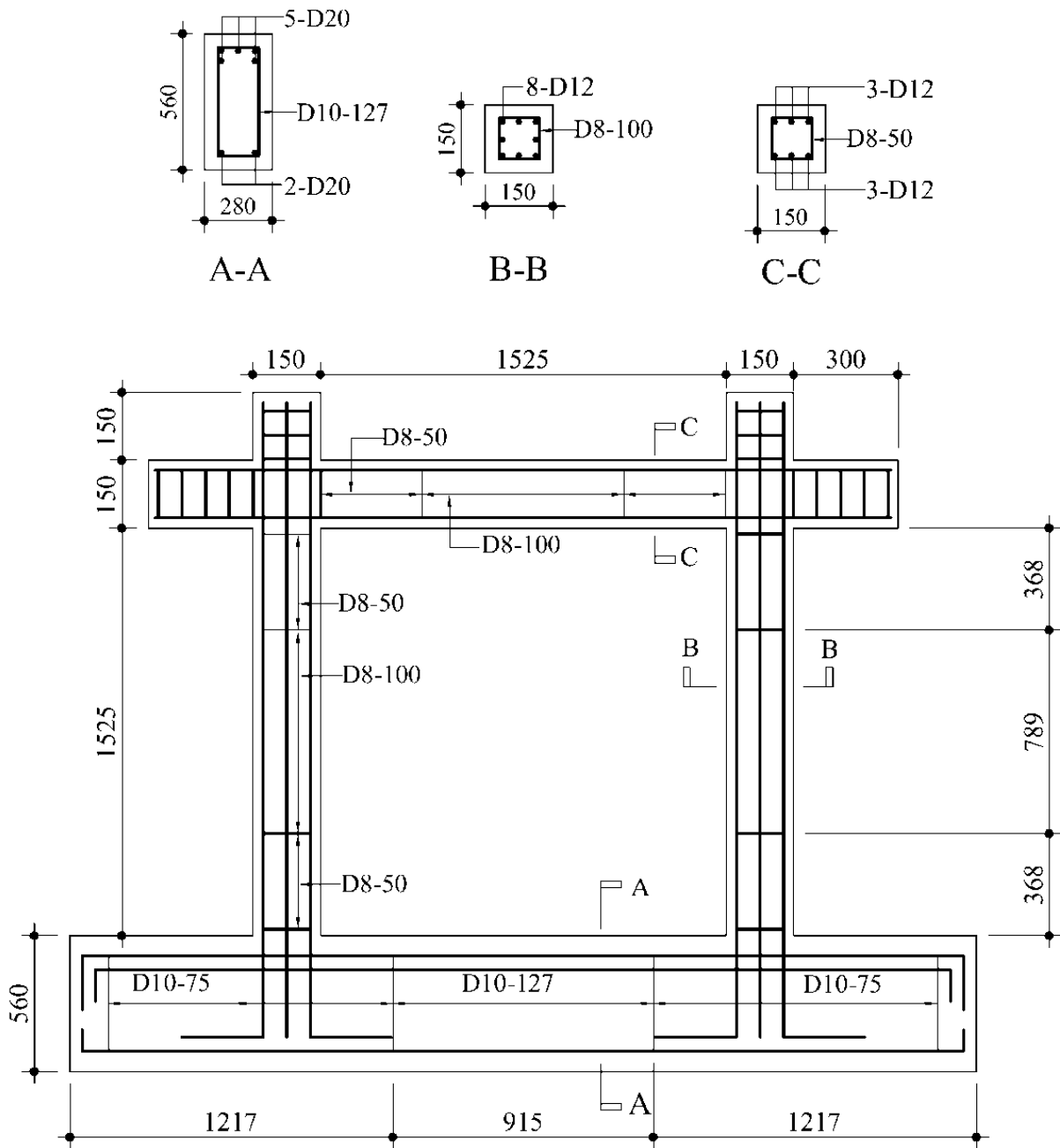


Figure 3.12 Geometry and reinforcement details of test model specimen

### 3.3.3 Construction of brick infills

As the RC frame specimens were half scale models, half scale brick units were used in construction of infill walls for the specimens A1, A2, C1 and C2 (Figure 3.17). The commonly used size of brick mass is 240mm×115mm×70mm. Therefore, local clay brick units were sliced into five pieces using diamond saw to obtain the half scale dimensions 115mm×70mm×45mm. For stretcher bond masonry infill wall

construction half-scaled bricks with 1:4 mortars (Portland cement: local river sand) were used.

The infill walls used in frames A1 and A2 had the wall height=1525 mm, width=1525 mm and wall thickness=100 mm. The thickness of walls for the specimens C1 and C2 was also 100 mm. On the other hand, the height of the wall was 1513 mm and the width was 1475 mm due to providing some gaps between the infills and the surrounding frames in the isolated infilled RC frames C1 and C2.

### **3.3.4 Gap Provisions for isolated infilled frames**

For C1 and C2, the non-structural infill wall was uncoupled from the surrounding frame by providing some structural gap between the infill wall and the surrounding frame elements. The clearance distance between the wall and the frame was determined by considering possible drift of the frame. The vertical gap between the infill and the RC column was kept  $50 \text{ mm} > 0.025h$ , the possible maximum drift of the RC frame (2.5% of storey height,  $h=1600 \text{ mm}$ ) whereas the horizontal gap between the loading beam and the infill was 12.5 mm. The gaps were filled with compressible filler materials (cork sheet was used as filler material). However, for the isolated infilled RC frame, some sort of lateral support was provided by a single layer of FC laminate applying 200 mm wide BWG 18 woven wire mesh with 12.7 mm square openings along the wall-frame interface to prevent the wall from falling in the out of plane direction. The most important assumption of such investigation with gap provision is that the initial stiffness of RC frame with infill wall will be reduced from the condition where the infill is in contact with the RC frame; so that the overall structure can remain flexible within the limits of the integrity of the surrounding frame. The current experimental investigation on isolated infill frames are considered to investigate whether the technique of providing gap in infilled frame is a justified preventive measure in minimizing the risk of “soft story” or “weak story” mechanism for those buildings where earthquake loads are considered in the structural design (Figures 3.17- 3.23).



Figure 3.13 Steel casing for the specimen base



Figure 3.14 Seismic detailing of the reinforcing steel



Figure 3.15 Casting of the specimens' bases in first step



Figure 3.16 Casting of columns of the specimens





Figure 3.17 Construction of brick infills in specimens C1, C2 and A1 (from front)



Figure 3.18 Application of cork sheets into gaps between the infill and the surrounding RC frame for the isolated infilled RC frame



Figure 3.19 Placement of the single layer cork sheet at the infill-RC beam interface and tetra layer cork sheet at the infill-RC column interface and application of wire mesh along the interfaces



Figure 3.20 Application of wire mesh with GI wire and nails along the surface area of the infill-RC column interface



Figure 3.21 Application of sand cement mortars on the specimen surface and the wire mesh fastened along the infill-RC column interface



Figure 3.22 Surface finishing of the isolated brick infilled RC frame specimen



Figure 3.23 Finished Specimens C1, C2 and A1 (from front)



Figure 3.24 Finished Specimens B1, B2, A2 (right column) and C1, C2 and A1 (left column)

### **3.3.5 Surface finishing and painting**

All the specimen frames A1, A2, B1, B2, C1 and C2 were plastered with 12.7 mm thick mortars (cement: sand=1:4). Afterward, the infill walls were painted with white wash while the frame elements were painted yellow for easy identification of the cracks. The walls were marked with blue lines of 50 mm spacing.

### **3.4 Laboratory Investigation**

The laboratory investigations were accomplished in two consecutive phases, i.e., phases-I and phase-II. In phase-I, cyclic in-plane lateral load, with increasing magnitude in each cycle, was applied on pairs of single bay, single story brick infilled RC frame (A1, A2), bare RC frame (B1, B2) and isolated infilled RC frame (C1, C2) model specimens, till their ultimate capacities were reached. Behaviors of the frames were evaluated through the observed strength and deformation characteristics along with hysteretic energy dissipation capacity and ductility. In phase-II, the previously damaged specimens were repaired with ferrocement laminates relabeled as AR1, AR2, BR1, BR2, CR1 and CR2 respectively; and tested following the same procedures as for the original frames.

#### **3.4.1 Test Phase-I: in-plane cyclic loading test of specimen frames A1, A2, B1, B2, C1 and C2**

In Test Phase-I, tests were performed on locally available brick infilled RC frame model specimens A1 and A2, bare RC frame B1 and B2, and isolated infilled RC frame specimens C1 and C2 (Figure 3.25a, 3.25b and 3.25c). The specimens were attached to the strong base of the test setup by means of four pairs of anchor bolts applying 178 kN compression forces by each pair of the anchor bolts on the fixing blocks. Two displacement transducers (DT) were positioned at top-north and top-south of specimen frames to measure the corresponding deflections while another DT was fitted to monitor in case of base movement of the specimens. The first cracking load, failure load, failure mode and corresponding deflections at the top of the frames for each incremental load were observed and recorded during testing. After the completion of laboratory investigations for Phase-I, damaged specimens were removed from the setup and repaired with FC laminates.



(a) In-plane cyclic load test of brick infilled RC frame



(b) In-plane cyclic load test of bare RC frame



(c) In-plane cyclic load test of isolated infilled RC frame

Figure 3.25 In-plane cyclic load test of the model specimens in Test Phase-I

A set of material tests were performed for concrete, masonry prisms, reinforcing bars used in construction of specimen are shown in Table 3.3(a).

**Table 3.3(a) Average Material Properties of the Construction Materials of the Model Specimens (Appendices A, B and D)**

Specimen	Test Models		
Concrete Cylinder (100mmx200mm)	Test Model A1		Test Model A2
	$f_c'_{(28 \text{ day})} = 21.94 \text{ MPa}$		$f_c'_{(28 \text{ day})} = 25.20 \text{ MPa}$
	$f_c'_{(\text{test day})} = 27.50 \text{ MPa}$		$f_c'_{(\text{test day})} = 32.21 \text{ MPa}$
	Test Model B1		Test Model B2
	$f_c'_{(28 \text{ day})} = 25.50 \text{ MPa}$		$f_c'_{(28 \text{ day})} = 23.13 \text{ MPa}$
	$f_c'_{(\text{test day})} = 31.30 \text{ MPa}$		$f_c'_{(\text{test day})} = 32.32 \text{ MPa}$
	Test Model C1		Test Model C2
	$f_c'_{(28 \text{ day})} = 24.91 \text{ MPa}$		$f_c'_{(28 \text{ day})} = 26.39 \text{ MPa}$
	$f_c'_{(\text{test day})} = 31.28 \text{ MPa}$		$f_c'_{(\text{test day})} = 29.62 \text{ MPa}$
Masonry Prism (230mmx230mmx 70mm)	Compressive strength of masonry prism for load parallel to bed joint = 9.15 MPa load perpendicular to bed joint = 7.41 MPa		
Reinforcement	Yield, MPa	Ultimate, MPa	% Elongation
8mm	424	532	18
12mm	417	624	15
20mm	324	456	19

**Table 3.3(b) Materials Used in FC Laminating for Repair of Damaged Specimens (Appendix C)**

FC Components	Description
Wire mesh	BWG 18 woven wire mesh with 12.7 mm square openings
Mortar	Mixing proportion of cement and sand = 1:2.5 Water cement ratio = 0.45 7 days average crushing strength (50 mm mortar cube): $f_{cm}$ for AR1 = 15.88 MPa $f_{cm}$ for AR2 = 17.49 MPa

### 3.4.2 Test Phase-II: In-plane cyclic test of repaired specimen frames AR1, AR2, BR1, BR2, CR1 and CR2

After in-plane cyclic testing, A1, A2, B1, B2, C1 and C2 were repaired by FC laminates and relabeled as AR1, AR2, BR1, BR2, CR1 and CR2 in Phase-II. The Table 3.3(b) and Table 3.4 illustrate the FC component materials and reinforcement parameters employed in the present research.

**Table 3.4 Reinforcement Parameters for FC Laminated Specimens AR1 and AR2**

Specimen Component	RC Frame	Brick Infill wall
Wire mesh Layer	Double	Single layer applied on both faces
Thickness of FC laminate (mm)	19	12.7(Applied on both faces of infill)
Volume Fraction of Reinforcement, $V_f$ (mm <sup>3</sup> /mm <sup>3</sup> )	0.0136	0.0102
Specific Surface of Reinforcement, $S_r$ (mm <sup>2</sup> /mm <sup>3</sup> )	0.0531	0.0398
Effective Area of Reinforcement per unit length, $A_{s_i}$ (mm <sup>2</sup> /mm)	0.1292	0.1295

1) Repair of the damaged specimens with FC laminates

a. Surface preparation for the repair of damaged specimens

All the damaged model specimens were carefully dismantled of the plaster of RC frames (for B1 and B2) or RC frames and the infills (for A1, A2, C1 and C2). The chipping process continued from either side of the cracks. The specimen frames were then washed with water jet to ensure all dust and loose debris was removed. In order to ensure proper bond between crack surfaces, cement slurry was sprayed over the cracks. Thereafter, a thin layer of mortar was applied all over the surface of the frames (for B1 and B2) or frames and the infills (for A1, A2, C1 and C2) (Figure 3.26-3.27)

b. FC laminating on the damaged infilled RC frame specimens A1 and A2

After surface preparation, double layer wire mesh on RC frames and single layer mesh on both sides of infills were placed by previously affixed nails ((Figure 3.28). Afterward mortar was applied on the wire mesh with the help of trowels ensuring penetration of mortar through the openings of the mesh. Thus, the applied mortar came in contact with the previously applied mortar securing the mesh in place with proper bonding. Finishing of the surface was performed using a trowel following the standard practice.

Finally, the repaired frame was cured for 28 days covering the FC laminated regions with moist hessians. The dimension of the sections of infill and the beam and columns were slightly changed in repaired specimens due to the addition of FC coating. In the original frames A1 and A2, the plaster was about 12.5 mm thick everywhere whereas in the repaired frames AR1 and AR2 the thickness became 19



mm. Table 3.4 describes the reinforcement parameters for FC laminated specimens AR1 and AR2. Additionally, Figure 3.28(a) and (b) illustrate the FC lamination procedures on the infilled RC frames.

c. FC laminating on the damaged bare RC frame specimens

After surface preparation, double layer wire mesh on RC frames was placed by previously affixed nails. Afterward, the same procedures were followed for repairing the bare RC frame specimens that previously discussed in case of infilled RC frames. In the original frames B1 and B2, the plaster was about 12.5 mm thick everywhere whereas in the repaired frames BR1 and BR2 the thickness became 19 mm. Table 3.5 depicts the reinforcement parameters for FC laminated specimens BR1 and BR2.

**Table 3.5 Reinforcement Parameters for FC Laminated Specimens BR1 and BR2**

Specimen Component	RC Frame
Wire mesh Layer	Double
Thickness of FC laminate (mm)	19
Volume Fraction of Reinforcement, $V_f$ (mm <sup>3</sup> /mm <sup>3</sup> )	0.0136
Specific Surface of Reinforcement, $S_r$ (mm <sup>2</sup> /mm <sup>3</sup> )	0.0531
Effective Area of Reinforcement per unit length, $A_{sf}$ (mm <sup>2</sup> /mm)	0.1292

d. FC laminating on the damaged isolated infilled RC frame specimens

For the isolated infilled RC frames, double layer wire mesh on RC frames was wrapped around the three faces of the columns and the beam with the affixed nails. No mesh was applied on infills. Further, the isolated infills were laterally supported again by a single layer of wire mesh along the gap between the frame elements and the infills (Figure 3.29).

Afterward the previously described procedures were followed for the completion of the FC repairing along the surface area of the applied wire mesh. In the original frames C1 and C2, the plaster was about 12.5 mm thick everywhere whereas in the repaired frames CR1 and CR2 the thickness became 19 mm (Figure 3.30-3.31).

Table 3.6 depicts the reinforcement parameters for FC laminated specimens CR1 and CR2.

**Table 3.6 Reinforcement Parameters for FC Laminated Specimens CR1 and CR2**

Specimen Component	RC Frame	Along the Gap between RC frame and the infill	Brick Infill wall
Wire mesh Layer	Double	250 mm wide single layer applied on both surfaces along the gap only	FC Laminate was not Applied
Thickness of FC laminate (mm)	19	12.7 (both surfaces along the gap)	
Volume Fraction of Reinforcement, $V_f$ ( $\text{mm}^3/\text{mm}^3$ )	0.0136	0.0102	
Specific Surface of Reinforcement, $S_r$ ( $\text{mm}^2/\text{mm}^3$ )	0.0531	0.0398	
Effective Area of Reinforcement per unit length, $A_{si}$ ( $\text{mm}^2/\text{mm}$ )	0.1292	0.1295	

## 2) Testing of repaired infilled RC frame

The repaired specimens AR1, AR2, BR1, BR2, CR1 and CR2 were tested following the same procedures as for the original frames using the same in-plane reverse cyclic loading test setup (Figure 3.32-3.37). Cyclic responses of the specimens along with the corresponding effect of FC were monitored until their ultimate capacities were reached. Seismic performance of the repairing with FC was assessed through observed strengths and deformation characteristics along with hysteretic energy dissipation capacity and ductility of the repaired frames.



Figure 3.26 Surface cleaning of damaged specimens after chipping of plasters



Figure 3.27 Shear sliding, mortar bed joint failure and corner crushing of the isolated in-fill have been identified clearly after chipping of the plasters



Figure 3.28(a) Wiremesh wrapped around the RC frame and the infill

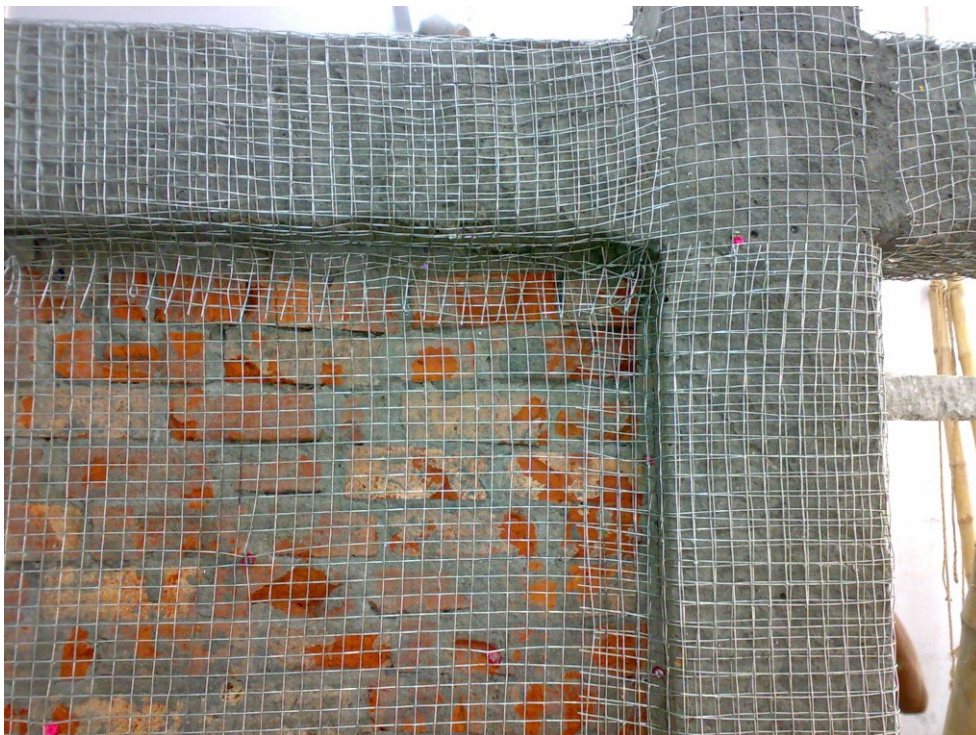


Figure 3.28(b) Closed up view of Wiremesh wrapped around the RC frame (two layers of wire mesh) and the infill (one layer of wiremesh)



Figure 3.29(a) Wrapping of wiremesh on isolated infilled RC frame to repair the bed joint failures of isolated infill wall



Figure 3.29(b) Gouting along the wrapped wiremesh around the RC frame and the infill RC frame interface



Figure 3.30 Close up view of wire mesh wrapping around the RC frame and infill-RC frame interface for the isolated infilled RC frames



Figure 3.31 Wiremesh wrapped specimens were plastered with rich mortars

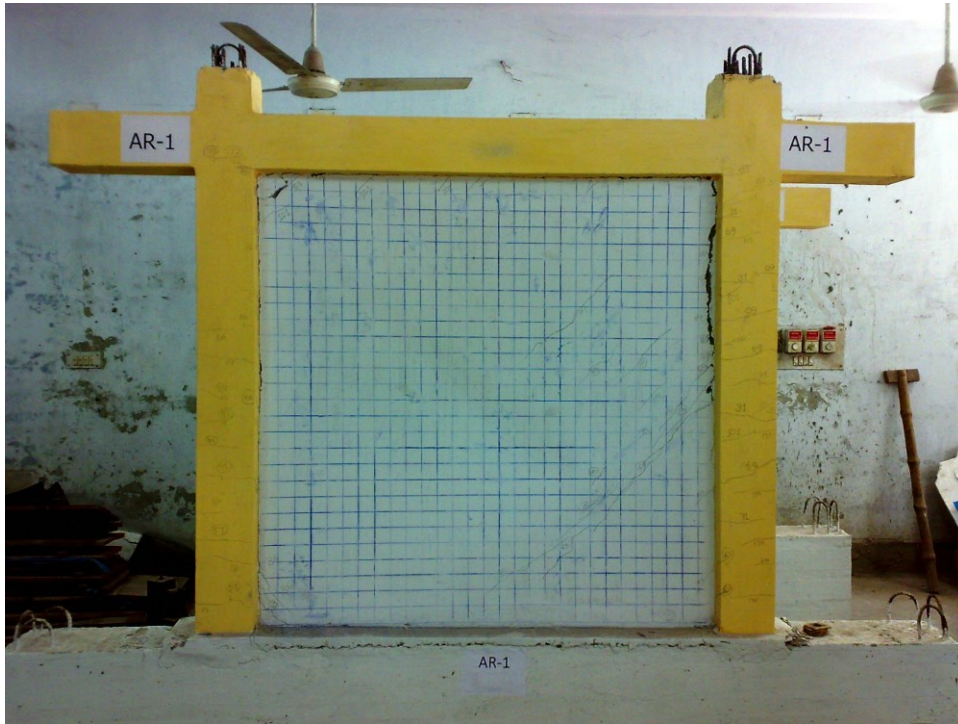


Figure 3.32 Test specimen AR1 after applying cyclic load in Test Phase-II

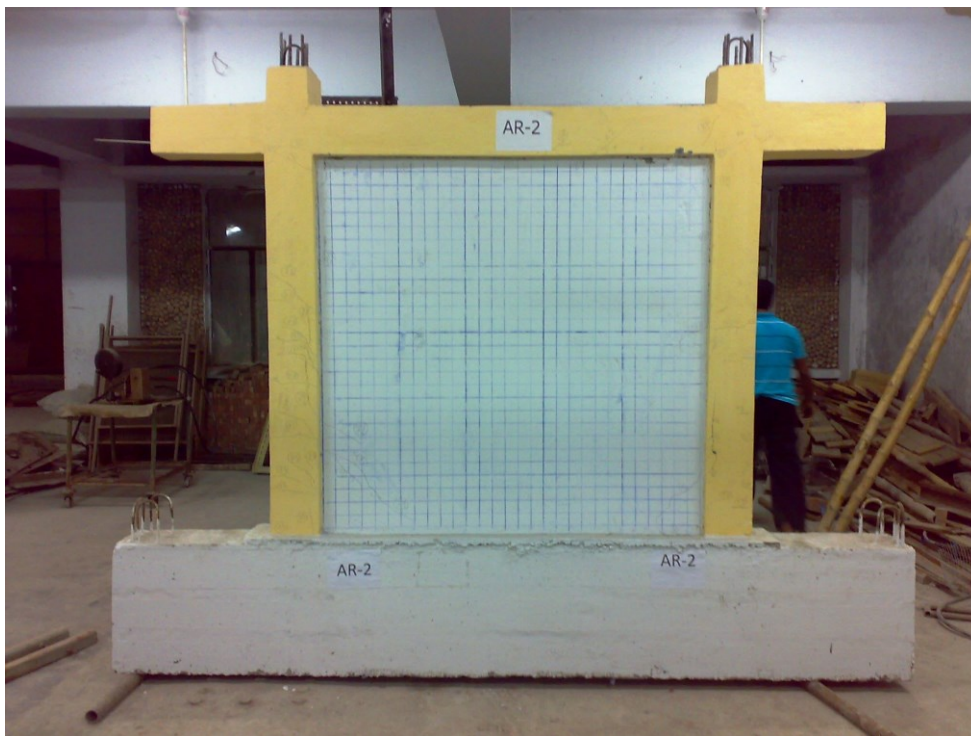


Figure 3.33 Test specimen AR2 after applying cyclic load in Test Phase-II

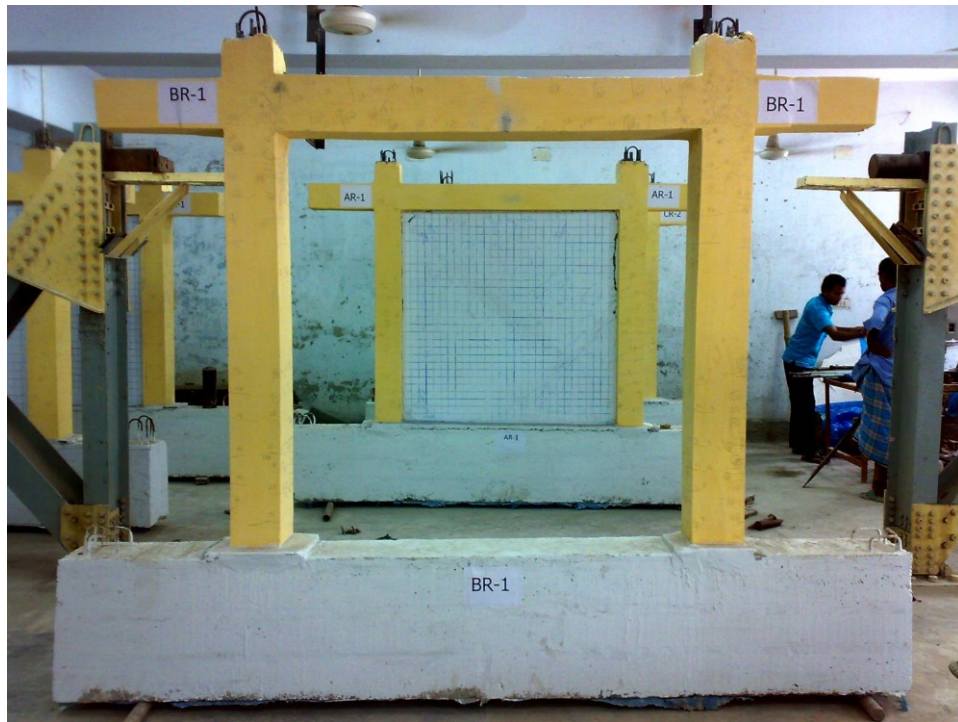


Figure 3.34 Test specimen BR1 after applying cyclic load in Test Phase-II



Figure 3.35 Test specimen BR2 after applying cyclic load in Test Phase-II



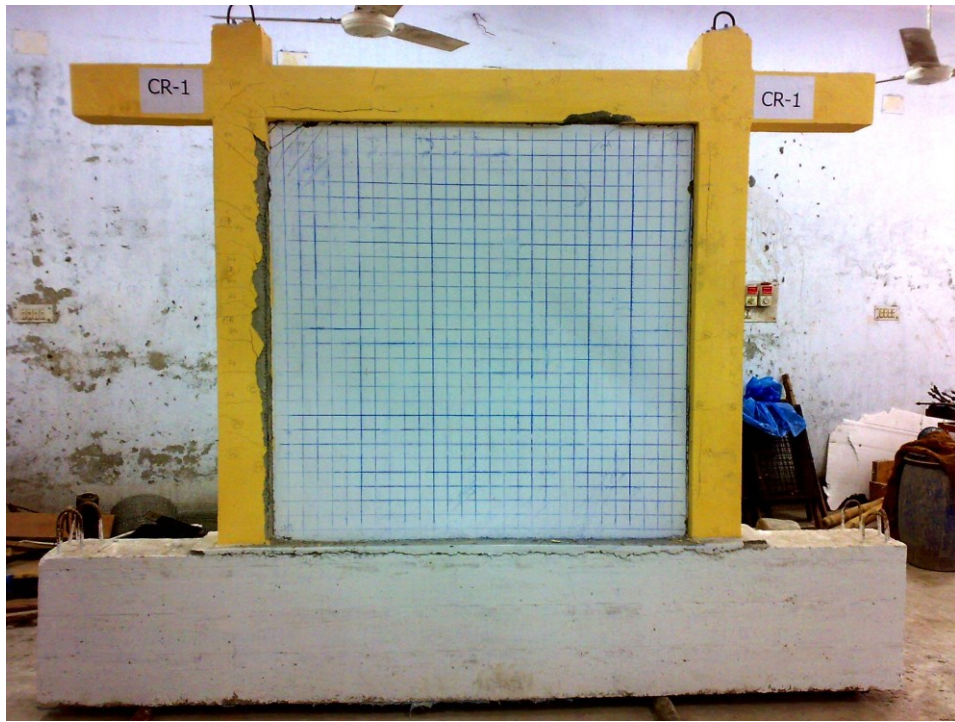


Figure 3.36 Test specimen CR1 after applying cyclic load in Test Phase-II

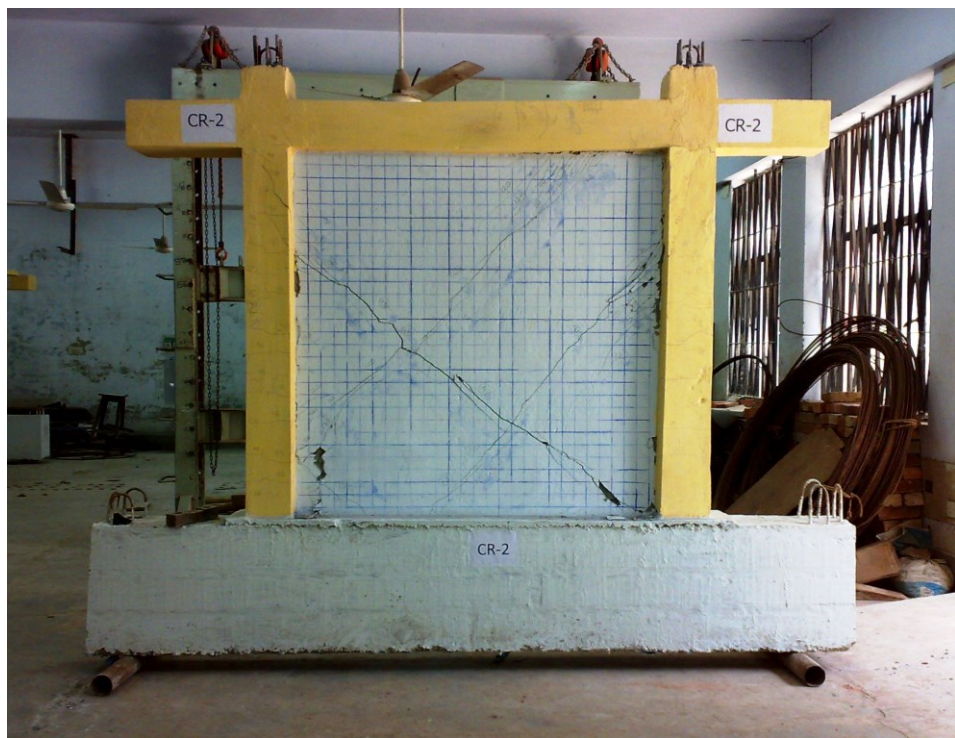


Figure 3.37 Test specimen CR1 after applying cyclic load in Test Phase-II

#### 4.1 Introduction

Crack patterns, initial stiffness, deflections, maximum lateral loads, and failure mechanism, lateral stiffness, energy dissipations and displacement ductility ratio were observed for original brick infilled RC frames (A1, A2), bare RC frames (B1, B2) and isolated infilled RC frames (C1, C2) as well as for the repaired infilled RC frames (AR1, AR2), repaired bare RC frames (BR1, BR2) and repaired isolated infilled RC frames (CR1, CR2) which are summarized in following sections.

#### 4.2 Experimental Results for Brick Infilled RC Frames

The experimental results on the brick infilled RC original frames and the FC laminated repaired infilled RC frames are summarized in the following Table 4.1. Along with, the failure mechanisms of the original and the repaired infilled RC frames are described in Table 4.2.

**Table 4.1 Summary of Experimental Results for A1, A2, AR1 and AR2**

Description	A1	A2	AR1	AR2
Frame cracking load (kN)	71	89	80	89
Displacement at frame cracking load (mm)	0.60	0.94	0.84	0.76
Infill cracking load (kN)	111	133	125	156
Displacement at infill cracking load (mm)	1.44	2.98	1.57	2.10
Maximum lateral load (kN)	169	178	222	178
Displacement at maximum lateral load (mm)	4.84	6.64	6.15	4.07
Initial stiffness (kN/mm) at first crack	119	95	95	117

**Table 4.2 Failure Mechanism of Original and Repaired Frames**

Test Model	Failure Mechanism
A1	Diagonal tensile splitting of brick masonry
A2	Diagonal tensile splitting of brick masonry, Partial corner crushing of infill
AR1	Tensile failure of wire mesh along the previous diagonal tensile cracks in infills, Partial corner crushing of infill
AR2	Shear failure of columns and beam, Partial corner crushing of infill Tensile failure of wire mesh along previous tensile cracks in infills

#### **4.2.1 Crack patterns of the original frames A1 and A2**

The crack patterns of original brick infilled RC frame models A1 and A2 at maximum lateral loads are shown in Figure 4.1(a) and Figure 4.1(b). Initial flexural cracks started to develop in columns during the second load cycle (71 kN and 89 kN respectively). The first cracks in infill started to form in the third cycle (111 kN and 133 kN respectively), appearing diagonally at the furthest corner from the loaded compression diagonal. This indicates that the infill was substantially bonded with the base as well as with the columns. The diagonal cracks in infills propagated through the brick units, confirming that the bond tensile strength of the brick-mortar interface of the masonry becomes higher due to tri-axial confined stress condition inside the masonry along with the confining stress due to the surrounding RC frames. As a consequence, tensile splitting of brick units was noted. During this loading cycle, infill corner crushing and shear sliding at the infill-RC beam interface were also observed. During the final loading cycle (169 kN and 178 kN respectively), both specimens A1 and A2 experienced major diagonal tension cracks in masonry along with dispersed flexural cracks along the overall length of the yielded RC columns, and shear cracks in columns near beam-column joints. A few flexural cracks also occurred in the beams at failure loads.

#### **4.2.2 Crack patterns of the repaired frame AR1 and AR2**

The crack patterns of AR1 and AR2 at failure loads are shown in Figure 4.2(a) and 4.2(b). In the test models AR1 and AR2, initial flexural cracks generated in columns

during the second loading cycle (80 kN and 88 kN respectively) were akin to those of original frames A1 and A2. The first cracks in infills started to form in the third cycle (125 kN and 156 kN respectively). In the final load cycle, corner crushing and separation of infill from surrounding frames were observed.

The failure load for repaired frame AR1 was 222 kN. AR1 failed due to major diagonal cracks in the wall at the same locations as in the original frames. This was due to the fact that the cracks in the original frames were not repaired; instead, the whole frame was coated with FC overlay to determine the shear capacity of the repair material itself. This left the crack zones weaker than the other parts of the frame. Consequently, the failure load was governed by the tensile strength of the FC wire mesh overlaid on the wall.

On the contrary, the maximum load for repaired specimen AR2, 178 kN, was governed by shear failure of the surrounding RC frame. Although few tension cracks developed in the infill wall, no cracks developed along the previous major diagonal cracks in the infill formed in test phase I. This reveals the fact that due to the rich mortar plastering, a strong bond was developed in the FC laminates-masonry wall composite. Consequently, cracks could not generate at the same location as previous major diagonal cracks. Strong infills-RC frame interaction led to shear failure of the RC frame due to unexpected stress concentration. It was, however, observed that the amount of crack openings (width of crack opening) in the FC laminated infill walls was significantly smaller than those of original frames. This reveals the superior capability of FC in protecting the damaged structure from large deformation as well as from environmental actions.

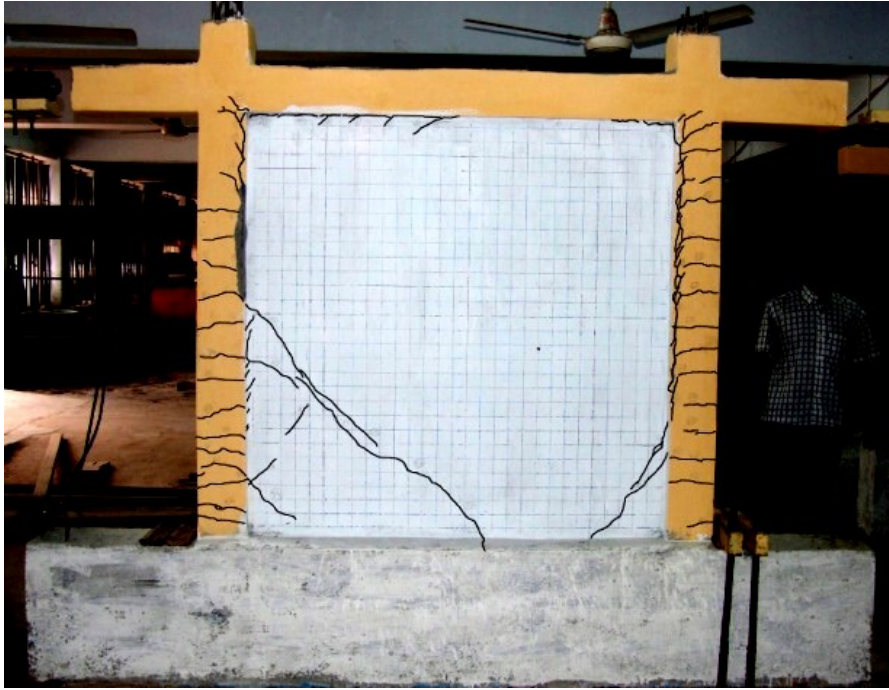


Figure 4.1(a) Crack patterns at maximum lateral load in brick infilled RC frame model specimen A1

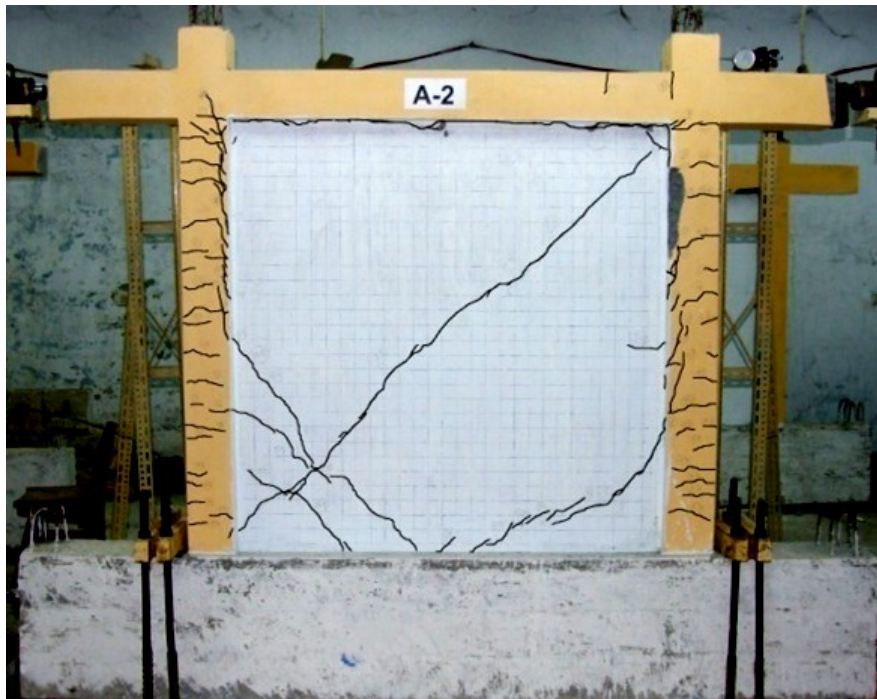


Figure 4.1(b) Crack patterns at maximum lateral load in brick infilled RC frame model specimen A2

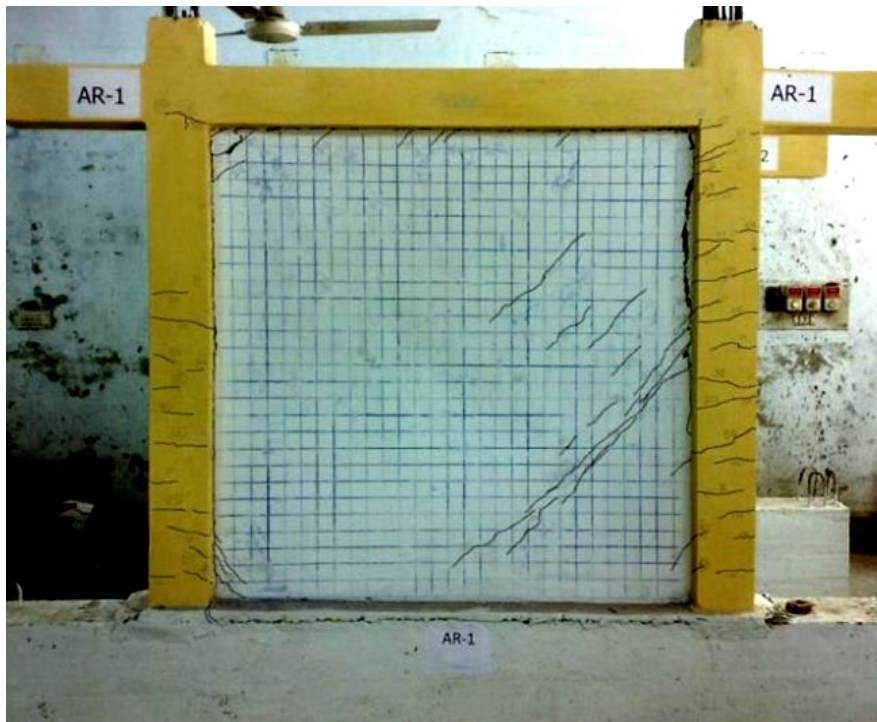


Figure 4.2(a) Crack patterns at peak load in repaired brick infilled RC frame model specimen AR1

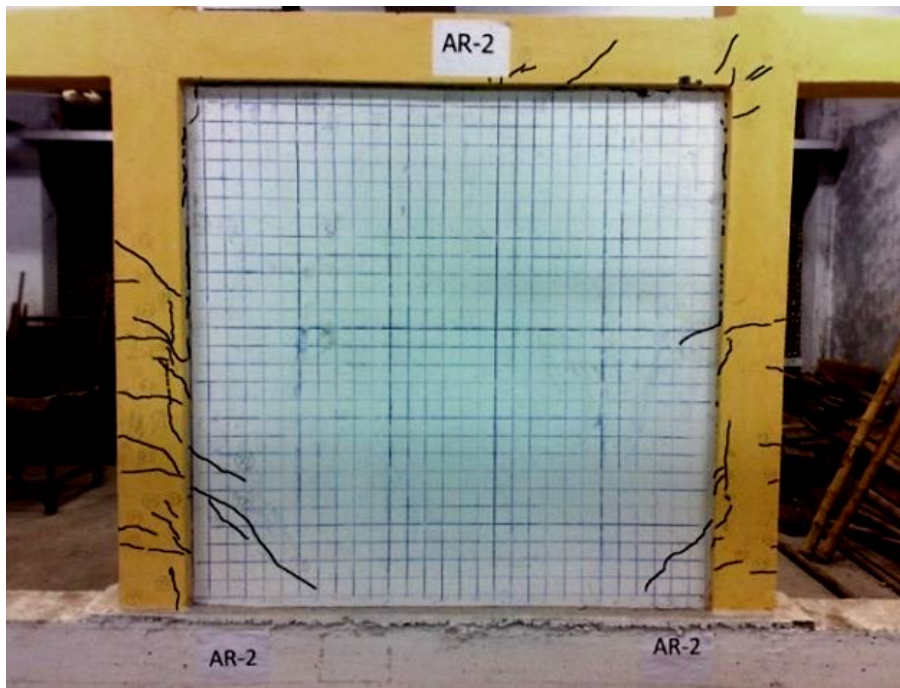


Figure 4.2(b) Crack patterns at peak load in repaired brick infilled RC frame model specimen AR2

### **4.2.3 Shear capacity of the original and the repaired brick infilled RC frames**

Maximum shear capacity is defined as the maximum lateral shear load applied at failure. From Table 4, the maximum shear capacity of original brick infilled RC frames A1 and A2 was noted as 169 and 178 kN respectively. According to the equation 2.6 in Chapter 2 demonstrated by Smith and Coull (1991), average diagonal tensile stress developed in the center of infill is around 0.88 MPa at failure which can be considered as the ultimate tensile strength of masonry infill (Appendix E). Furthermore, it has been confirmed that the calculated maximum horizontal shear load (165.27 kN) based on the equation 2.8 in Chapter 2 demonstrated by Smith and Coull (1991) regarding diagonal tensile failure of infill is approximately equal (variation within 5%) to the average maximum shear capacity (173 kN) obtained from the present laboratory investigation (Appendix-E).

Nonetheless, after the frame was repaired using FC laminates, the in-plane shear capacity for AR1 (222 kN) became 32% higher than that of original frame A1 (169 kN). For AR2, the maximum shear capacity (178 kN) against in-plane cyclic load was unchanged compared to original frame A2.

The lateral load versus story drift (sample calculation is included in Appendix E) of the original and repaired frames is shown in Figure 4.3(a) and 4.3(b) clearly demonstrating the effectiveness of the repair methodology using FC laminates. Since the failure of the repaired frame AR1 was diagonal tensile failure, it can be inferred that the capacity of the repaired frame depends on the tensile strength of FC laminates. It can be thus said that the combined shear capacity of the two layers of FC is higher than that of the infill wall.

As the specimen AR2 failed in shear due to strong infills, it can be inferred that if the cracks in masonry and RC frame are repaired before applying FC coating, then the infill will contribute to the load carrying capacity of FC. That would have resulted in a much higher lateral load capacity. It can, thus be inferred that, if FC laminates is applied to any existing un-distressed infill wall along with ensuring enhanced shear capacity of RC columns and beams, the capacity of the infilled frame will be significantly improved.

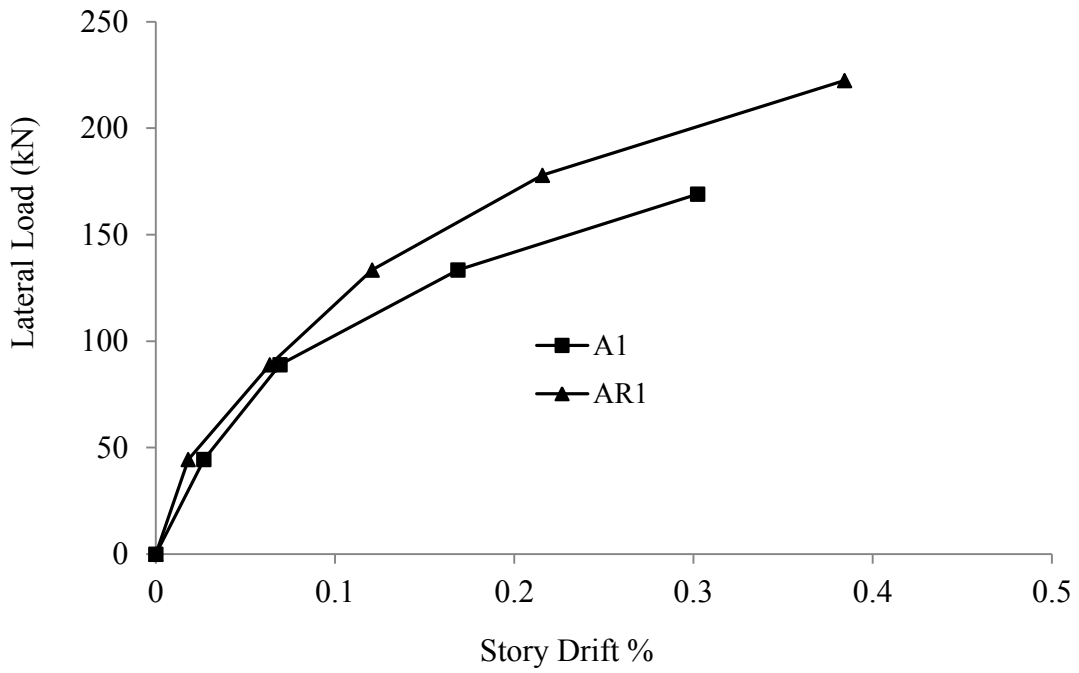


Figure 4.3(a) Lateral load versus story drift in original brick infilled RC frames (A1, A2)

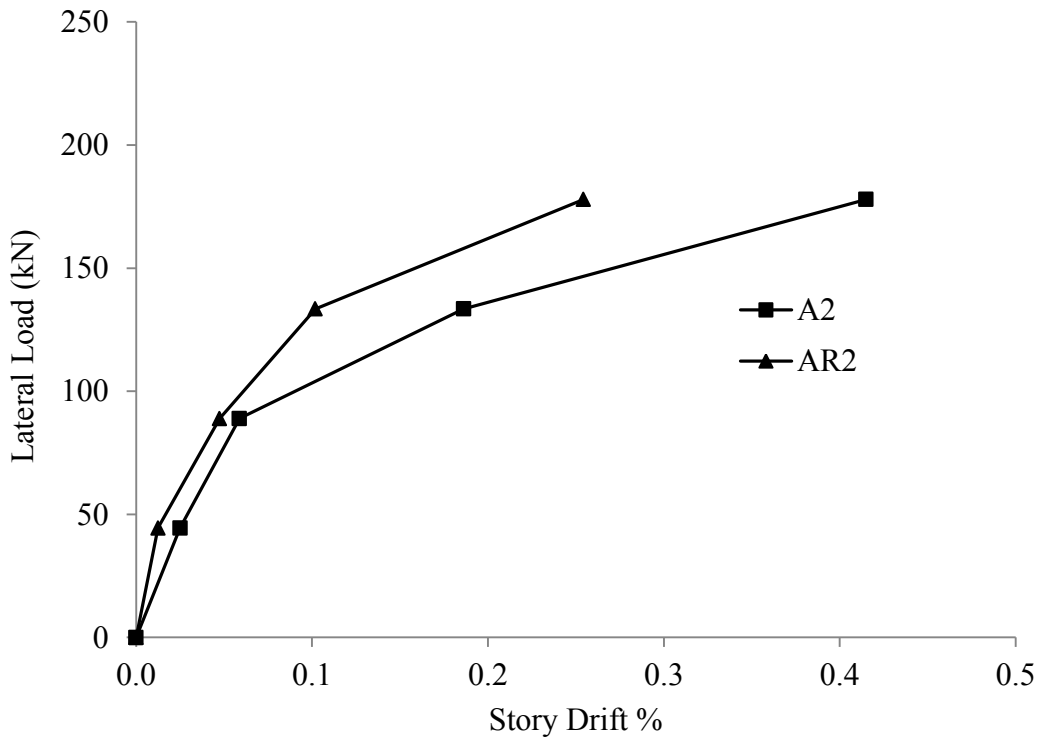


Figure 4.3(b) Lateral load versus story drift in FC laminated repaired brick infilled RC frames (AR1, AR2)



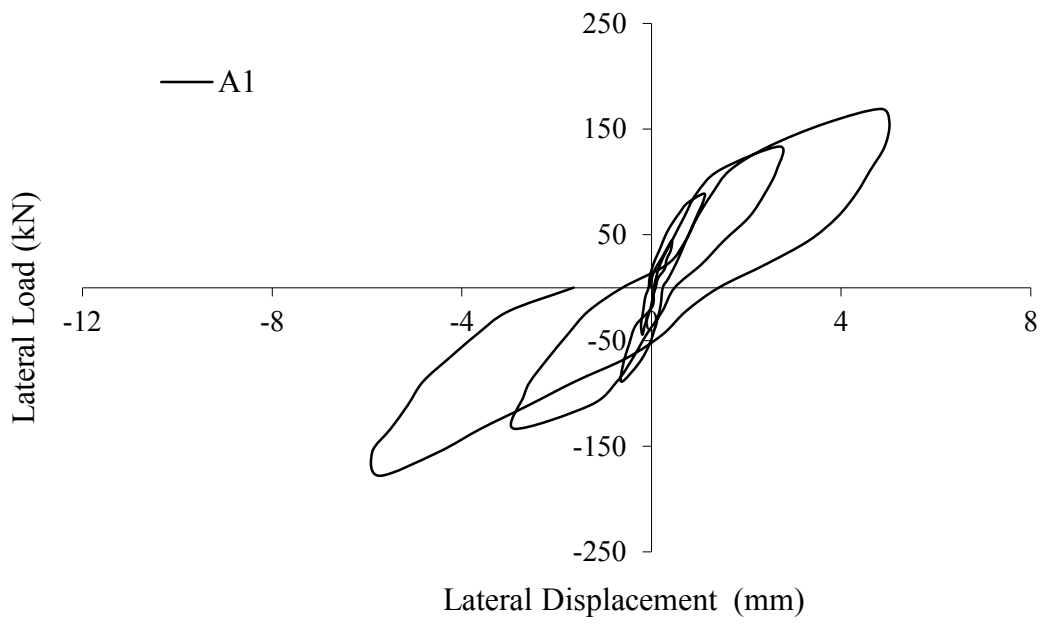


Figure 4.4(a) Hysteretic load-displacement curves in Test Model A1

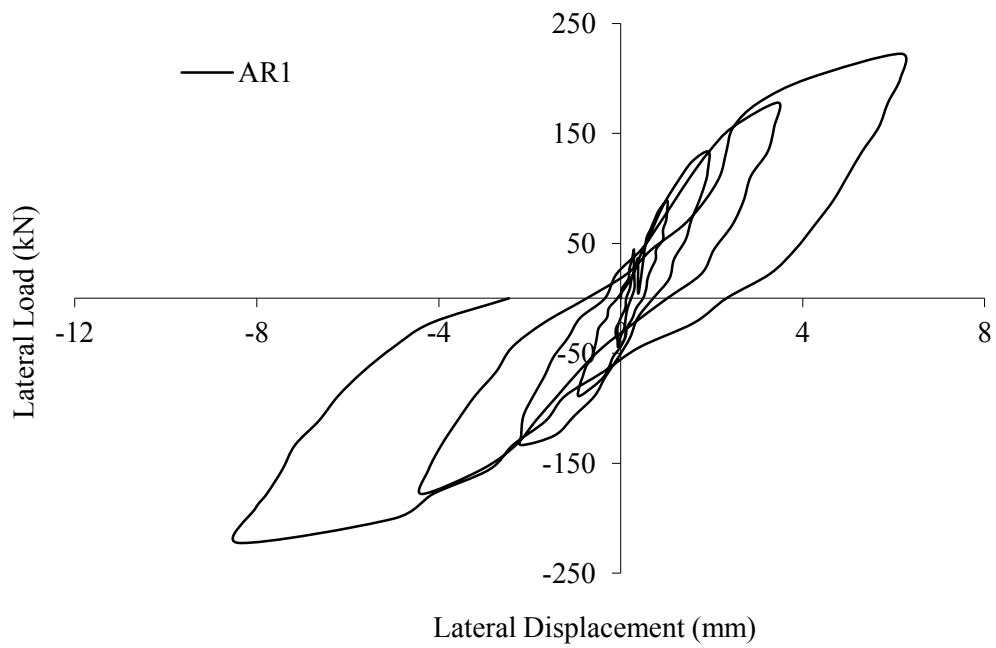


Figure 4.4(b) Hysteretic load-displacement curves in Test Model AR1

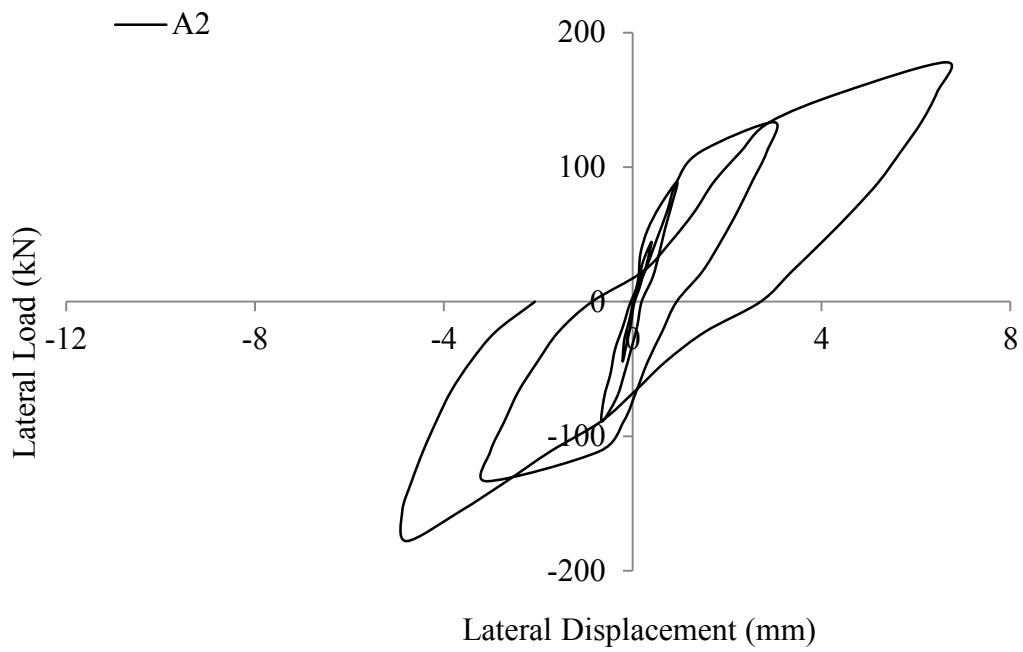


Figure 4.4(c) Hysteretic load-displacement curves in Test Model A2

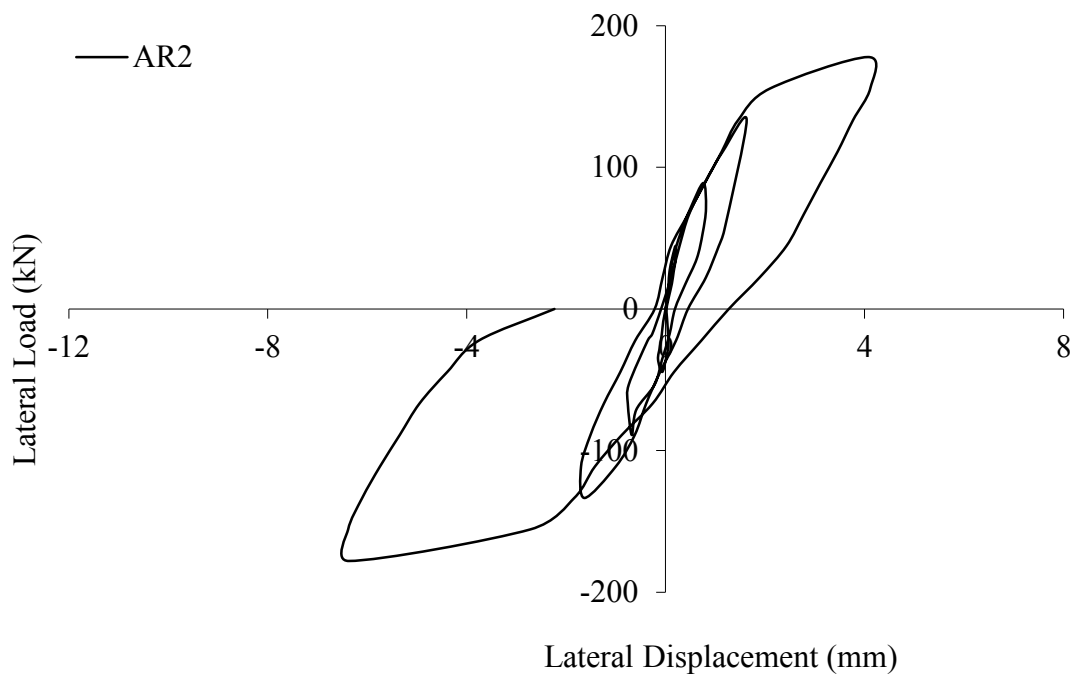


Figure 4.4(d) Hysteretic load-displacement curves in Test Model AR2

#### **4.2.4 Comparative hysteretic behavior of the original and the repaired infilled RC frames**

The hysteretic behaviors of original brick infilled RC frame specimens A1, A2 and repaired specimens AR1, AR2 are presented in Figures 4.4(a)-(d). According to the load-deflection behavior, original brick infilled RC frames and repaired infilled RC frame with FC exhibited basically same peak load except repaired specimen AR1. However, FC laminated repaired specimens exhibited better hysteresis behaviors as the more accelerated lateral displacements for similar intensity of lateral loads were observed in original specimens A1 and A2 compared to AR1 and AR2.

#### **4.2.5 Comparative lateral stiffness of the original and the repaired infilled RC frames**

Table 4.1 shows initial stiffness of original frames A1 and A2 along with repaired frames AR1 and AR2 obtained from the experimental results. The lateral stiffness of the specimens before the generation of cracks is defined as the initial stiffness (Imran and Aryanto, 2009). It has been revealed that the initial stiffness of the repaired frame AR1 was 17% higher than the original frame A1. And for AR2, the initial stiffness became 49% higher than the original frame A2 (calculation shown in Appendix E).

Furthermore, Figure 4.5(a) and Figure 4.5(b) illustrate comparative stiffness degradation with respect to story drift at peak loads in each cycle establishing that stiffness degradation as well as story drift was less in case of repaired specimens AR1 and AR2.

Alternatively, AR2 shows less energy dissipation than A2, due to shear failure of RC columns prior to the complete collapse of FC laminated infills.

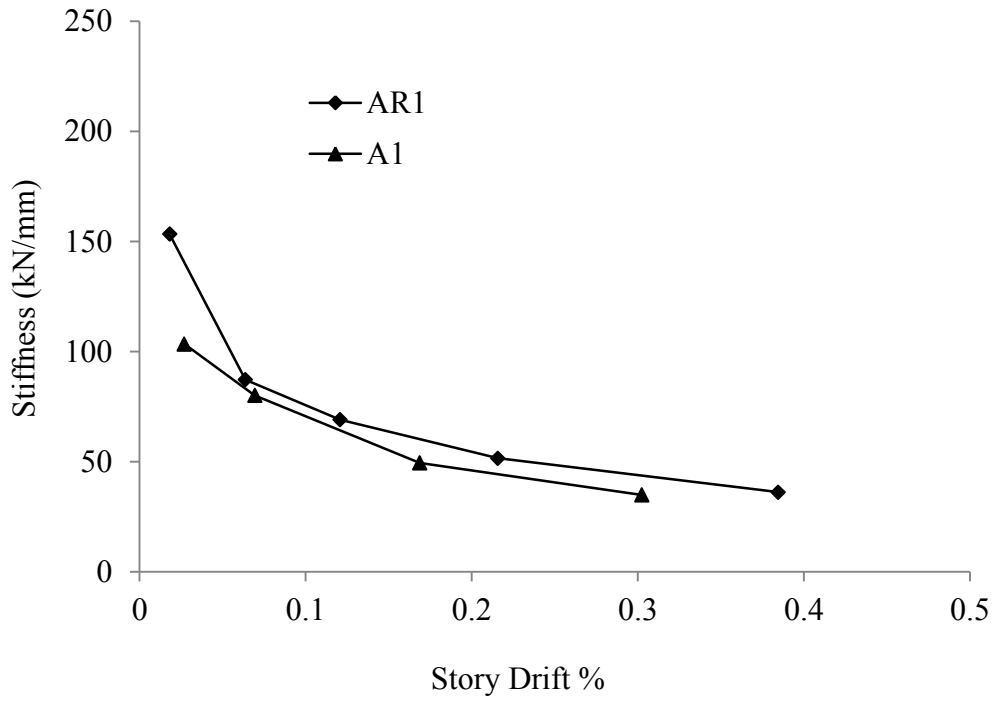


Figure 4.5(a) Comparison of stiffness degradation in each loading cycle with respect to story drift in original specimen A1 and AR1

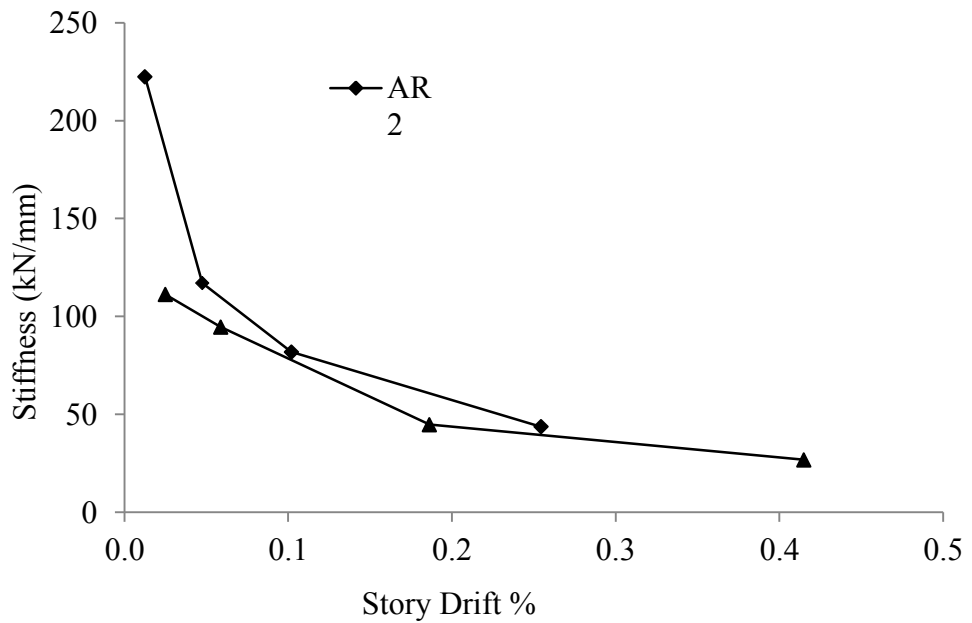


Figure 4.5(b) Comparison of stiffness degradation in each loading cycle with respect to story drift in repaired specimens A2 and AR2

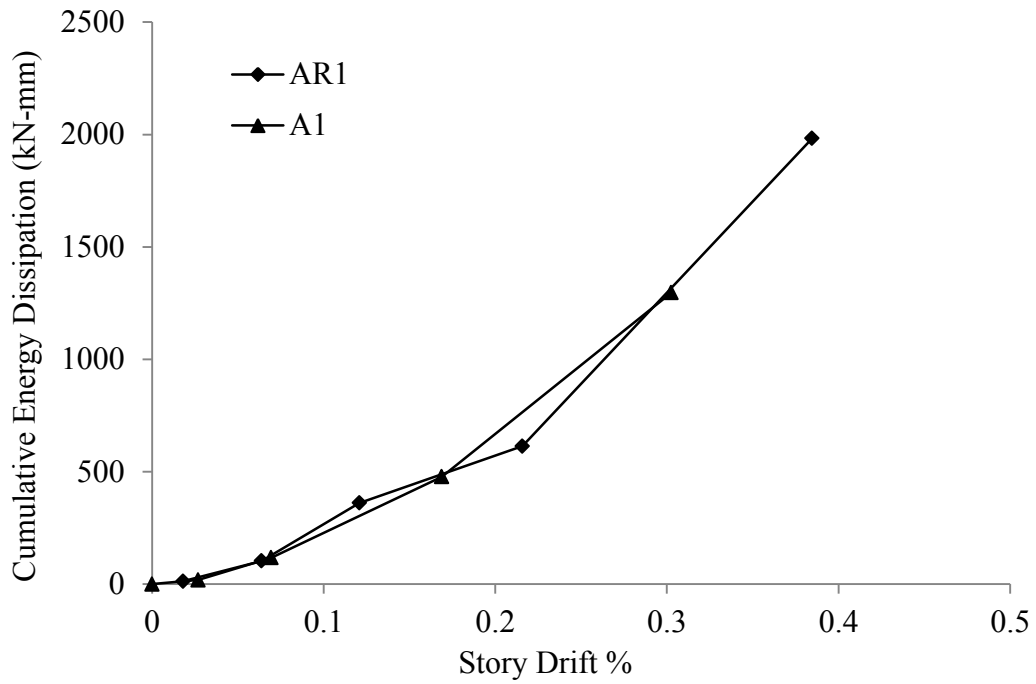


Figure 4.6(a) Comparison of cumulative energy dissipation in each loading cycle with respect to story drift in original specimen A1 and AR1

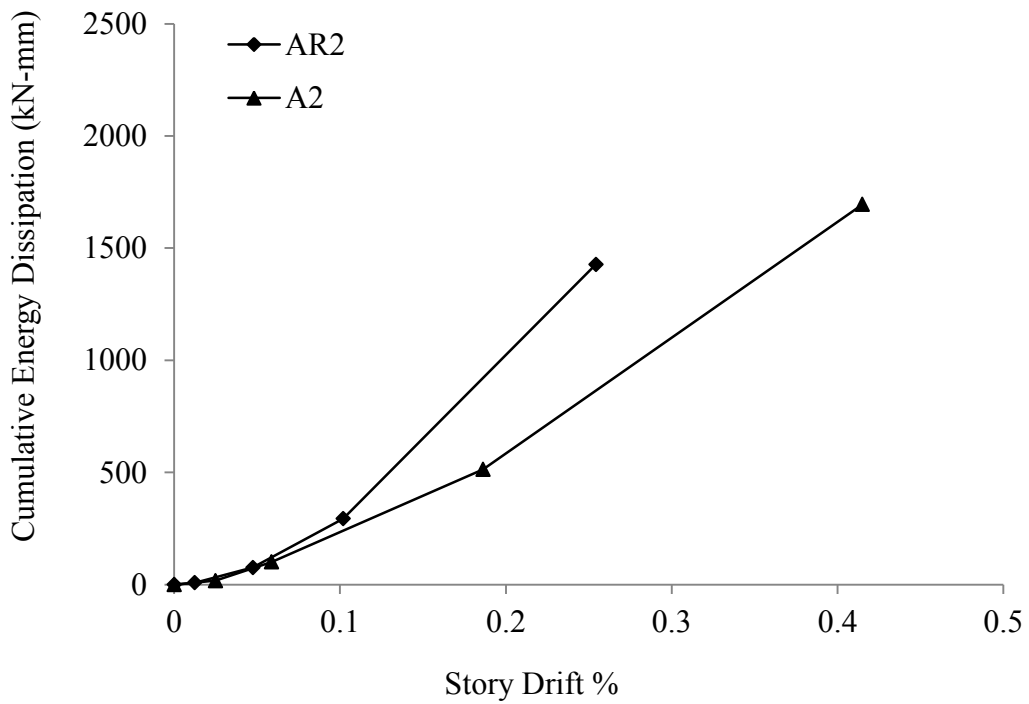


Figure 4.6(b) Comparison of cumulative energy dissipation in each loading cycle with respect to story drift in repaired specimens A2 and AR2

#### 4.2.6 Comparative energy dissipation of the original and the repaired infilled RC frames

Figure 4.6(a) and 4.6(b) represent the comparative cumulative energy dissipation behavior (sample calculation of energy dissipation is shown in Appendix E) for respective story drift of FC laminated repaired frames AR1, AR2 with original frames A1 and A2. The energy dissipated in each load cycle is evaluated as the area covered by the corresponding hysteretic loop.

The Figure 4.6(a) and (b) signify that cumulative energy dissipation of AR1 was same as original frame A1 as both the specimens experienced similar mode of failure in infills.

#### 4.2.7 Displacement ductility ratio of the original and the repaired infilled RC frames

**Table 4.3 Ductility Ratio of Test Model Specimens**

Description	Model A1	Model A2	Model AR1	Model AR2
Shear load at first yielding of steel (kN)	89	89	133	133
Displacement at 1 <sup>st</sup> yielding of steel (mm)	0.95	0.93	1.93	1.46
Maximum lateral load (kN)	169	178	222	178
Displacement at maximum shear load (mm)	5.73	6.64	8.40	6.37
Ductility ratio, $\mu$	6.03	7.14	4.35	4.36

Table 4.3 summarizes the ductility ratio of original brick infilled RC frame models (A1 and A2) and FC laminated repaired models (AR1 and AR2). Here the ductility ratio is defined as the ratio of the displacement of frame at maximum shear load to the displacement at 1<sup>st</sup> yielding of steel. The yielding of reinforcing steel seems already had been occurred in A1 and A2. Therefore, it is anticipated that only the embedded wire meshes in ferrocement have been yielded for the repaired specimens. It is observed that shear load at first yielding of FC wire mesh was 133 kN both for AR1 and AR2 which was around 40% larger than the original specimens A1 and A2.

### 4.3 Experimental Results for Bare RC Frames

The experimental results on the bare RC original frames and the FC laminated repaired bare RC frames are summarized in the following Table 4.4. Along with, the failure mechanisms of the original and the repaired bare RC frames are described in Table 4.4.

**Table 4.4 Summary of Experimental Results for B1, B2, BR1 and BR2**

Description	B1	B2	BR1	BR2
Frame cracking load (kN)	9	7	16	9
Displacement at frame cracking load (mm)	2.97	1.51	6.68	4.26
Maximum lateral load (kN)	27	42	36	42
Displacement at maximum lateral load (mm)	14.33	27.09	19.92	40.30
Initial stiffness at first crack (kN/mm)	3	4	2	2

**Table 4.5 Failure Mechanism of Original and Repaired Bare RC Frames**

Test Model	Failure Mechanism
B1	Flexural cracks and yielding of reinforcement in tension zones of the RC frame with diagonal cracks in beam –column joints
B2	Flexural cracks and yielding of reinforcement in tension zones of the RC frame with diagonal cracks in beam –column joints
BR1	Flexural cracks in the tension zones of the RC frame with diagonal cracks in beam –column joints and yielding of FC wire mesh
BR2	Flexural cracks in the tension zones of the RC frame with diagonal cracks in beam –column joints and yielding of FC wire mesh

#### 4.3.1 Crack patterns of the original frames B1 and B2

The crack patterns of original Bare RC frame models B1 and B2 at maximum lateral loads are shown in Figure 4.7(a) and Figure 4.7(b) respectively. Initial flexural cracks started to develop in columns in tension zones during the second load cycle (9 kN and 7 kN respectively). Initial stiffness at cracking loads were around 3 kN/mm and 4 kN/mm respectively for B1 and B2. During the final loading cycle (27 kN and 42 kN respectively), both specimens B1 and B2 experienced prominent

flexural cracks along the columns and beams at tension zones and diagonal cracks in beam-column joints.



Figure 4.7(a) Crack patterns at maximum lateral load in RC Bare frame model specimen B1



Figure 4.7(b) Crack patterns at maximum lateral load in RC Bare frame in specimen B2





Figure 4.8(a) Crack patterns at peak load in Repaired RC Bare frame model specimen BR1



Figure 4.8(b) Crack patterns at peak load in repaired RC Bare frame specimen BR2

### **4.3.2 Crack patterns of the repaired frame BR1 and BR2**

The crack patterns of BR1 and BR2 at failure loads are shown in Figure 4.8(a) and Figure 4.8(b) respectively. In the test models BR1 and BR2, initial flexural cracks generated in the columns and beams during the second loading cycle in 16 kN and 9 kN respectively. During the final loading cycle (36 kN and 42 kN respectively), both specimens BR1 and BR2 experienced flexural cracks along the columns and beams at tension zones and diagonal shear cracks in beam-column joints. BR1 and BR2 yielded with major tensile cracks in the frame at the same locations as in the original frames. This was due to the fact that the cracks in the original frames were not repaired; instead, the whole frame was coated with FC overlay to determine the shear and flexural capacity of the repair material itself. This left the crack zones weaker than the other parts of the frame. Consequently, the yielding of the repaired frames was governed by the tensile strength of the FC wire mesh overlaid on the frames. It was, however, observed that the extent of crack openings (width of crack opening) in the FC laminated frames was significantly smaller than those of original frames. On the other hand, the cracks were more dispersed in the FC laminated repaired frames. This reveals the capability of FC in protecting the damaged structure from large deformation.

### **4.3.3 Shear capacity of the original and the repaired bare RC frames**

Table 4.4 presents the shear capacities of bare RC frames B1 and B2 at yielding as 27 kN and 42 kN respectively. Nonetheless, after the frame was repaired using FC overlay, the in-plane shear capacity for BR1 (36 kN) became 33% higher than that of original frame B1. For BR2, the maximum shear capacity (42 kN) against in-plane cyclic load was unchanged compared to original frame B2. The lateral load-displacement characteristics of the original and repaired frames are shown in Figure 4.9(a) and Figure 4.9(b) clearly demonstrating the effectiveness of the repair methodology using FC overlay. It can be inferred that the capacity of repaired frame was depended on the tensile strength of Ferrocement overlay. It can be thus said that the combined shear capacity of the two layers of FC is higher or at least equal to the RC frame.

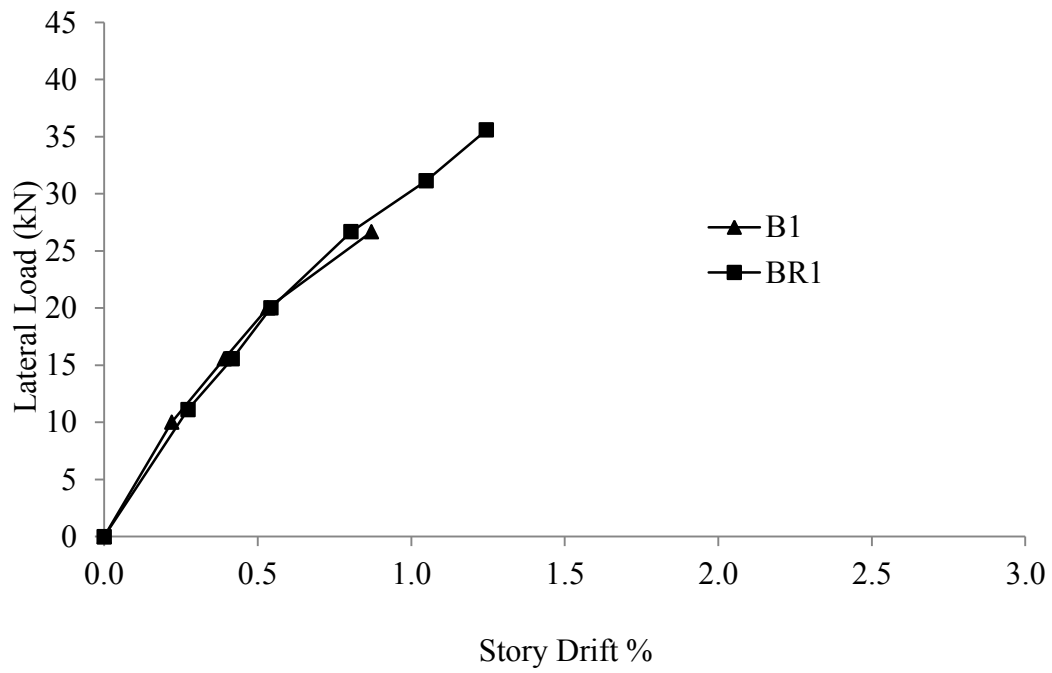


Figure 4.9(a) Lateral Load versus Story Drift in Original and Repaired Bare RC Frames (B1, BR1)

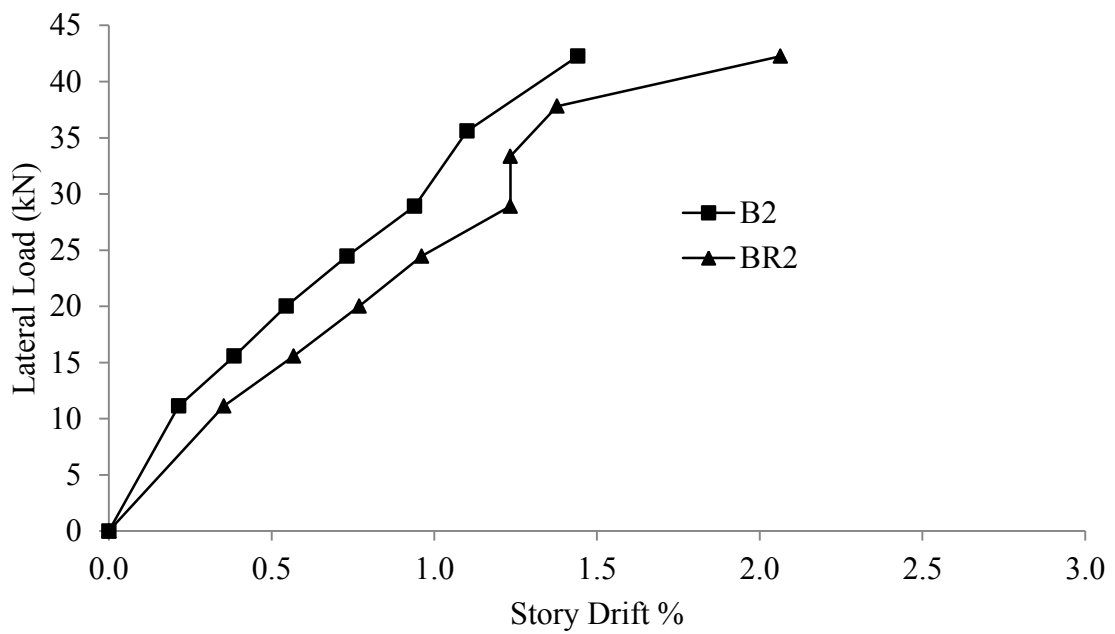


Figure 4.9(b) Lateral Load versus Story Drift in in Original and Repaired Bare RC Frames (B2, BR2)

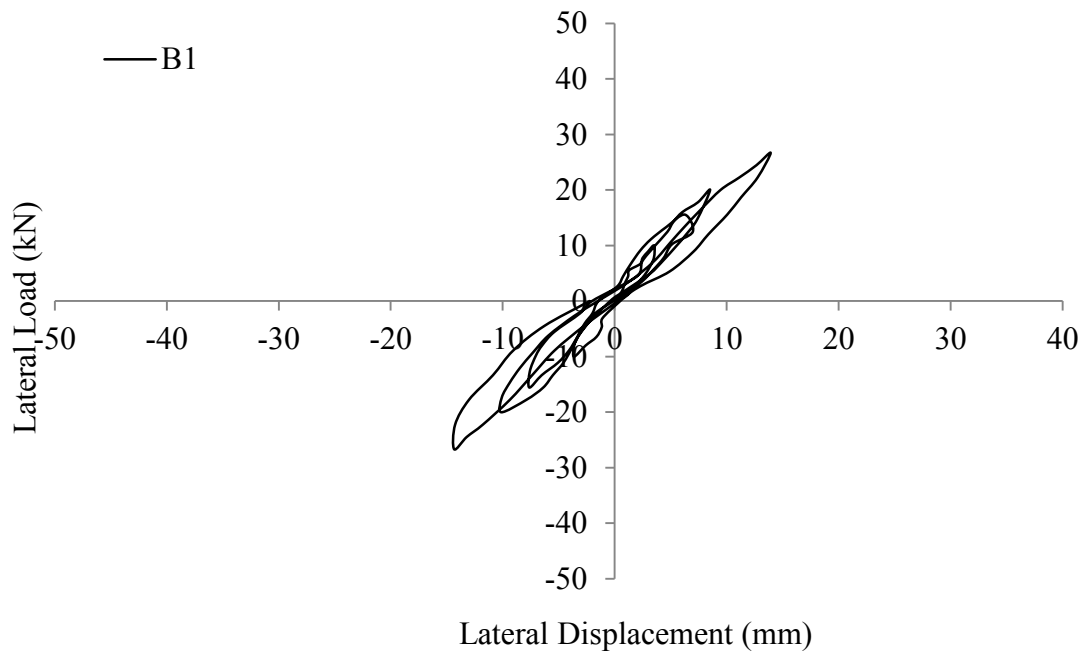


Figure 4.10(a) Hysteretic load-displacement curves in Test Model B1

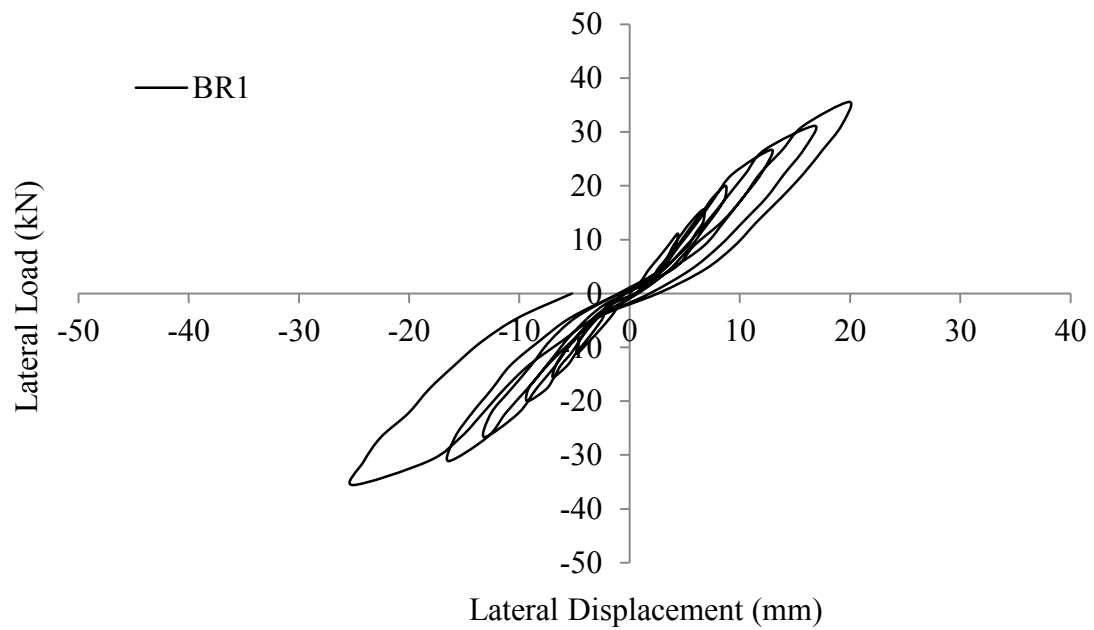


Figure 4.10(b) Hysteretic load-displacement curves in Test Model BR1

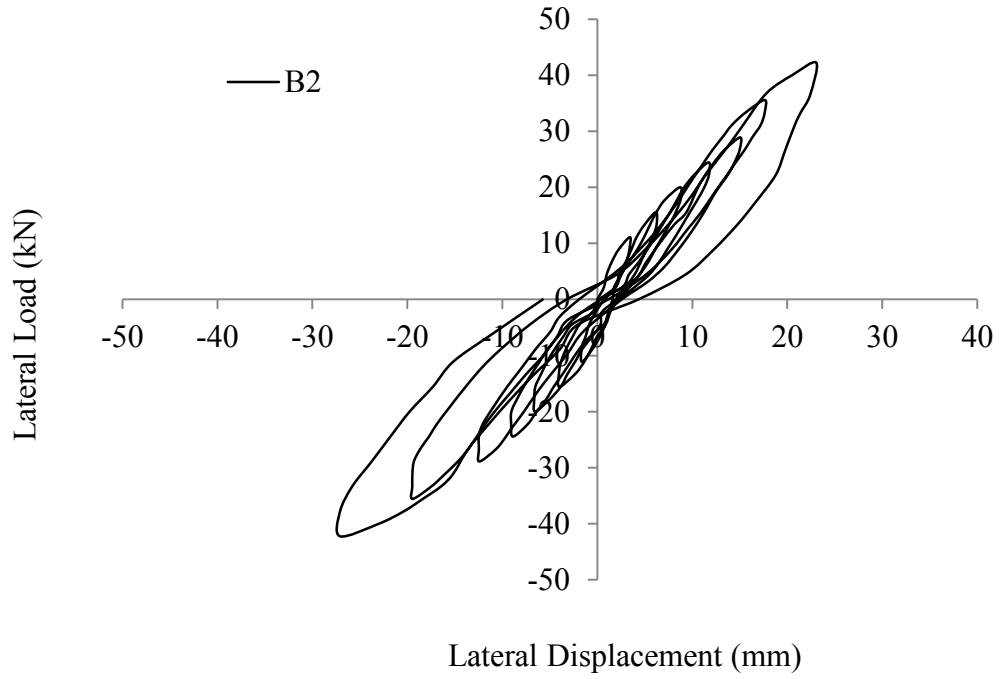


Figure 4.10(c) Hysteretic load-displacement curves in Test Model B2

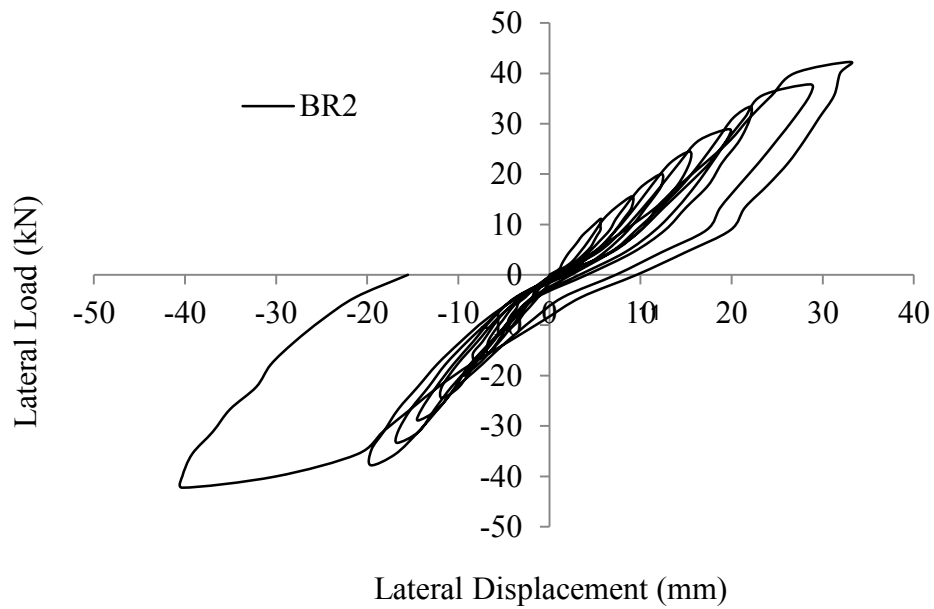


Figure 4.10(d) Hysteretic load-displacement curves in Test Model BR2

#### **4.3.4 Comparative hysteretic behavior of the original and the repaired frames bare RC frame**

The hysteretic behaviors of original bare RC frame specimens B1, B2 and repaired specimens BR1, BR2 are presented in Figure 4.10(a)-(d). According to load-deflection behavior, original bare RC frames and repaired bared RC frame with FC exhibited basically same or larger peak load.

#### **4.3.5 Comparative lateral stiffness of the original and the repaired bare RC frames**

Table 4.4 shows initial stiffness of original frames B1 and B2 along with repaired frames BR1 and BR2 obtained from the experimental results. The lateral stiffness of the specimens before the generation of cracks is defined as the initial stiffness (Imran & Aryanto, 2009). It has been revealed that the initial stiffness of the repaired frame BR1 was around 22% less than the original frame B1. And for BR2, the initial stiffness became around 52% less than the original frame B2.

Furthermore, Figure 4.11(a) and Figure 4.11(b) illustrate comparative stiffness degradation with respect to story drift at peak loads in each cycle establishing that stiffness degradation as well as story drift was higher in case of repaired specimens BR1 and BR2.

#### **4.3.6 Comparative energy dissipation of the original and the repaired bare RC frames**

Figure 4.12(a) and Figure 4.12(b) represents the comparative cumulative energy dissipation behavior for respective story drift of FC laminated repaired frames BR1, BR2 with original frames B1 and B2. The energy dissipated in each load cycle is evaluated as the area covered by the corresponding hysteretic loop. The Figure 4.12(a) and Figure 4.12(b) signify that cumulative energy dissipation of BR1 and BR2 were higher than the original frame B1 and B2 due to higher energy dissipation capacity of FC laminates.

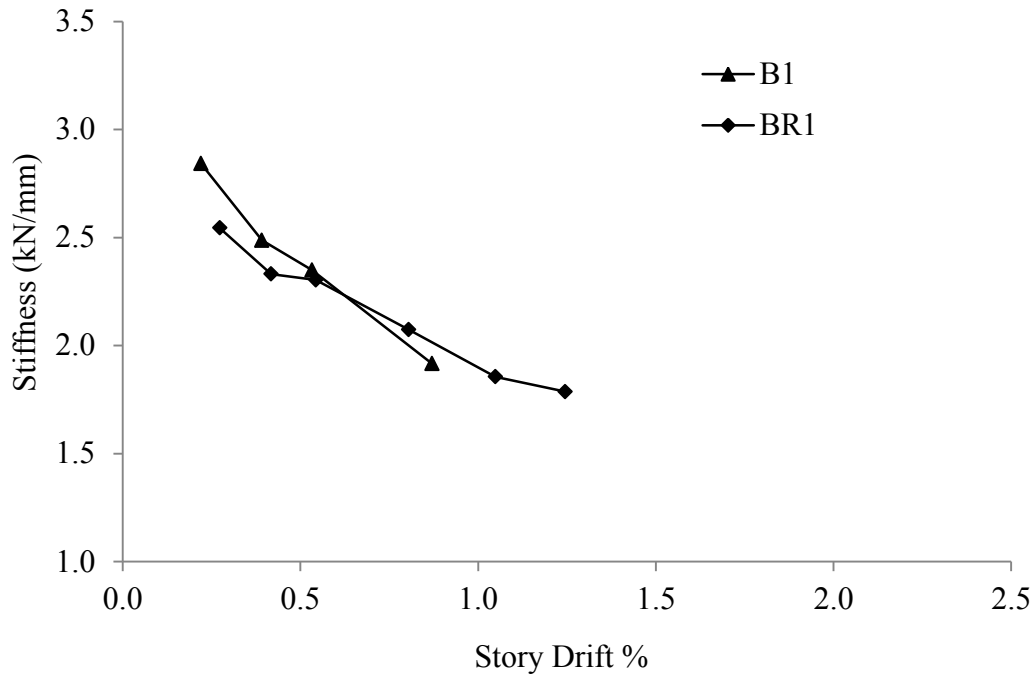


Figure 4.11(a) Comparison of stiffness degradation in each loading cycle with respect to story drift in original specimen B1 and BR1

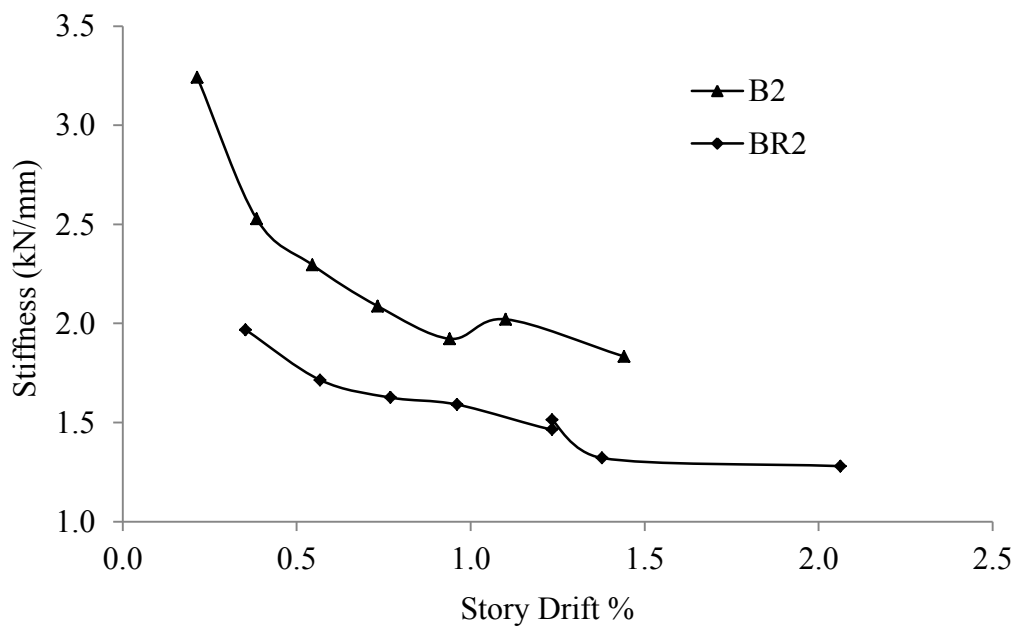


Figure 4.11(b) Comparison of stiffness degradation in each loading cycle with respect to story drift in repaired specimens B2 and BR2

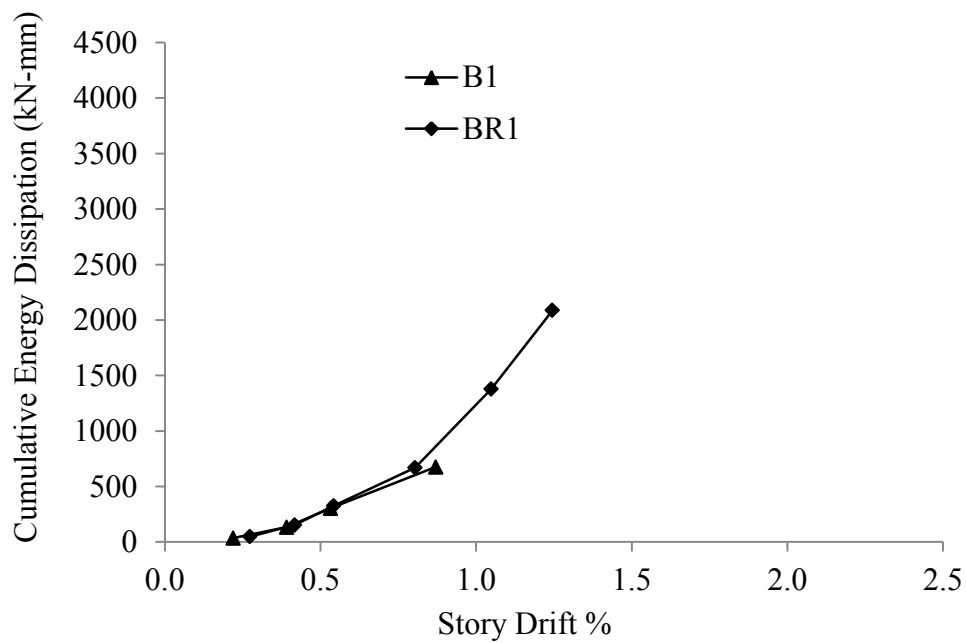


Figure 4.12(a) Comparison of cumulative energy dissipation with respect to story drift in original specimen B1 and BR1

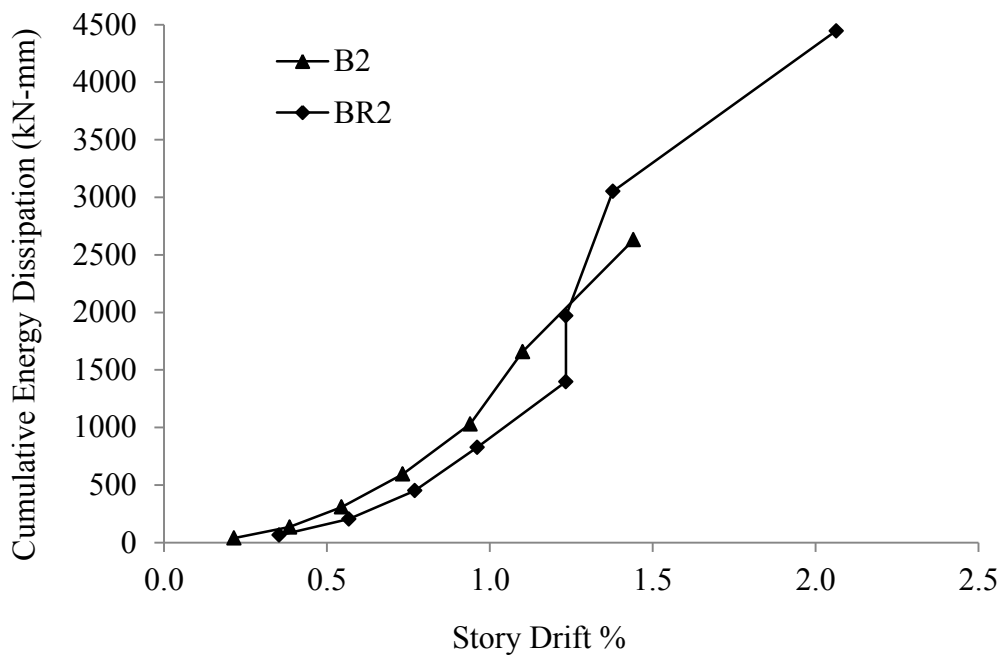


Figure 4.12(b) Comparison of cumulative energy dissipation with respect to story drift in repaired specimens B2 and BR2



#### 4.3.7 Displacement ductility ratio of the original and the repaired bare RC frames

Table 4.6 summarizes the ductility ratio of original bare RC frame models (B1 and B2) and FC laminated repaired models (BR1 and BR2). It should be noted that yielding of reinforcing steel already had been occurred in B1 and B2. Therefore, only the embedded wire meshes in ferrocement have been yielded for the repaired specimens. It is observed that highest recorded lateral load at yielding of FC wire mesh was 36 kN for BR1 and 42 kN for BR2. The ductility ratio with respect to maximum recorded lateral load for BR1 and BR2 were around 2.

**Table 4.6 Ductility Ratio of Bare RC Frame Specimens**

Description	Model B1	Model B2	Model BR1	Model BR2
Shear load at first yielding of steel (kN)	16	31	22	36
Displacement at 1 <sup>st</sup> yielding of steel (mm)	6.04	14.17	9.36	23.34
Maximum lateral load (kN)	27	42	36	42
Displacement at maximum shear load (mm)	14.33	27.09	19.92	40.30
Ductility ratio, $\mu$	2.37	1.91	2.13	1.73

#### 4.4 Experimental results for isolated brick infilled RC frames

The experimental results on the isolated brick infilled RC original frames and the FC laminated repaired isolated infilled RC frames are summarized in the following Table 4.7. Along with, the failure mechanisms of the original and the repaired isolated infilled RC frames are described in Table 4.8.

**Table 4.7 Summary of experimental results for C1, C2, CR1 and CR2**

Description	C1	C2	CR1	CR2
Frame cracking load (kN)	67	89	107	45
Displacement at frame cracking load (mm)	1.27	1.20	1.41	0.25
Infill cracking load (kN)	NA	NA	NA	80
Displacement at infill cracking load (mm)	NA	NA	NA	0.89
Maximum lateral load (kN)	111	107	174	187
Maximum Displacement (mm)	18.26	30.84	19.72	30.84
Initial stiffness (kN/mm) at first crack	105	74	75	178

**Table 4.8 Failure mechanism of original and repaired isolated infilled frames**

Test Model	Failure Mechanism
C1	Flexural cracks in columns and beams; shear cracks in columns near beam-column joints; cracks along the wire mesh attached as horizontal support at the periphery of isolated wall and the surrounding RC frames; no cracks in isolated brick infilled wall
C2	Flexural cracks in columns and beams; shear cracks in columns near beam-column joints; cracks along the wire mesh attached as horizontal support at the periphery of isolated wall and the surrounding RC frames; no cracks in isolated brick infilled wall
CR1	Flexural cracks in columns and beams; shear cracks in columns near beam-column joints; cracks along the wire mesh attached as horizontal support at the periphery of isolated wall and the surrounding RC frames; no cracks in isolated brick infilled wall
CR2	Flexural cracks in columns and beams; shear cracks in columns near beam-column joints; diagonal tension cracks in isolated brick infilled wall

#### 4.4.1 Crack patterns of the original frames C1 and C2

The crack patterns of original isolated brick infilled RC frame models C1 and C2 at maximum lateral loads are shown in Figure 4.13(a) and Figure 4.13(b). The specimen C1 and C2 experiences diagonal tensile cracks along the wire mesh laminated along the periphery of the isolated wall and the surrounding frame at second load cycle at 80 kN and 89 kN load respectively. Initial flexural cracks

started to develop in columns and beams during the second load cycle. Corner crushing of the isolated infill was observed in the 3<sup>rd</sup> load cycle at 133 kN load for C1 and at 156 kN for C2. During the final loading cycle (174 kN and 187 kN respectively), both specimens C1 and C2 experienced large extent of flexural cracks along the tension zones of the yielded RC columns, as well as diagonal shear cracks in columns near beam-column joints. Several flexural cracks also occurred in the beams at failure loads. Moreover, the bed joint failure of brick wall was also noted in the specimen C2 along the edge of the wire mesh laminated to the infill as a horizontal support.

#### **4.4.2 Crack patterns of repaired frame CR1 and CR2**

The crack patterns of CR1 and CR2 at failure loads are shown in Figure 4.14(a) and Figure 4.14(b). In the test models CR1 initial flexural cracks generated in columns during the third loading cycle (at 107 kN). Corner crushing of the isolated infill and flexural cracks in the beam were also observed in the same cycle. During the final load cycle (174 kN) diagonal shear failure of columns with yielding of reinforcement were noted in specimen CR1.

In the test models CR2 initial flexural cracks generated in columns during the 2<sup>nd</sup> loading cycle (at 45 kN). Diagonal shear cracks in columns and diagonal tension cracks in the infills were initiated in the third load cycle (at 80 kN). During the final load cycle (187 kN) diagonal shear failure of columns and with yielding of reinforcement and diagonal tension failure of the infill were noted. Shear sliding of the isolated infill and flexural cracks in the beam were also observed in the same cycle. A few flexural cracks in the beam were also observed.

The failure mechanism of CR2 indicates that the infill was substantially bonded with the base as well as with the columns due to the application of wire mesh with rich mortars along the periphery of the isolated infill and the surrounding RC frame as a support for the out of plane failure.

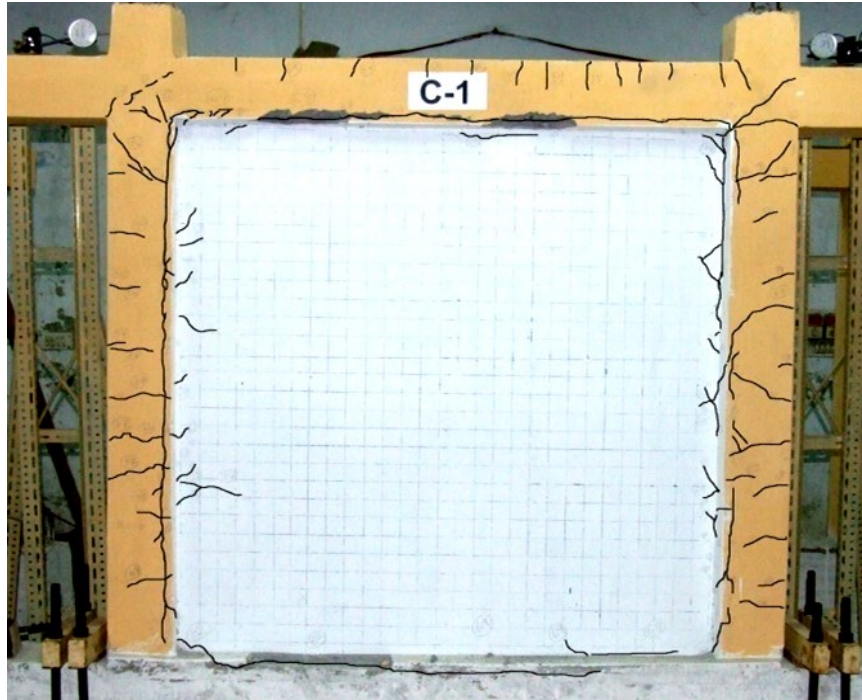


Figure 4.13(a) Crack patterns at maximum lateral load in isolated infilled RC frame model specimen C1



Figure 4.13(b) Crack patterns at maximum lateral load in isolated infilled RC frame specimen C 2

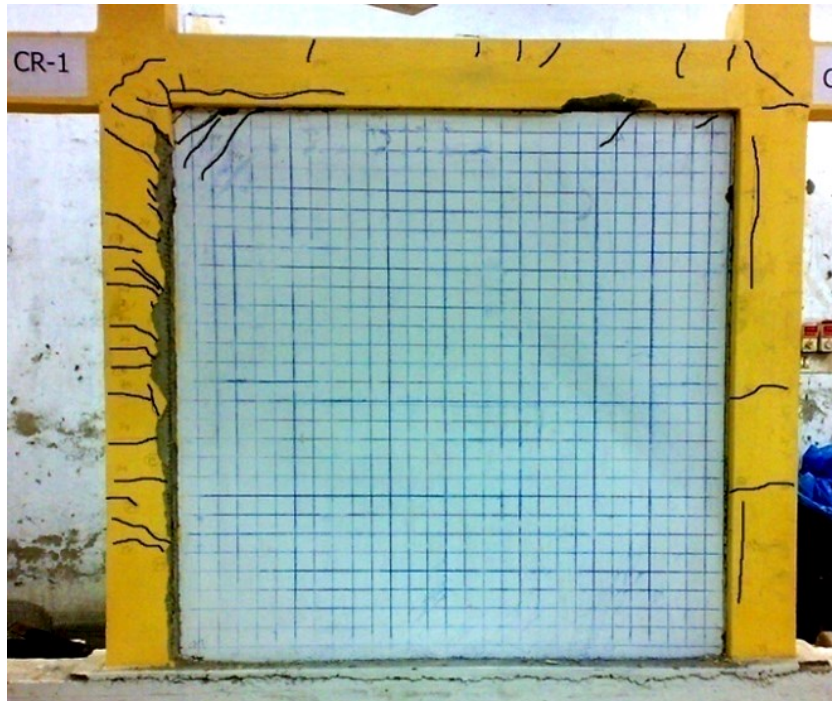


Figure 4.14(a) Crack patterns at peak load in repaired isolated infilled RC frame model specimen CR1



Figure 4.14(b) Crack patterns at peak load in repaired isolated infilled RC frame model specimen CR2

The width of the applied wire mesh was large enough to contribute to the in-plane strength of the overall frame. Moreover, due to the rich mortar plastering, a strong bond was developed in the FC laminates-RC columns-masonry wall composite. Consequently, cracks could not generate at the same location as previous major diagonal cracks. Strong infills-RC frame interaction led to shear failure of the RC frame due to unexpected stress concentration. It was, however, observed that the amount of crack openings (width of crack opening) in the FC laminated infill walls was significantly smaller than those of original frames. This reveals the superior capability of FC in protecting the damaged structure from large deformation as well as from environmental actions.

#### **4.4.3 Shear capacity of original and the repaired isolated infilled RC frames**

From Table 4.7, the maximum shear capacity of original isolated brick infilled RC frames C1 and C2 was noted as 111 and 107 kN respectively. Nonetheless, after the frame was repaired using FC overlay, the in-plane shear capacity for CR1 (174 kN) became 55% higher than that of original frame C1. For CR2, the maximum shear capacity (187 kN) against in-plane cyclic load was 75% increase compared to original frame C2. The comparative lateral load-displacement curves of the original and repaired isolated infilled RC frames are shown in Figure 4.15(a) and Figure 4.15(b) clearly demonstrating the effectiveness of the repair methodology using FC overlay for increasing shear capacity of the isolated infilled frame.

#### **4.4.4 Comparative hysteretic behavior of the original and the repaired isolated infilled RC frames**

The hysteretic behaviors of original isolated brick infilled RC frame specimens C1, C2 and repaired specimens CR1, CR2 are presented in Figure 4.16(a) and Figure 4.16(b).

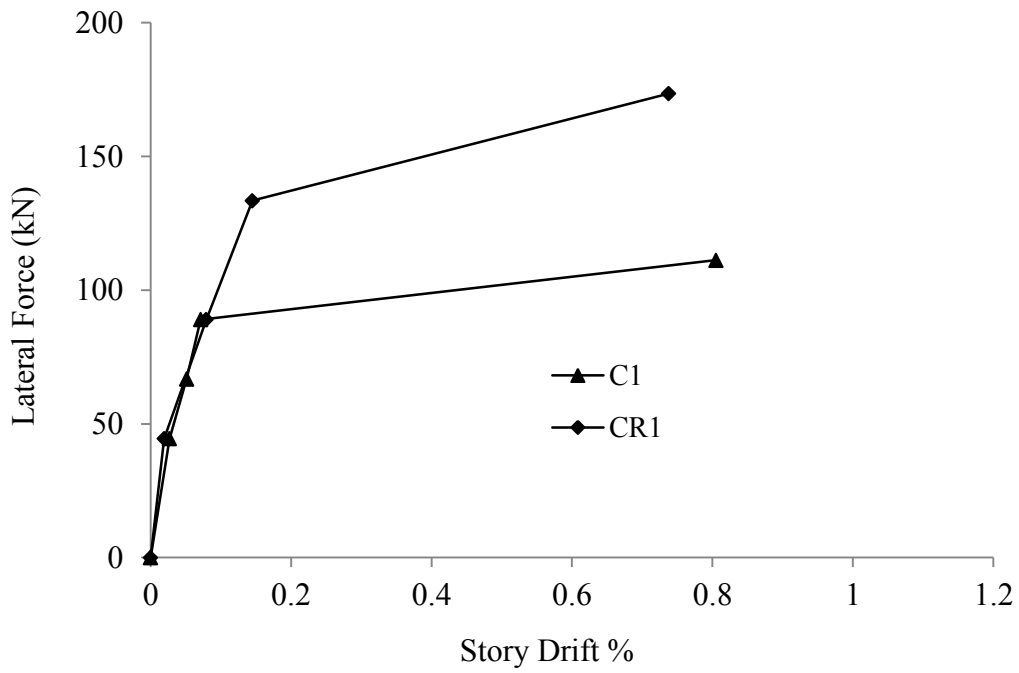


Figure 4.15(a) Comparative lateral forces versus story drift in each loading cycle in original isolated infilled RC frames (C1, C2)

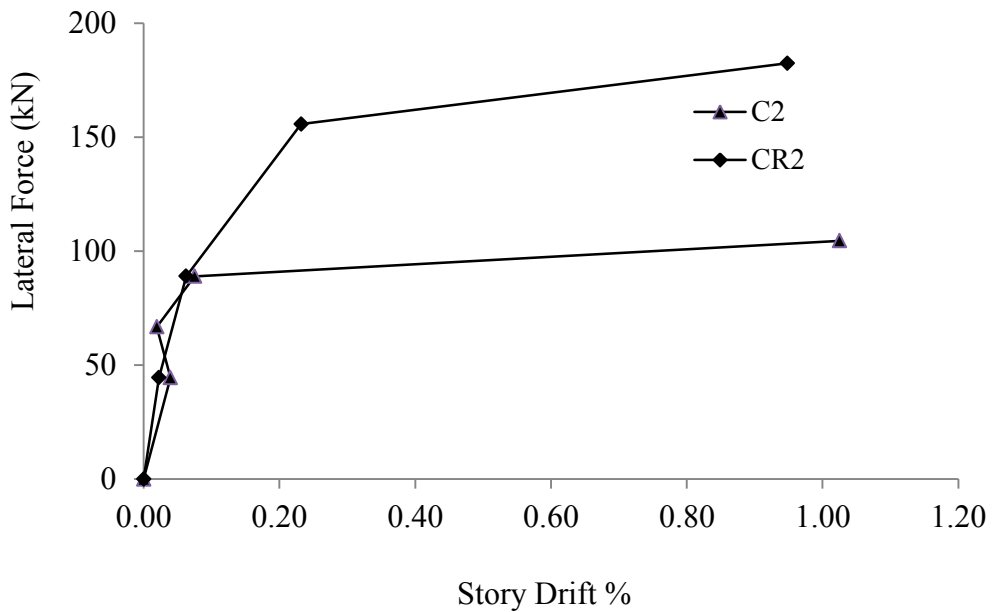


Figure 4.15(b) Comparative lateral forces versus story drift in each loading cycle in FC laminated repaired isolated infilled RC frames (CR1, CR2)

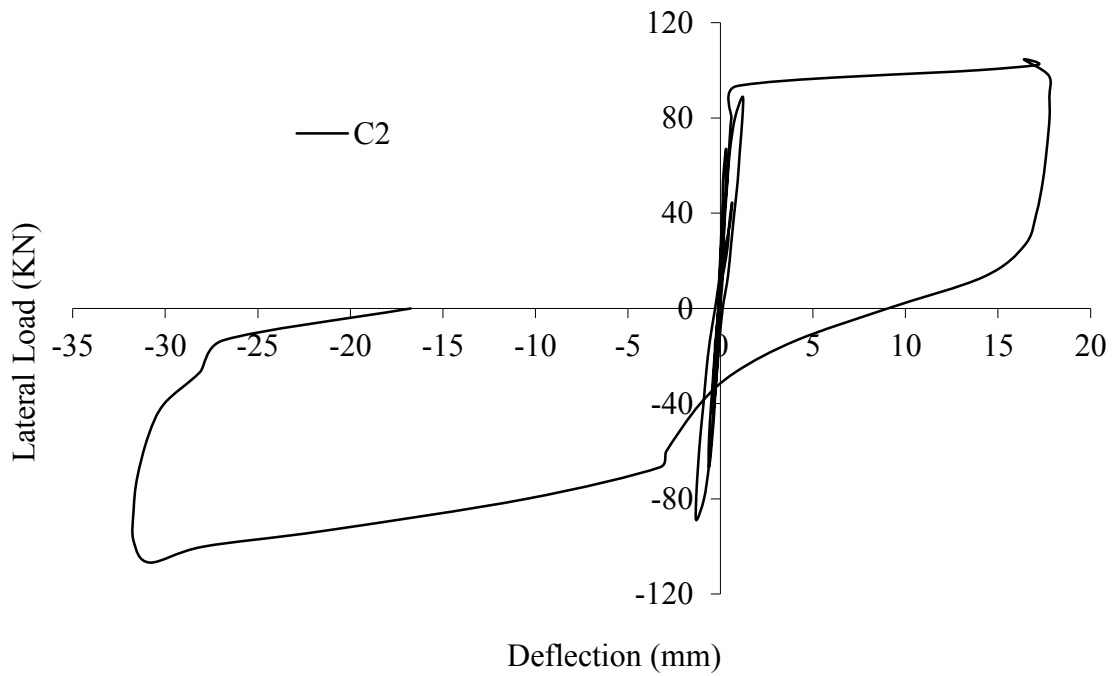
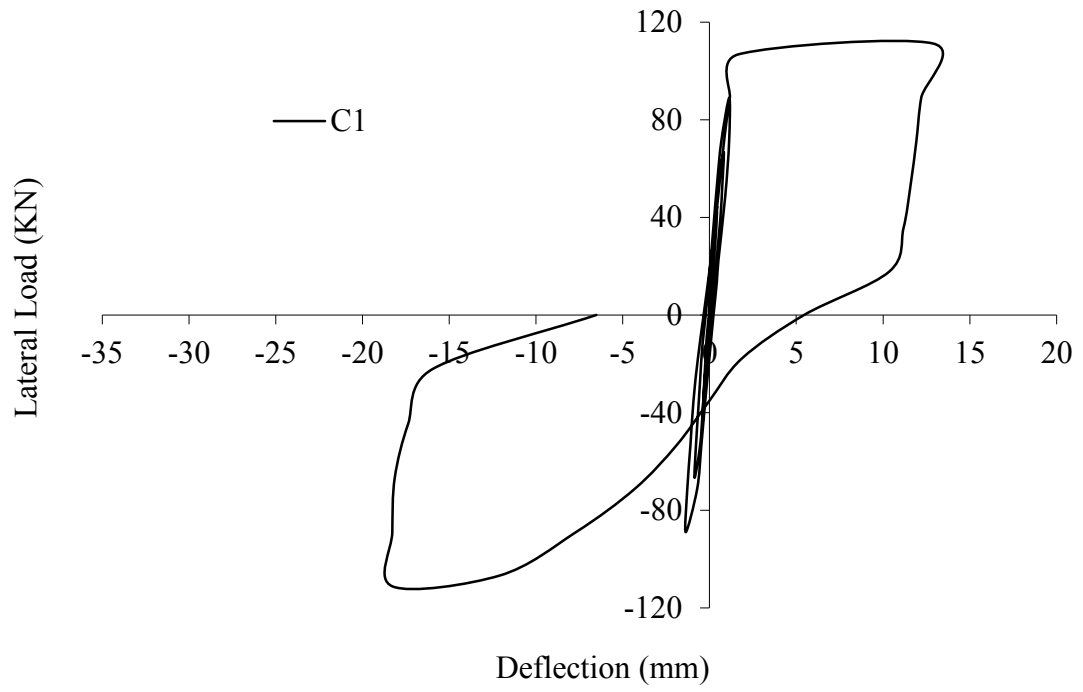


Figure 4.16(a) Hysteretic Load-Displacement Curves for Test Model C1 and C2



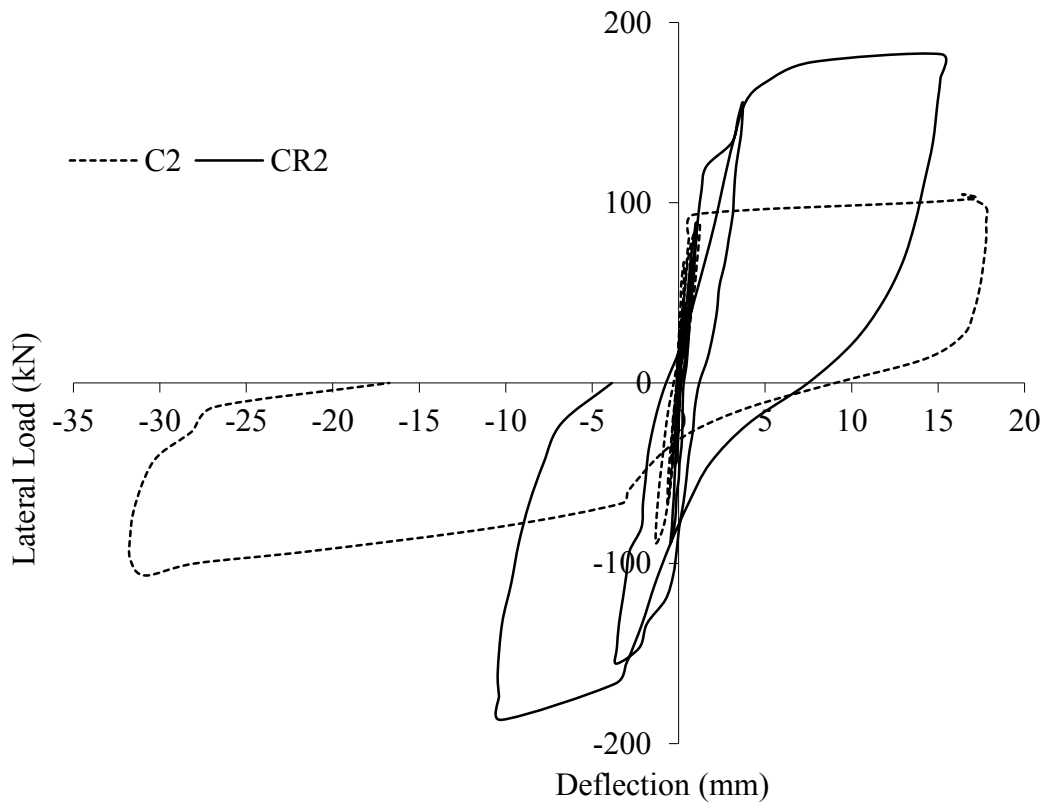
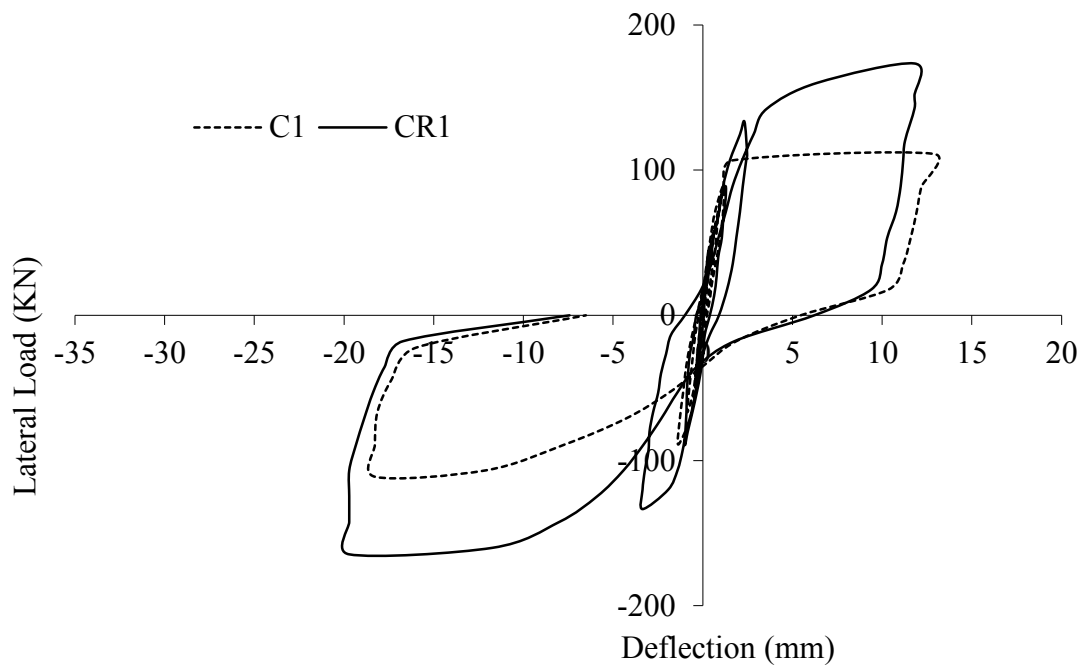


Figure 4.16(b) Comparison of Hysteretic Load-Displacement Curves between C1 and CR1 and between C2 and CR2

According to load-deflection behavior, initial stiffnesses of the original brick infilled RC frames were large until the generation of tensile cracks FC wire mesh along the connections of infill and the surrounding RC frames. Both the frames C1 and C2 exhibited large energy dissipation and lateral displacements after the compressive deformation of the filler materials (cork sheet). The FC laminated repaired isolated infilled RC frames CR1 and CR2 exhibited higher peak load less deformation compared to the original frames which indicate FC laminated repaired specimens exhibited better hysteresis behaviors as the more accelerated lateral displacements for similar intensity of lateral loads were observed in original specimens C1 and C2 compared to CR1 and CR2.

#### **4.4.5 Comparative lateral stiffness of original (C1, C2) and FC laminated repaired frames (CR1, CR2)**

Figure 4.17(a) and Figure 4.17(b) illustrate comparative stiffness degradation with respect to story drift at peak loads in each cycle establishing that stiffness degradation as well as story drift did not differentiate substantially for the original and the repaired specimens.

#### **4.5.6 Comparative energy dissipation of original (A1, A2) and FC laminated repaired frames (AR1, AR2)**

Figure 4.18(a) and Figure 4.18(b) represents the comparative cumulative energy dissipation behavior for respective story drift of FC laminated repaired frames CR1, CR2 with original frames C1 and C2. The energy dissipated in each load cycle is evaluated as the area covered by the corresponding hysteretic loop. The Figures 4.18(a) and 4.18(b) signify that cumulative energy dissipation of CR1 and CR2 was less as compared to the original frames C1 and C2.

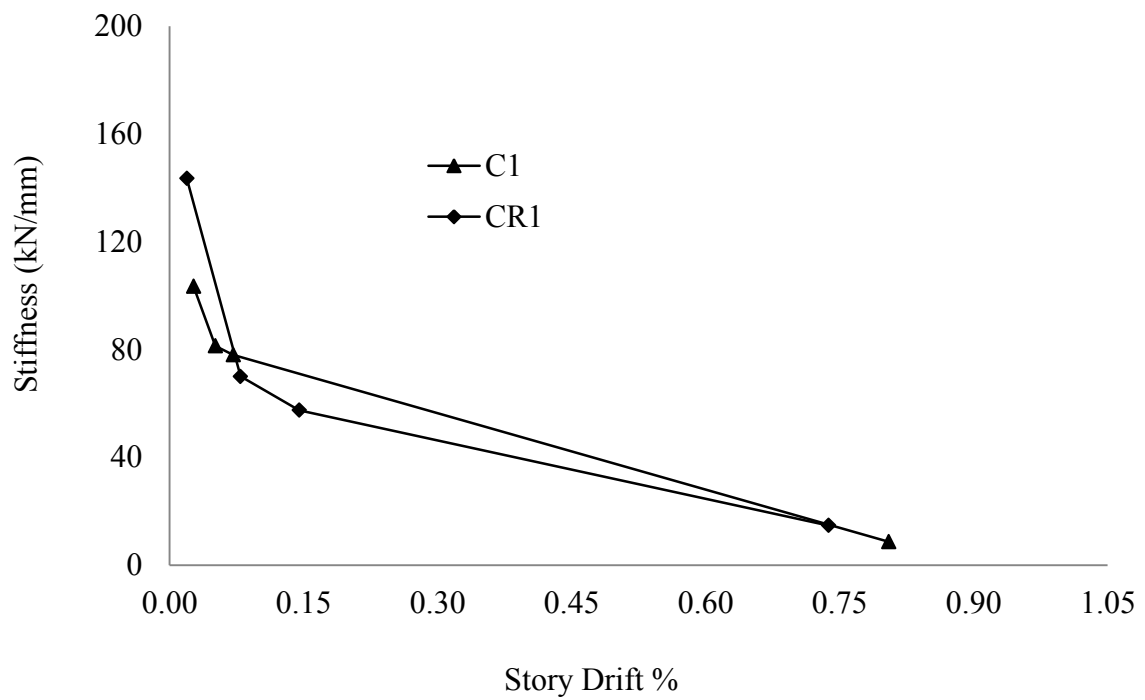


Figure 4.17(a) Comparison of stiffness degradation in each loading cycle with respect to story drift in original specimen C1

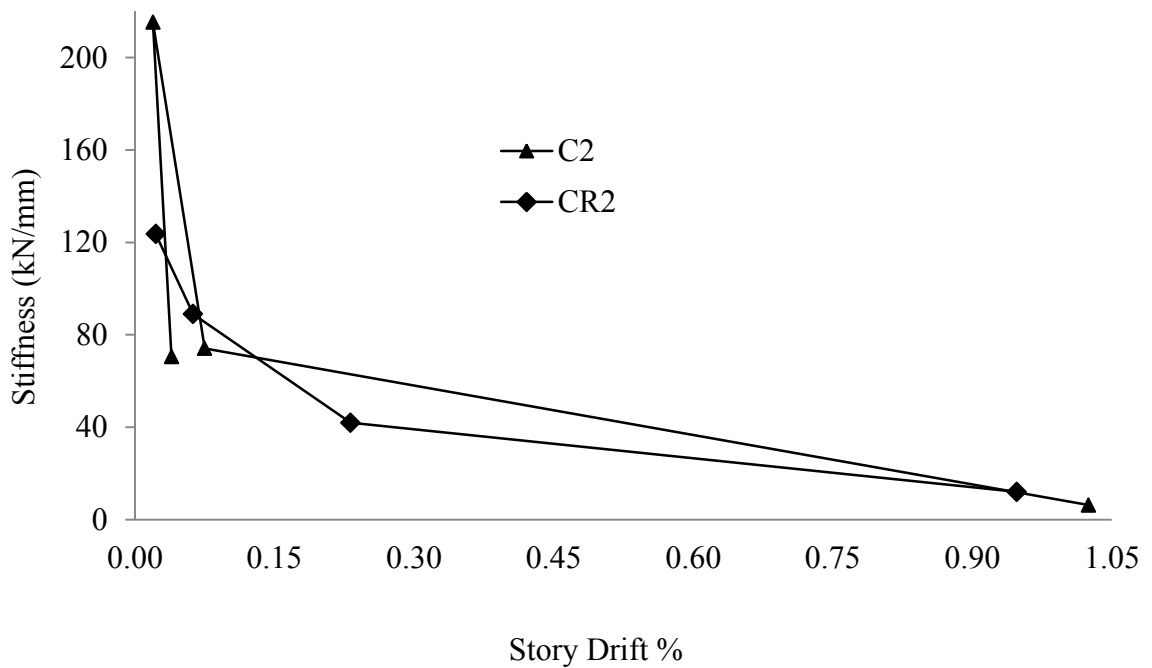


Figure 4.17(b) Comparison of stiffness degradation in each loading cycle with respect to story drift in repaired specimens C2 and CR2

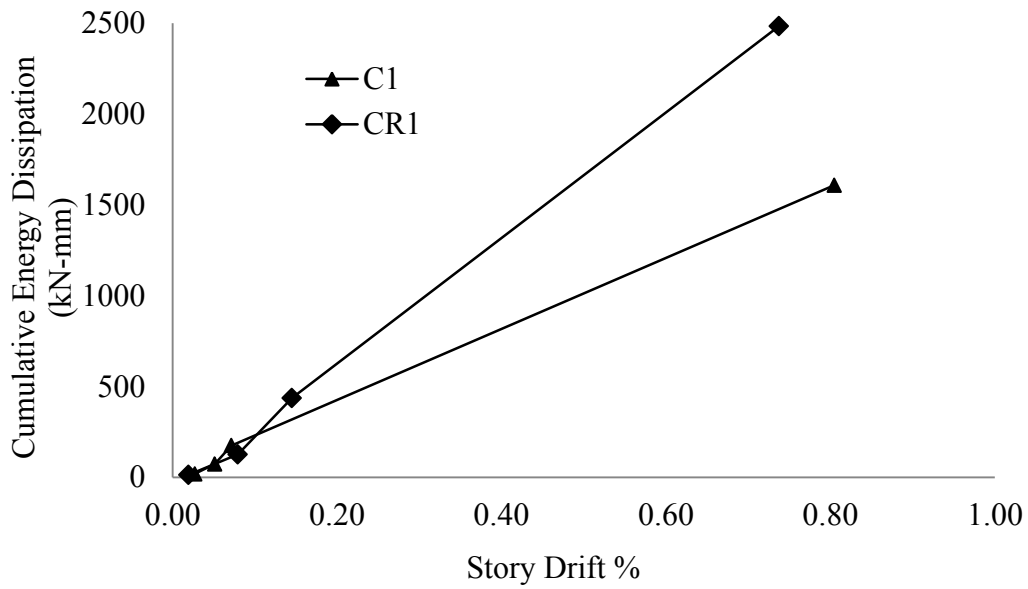


Figure 4.18(a) Comparison of cumulative energy dissipation in each loading cycle with respect to story drift in original specimen C1 and CR1

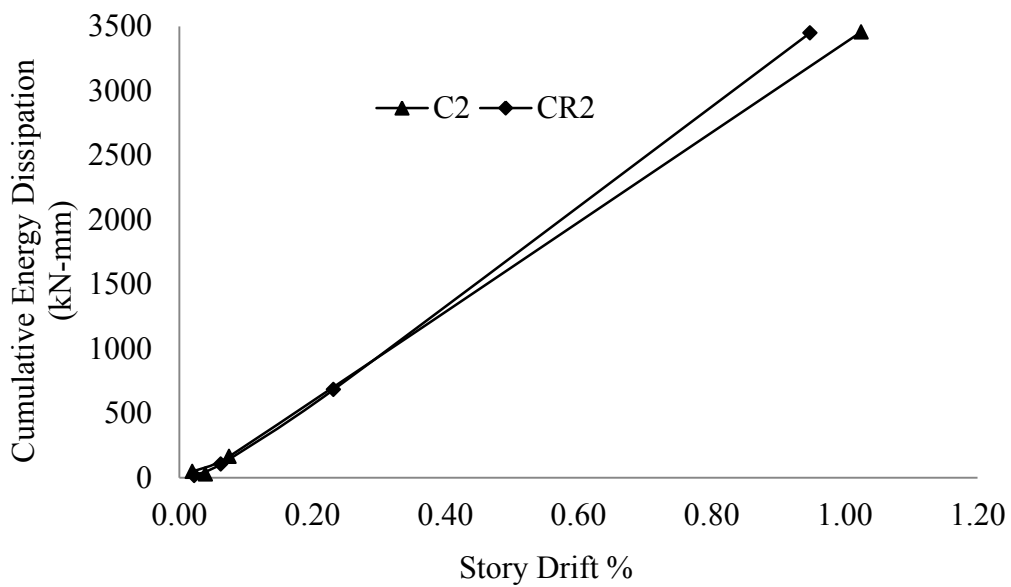


Figure 4.18(b) Comparison of cumulative energy dissipation in each loading cycle with respect to story drift in repaired specimens C2 and CR2

#### 4.5.7 Displacement ductility ratio of the original and the repaired isolated infilled RC frames

Table 4.9 summarizes the ductility ratio of original isolated brick infilled RC frame models (C1 and C2) and FC laminated repaired models (CR1 and CR2). It should be noted that yielding of reinforcing steel already had been occurred in C1 and C2. Therefore, only the embedded wire meshes in ferrocement have been yielded for the repaired specimens. It is observed that shear load at first yielding of FC wire mesh was 142 kN and 156 kN for CR1 and CR2 respectively which was around 33% and 66% larger than the original specimens C1 and C2.

**Table 4.9 Ductility Ratio of Test Model Specimens**

Description	Model C1	Model C2	Model CR1	Model CR2
Shear load at first yielding of steel (kN)	107	93	142	156
Displacement at 1 <sup>st</sup> yielding of steel (mm)	1.66	0.90	3.57	3.71
Maximum lateral load (kN)	111	105	174	187
Displacement at maximum shear load (mm)	12.88	16.40	11.80	15.17
Ductility ratio, $\mu$	7.76	18.22	3.30	4.08

Ductility ratio of the repaired frames CR1 and CR2 are 63% and 78% less than the original frames C1 and C2 respectively which proves the superior quality of FC laminates to keep the structural members in serviceability limits.

## **4.5 Comparative Cyclic Behaviors of Brick Infilled RC Frames, Bare RC Frames and Isolated Brick Infilled RC Frame**

### **4.5.1 Later forces versus story drift**

Figure 4.19 explains the story drifts with respect to the maximum lateral forces in each cycle for brick infilled RC frames, bare RC frames and the isolated infilled RC frames. Moreover, Figure 4.19 proves that isolated infilled RC frame exhibits the substantial lateral deformation similar to bare RC frames after initial stiffening characteristics akin to infilled RC frames until around 89 kN of lateral load.

### **4.5.2 Energy dissipation versus story drift**

Figure 4.20 explains the distinctive energy dissipation capacities with respect to story drifts in each cycle for brick infilled RC frames, bare RC frames and the isolated infilled RC frames. Figure 4.20 proves the substantial energy dissipation characteristics of the isolated infilled frames compared to brick infilled isolated RC frames and bare RC frames.

### **4.5.3 Stiffness versus story drift**

Figure 4.21 represent the differential stiffness degradation characteristics with respect to story drifts in each cycle for brick infilled RC frames, bare RC frames and the isolated infilled RC frames. Rapid degradation of stiffness for isolated infilled RC frame has been represented compared to the infilled RC frame.

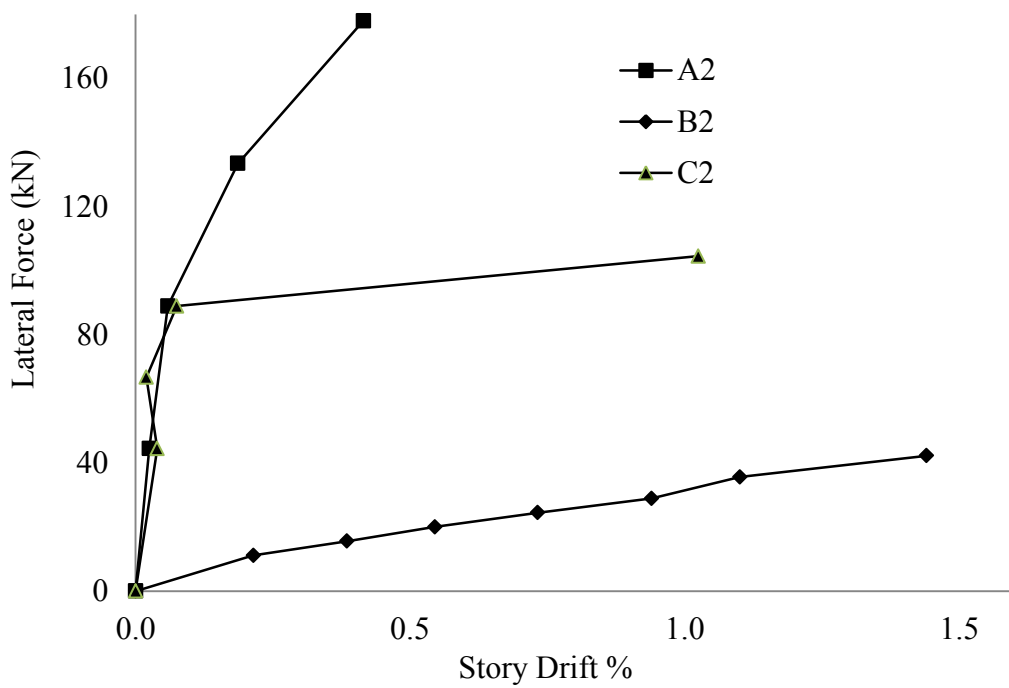
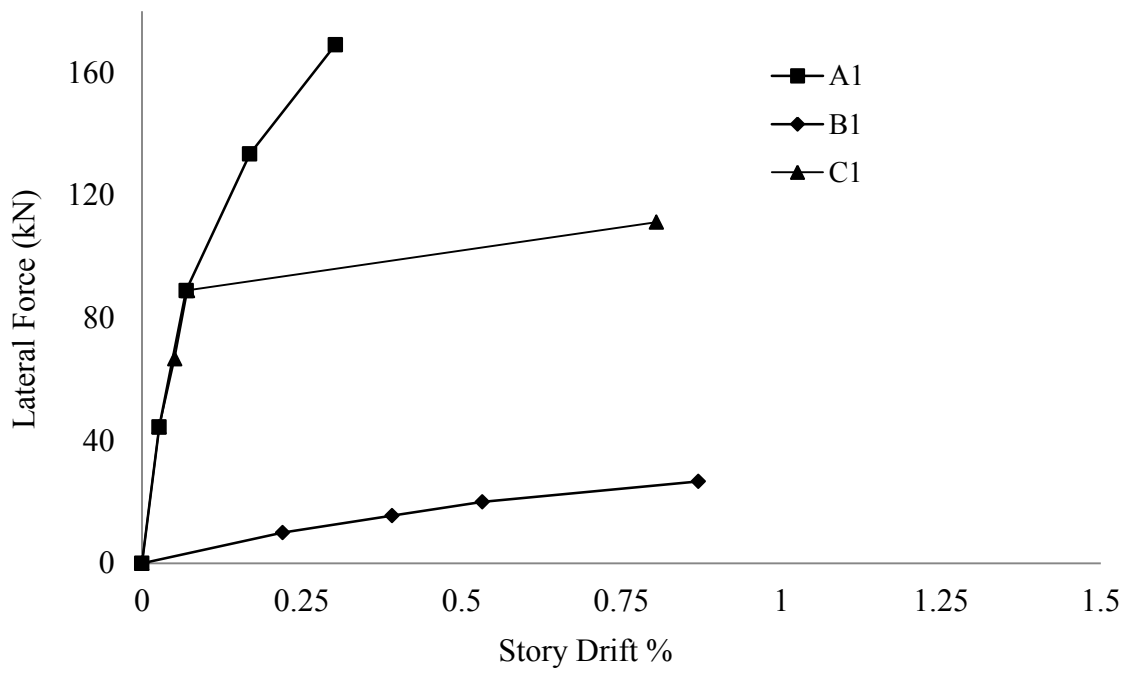


Figure 4.19 Comparison of story drift with respect to maximum lateral forces in each cycle for brick infilled RC frames (A1 and A2), Bare RC frame (B1 and B2) and isolated brick infilled RC frames (C1 and C2)

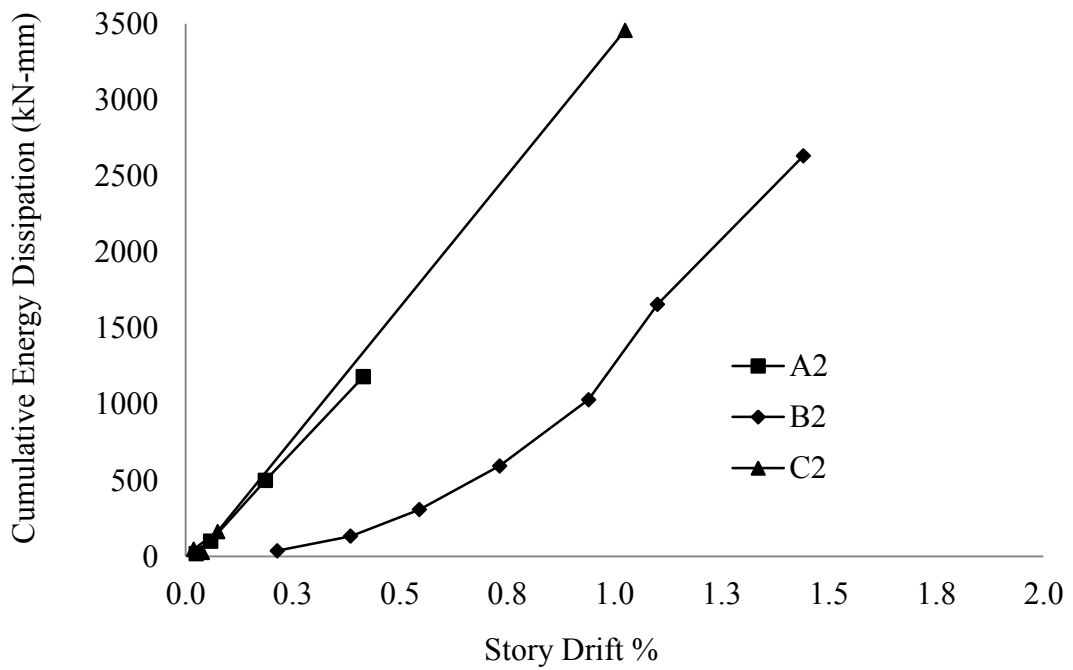
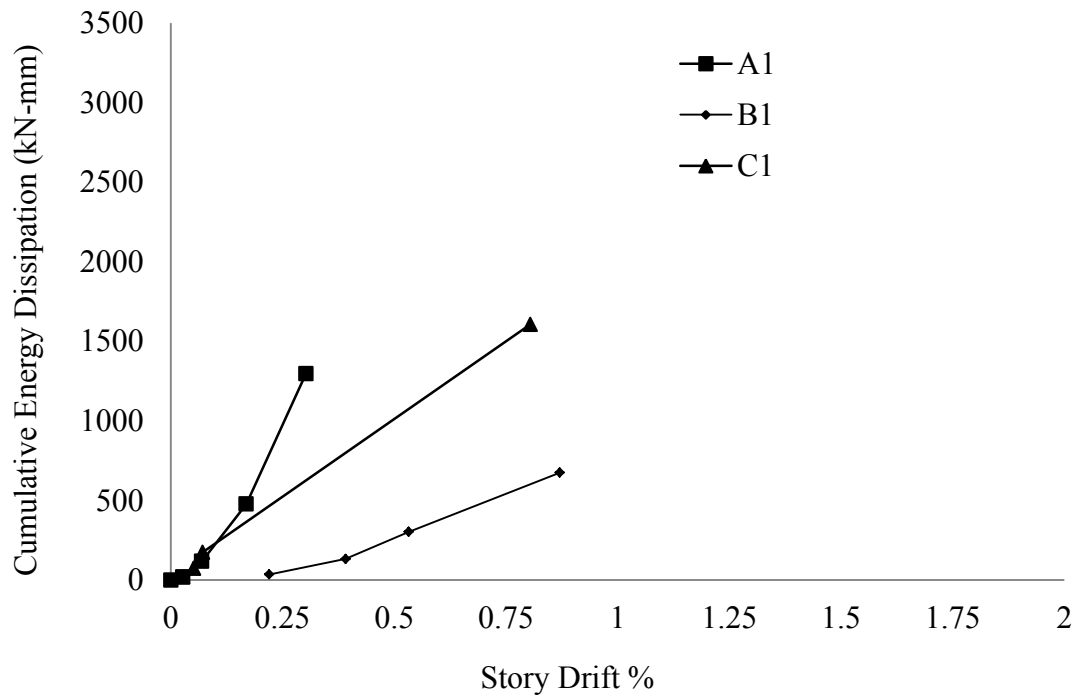


Figure 4.20 Comparison of story drift with respect to cumulative energy dissipation in each cycle for brick infilled RC frames (A1 and A2), Bare RC frame (B1 and B2) and isolated brick infilled RC frames (C1 and C2)



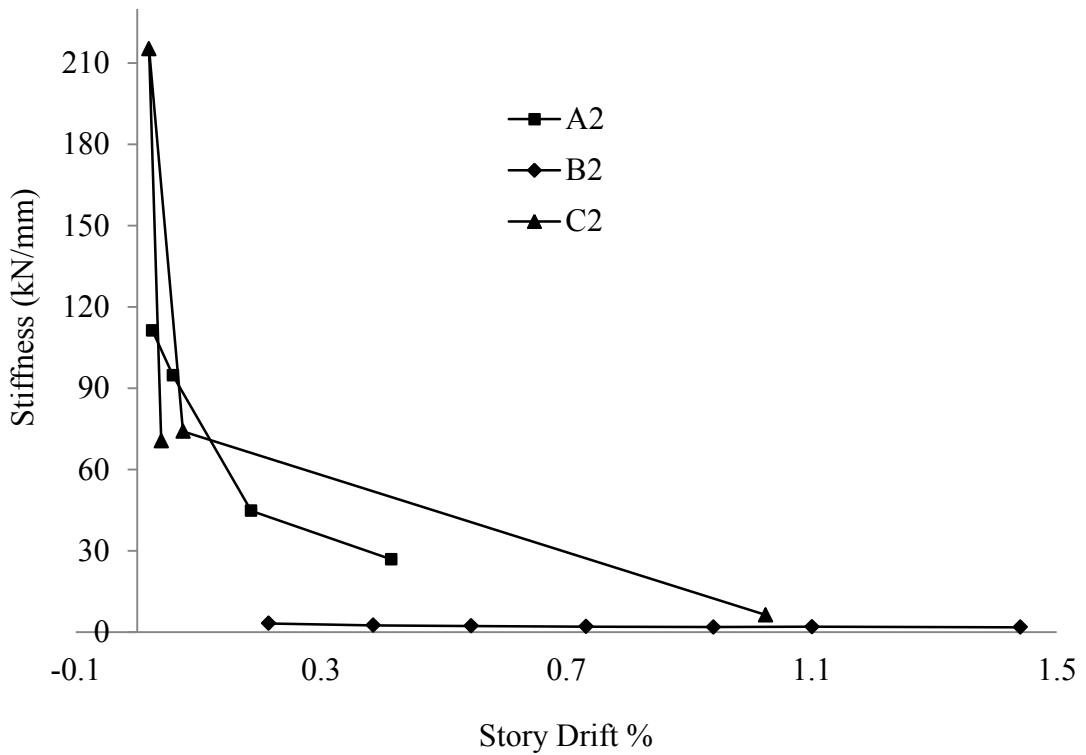
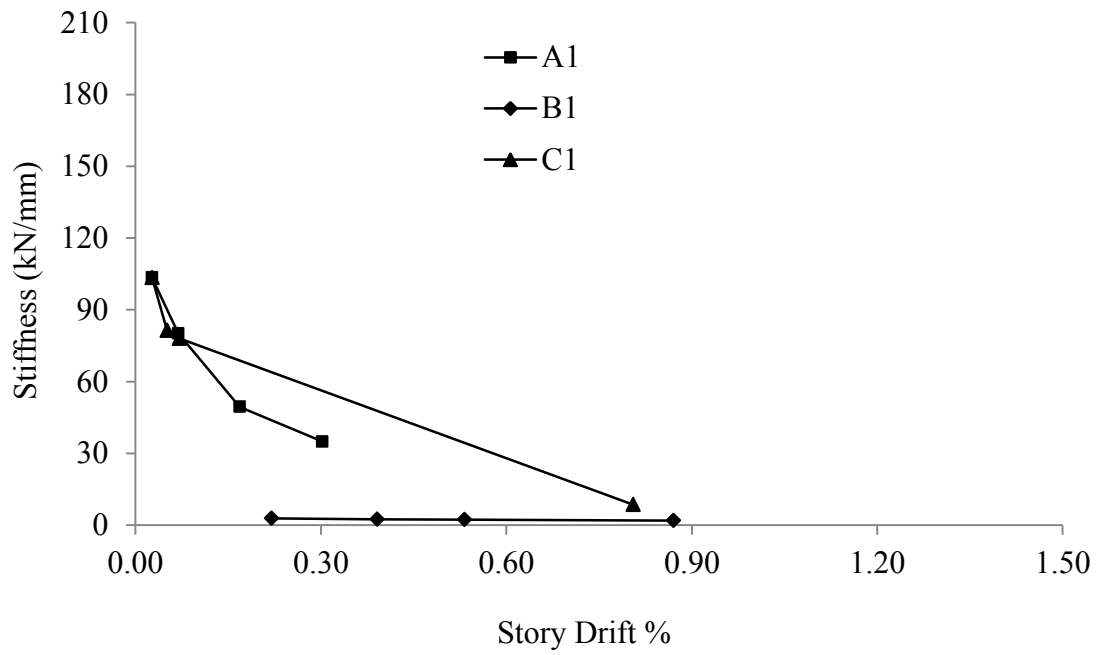


Figure 4.21 Comparison of story drift with respect to stiffness in each cycle for brick infilled RC frames (A1 and A2), Bare RC frame (B1 and B2) and isolated brick infilled RC frames (C1 and C2)

#### 4.6 Overall Comparative Behaviors of Infilled, Bare and Isolated Brick Infilled RC Frames

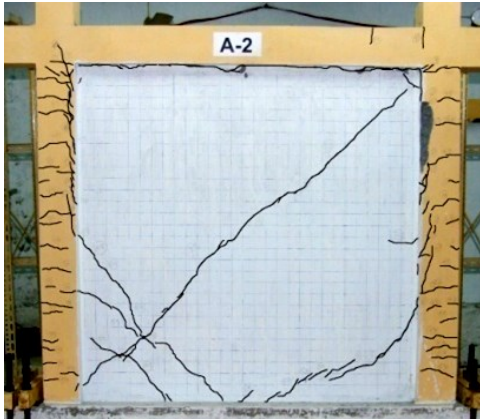
Experimental Results for original and repaired brick infilled, bare and isolated brick infilled RC frames have been summarized in the present section. Frame cracking loads, infill cracking loads, lateral loads at first yielding of the embedded steel, maximum lateral loads, initial stiffness and the ductility the specimens have been summerized in Table 4.10.

**Table 4.10 Brief Summary of Experimental Results**

Description	Brick Infilled RC Frames				Bare RC Frames				Isolated Brick Infilled RC Frames			
	Original		Repaired		Original		Repaired		Original		Repaired	
	A1	A2	AR1	AR2	B1	B2	BR1	BR2	C1	C2	CR1	CR2
Frame cracking load (kN)	71	89	80	89	9	7	16	9	67	89	107	45
Infill cracking load (kN)	111	133	125	156	NA	NA	NA	NA	NA	NA	NA	80
Lateral load at first yielding of steel	89	89	133	133	16	31	22	36	107	93	142	156
Maximum lateral load (kN)	169	178	222	178	27	42	36	42	111	107	174	187
Initial stiffness (kN/mm) at first crack	119	95	95	117	3	4	2	2	105	74	75	178
Ductility ratio, $\mu$	6.0	7.1	4.4	4.4	2.4	1.9	2.1	1.7	7.8	18.2	3.3	4.1

Additionally, crack patterns and failure mechanisms of original and FC laminated repaired specimens are summarized in Figure 4.22(a)-(c) and Figure 4.23(a)-(c). Comparative hysteretic behaviors of original and repaired frames are also represented in Figure 4.24. Moreover, comparative shear capacity, cumulative energy dissipation and stiffness degradation of brick infilled RC Frames, Bare RC Frames and Isolated Brick Infilled RC Frames are illustrated in Figure 4.25. Finally, the effect of FC overlay on the shear capacity, stiffness degradation and energy

dissipation of the infilled RC frame, bare RC frames and isolated brick infilled RC frames represented in Figure 4.26.



(a) Brick infilled RC frame

Failure Mechanism of Brick Infilled RC Frame:

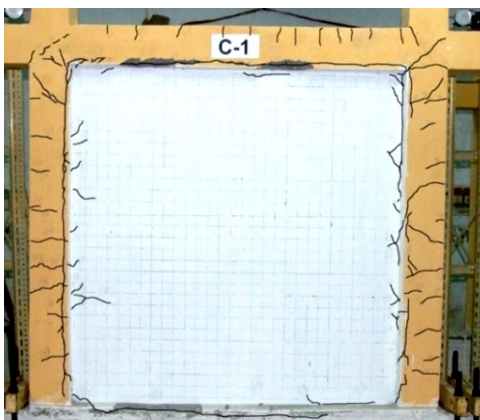
- 1) Diagonal tensile splitting of brick masonry
- 2) Partial corner crushing of infill



(b) Bare RC frame

Failure Mechanism of Bare RC Frame:

- 1) Flexural cracks and yielding of reinforcement in tension zones of the RC frame
- 2) Diagonal cracks in beam – column joints

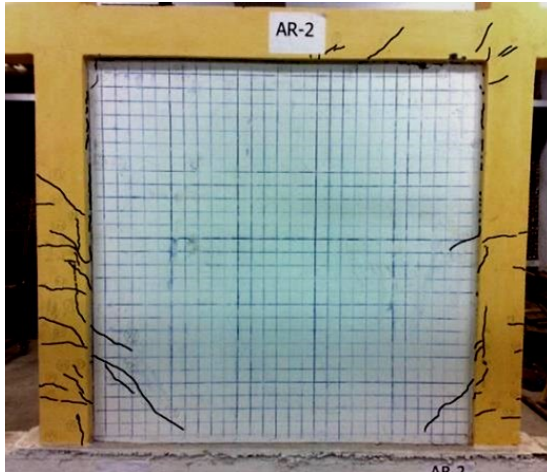


(c) Isolated brick infilled RC frame

Failure Mechanism of Isolated Brick Infilled RC Frame:

- 1) Flexural cracks in columns and beams
- 2) Shear cracks in columns near beam-column joints;
- 3) Cracks along the wire mesh attached as horizontal support at the periphery of isolated wall and the surrounding RC frames

Figure 4.22 Comparative Crack Patterns and Failure Mechanisms of Original Brick Infilled, Bare and Isolated Brick Infilled RC Frames



(a) Repaired brick infilled RC frame

Failure Mechanism of Repaired Brick Infilled RC Frame:

- 1) Tensile failure of wire mesh along the previous diagonal tensile cracks in infills
- 2) Partial corner crushing of infill
- 3) Shear failure of columns and beam, Partial corner crushing of infill



(b) Repaired bare RC frame

Failure Mechanism of Repaired Bare RC Frame:

- 1) Flexural cracks in the tension zones of the RC frame
- 2) Diagonal cracks in beam –column joints and yielding of FC wire mesh



(c) Repaired isolated brick infilled RC frame

Failure Mechanism of Repaired Isolated Brick Infilled Frame:

- 1) Flexural cracks in columns and beams
- 2) Shear cracks in columns near beam-column joints
- 3) Cracks along the wire mesh attached as horizontal support at the periphery of isolated wall and the surrounding RC frames

Figure 4.23 Comparative Crack Patterns and Failure Mechanisms of Repaired Brick Infilled, Bare and Isolated Brick Infilled RC Frames

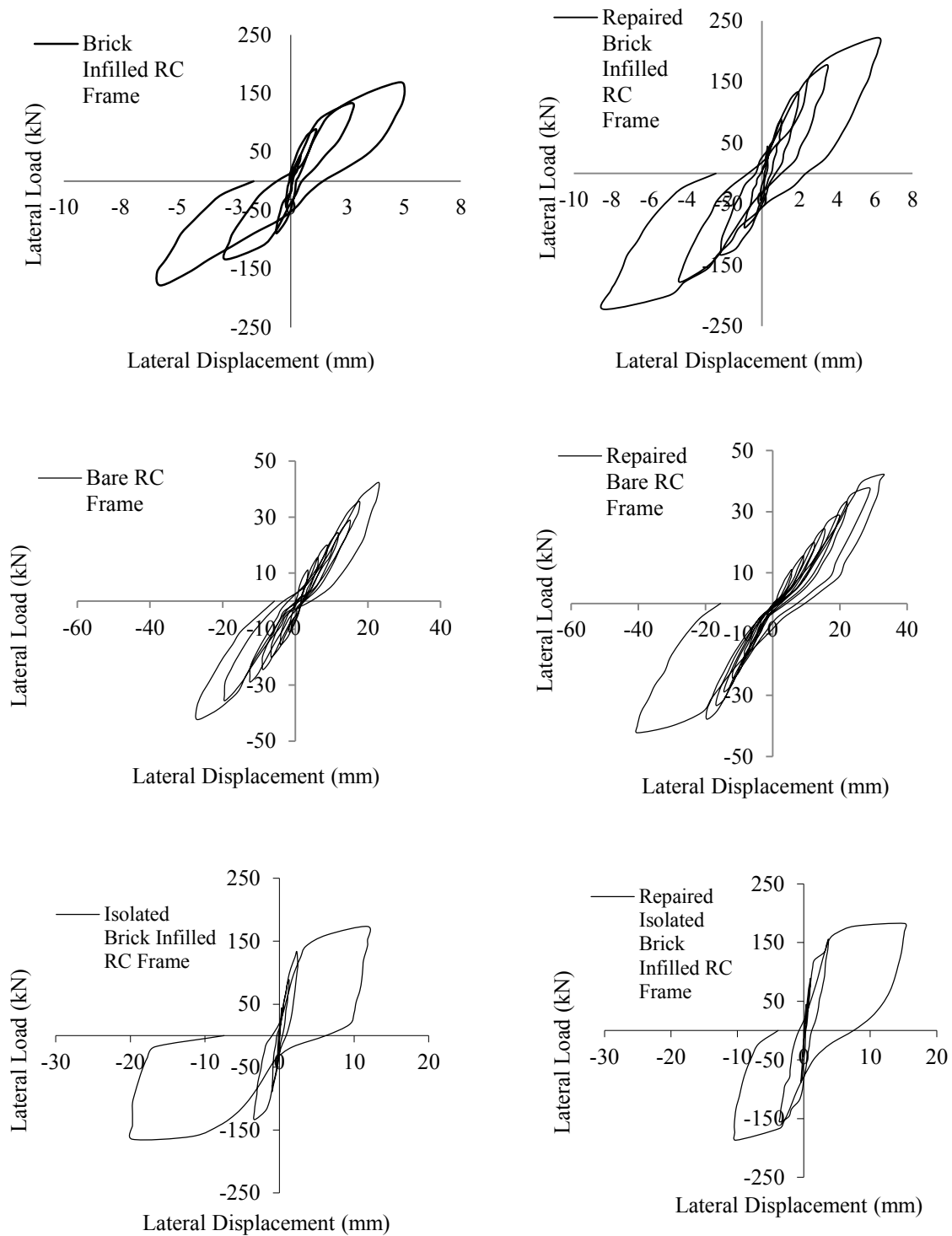


Figure 4.24 Comparative Hysteretic Behavior of Original and Repaired Brick Infilled, Bare and Isolated Brick Infilled RC Frames

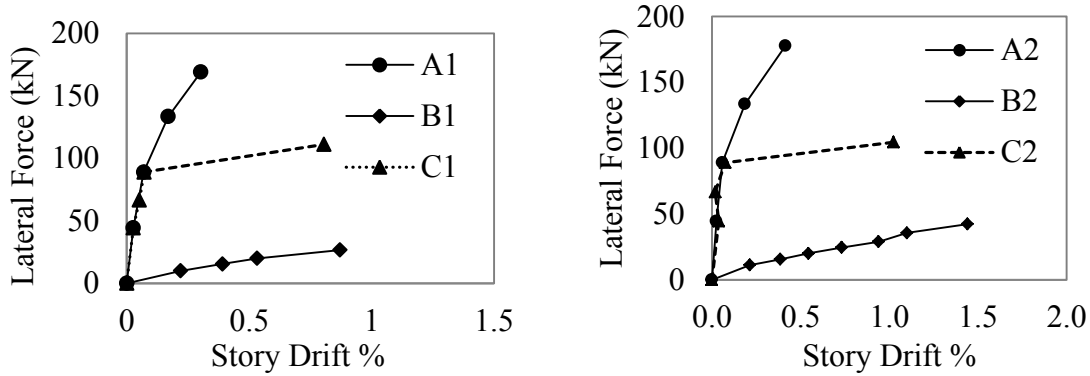


Figure 4.25 (a) Comparative shear capacity

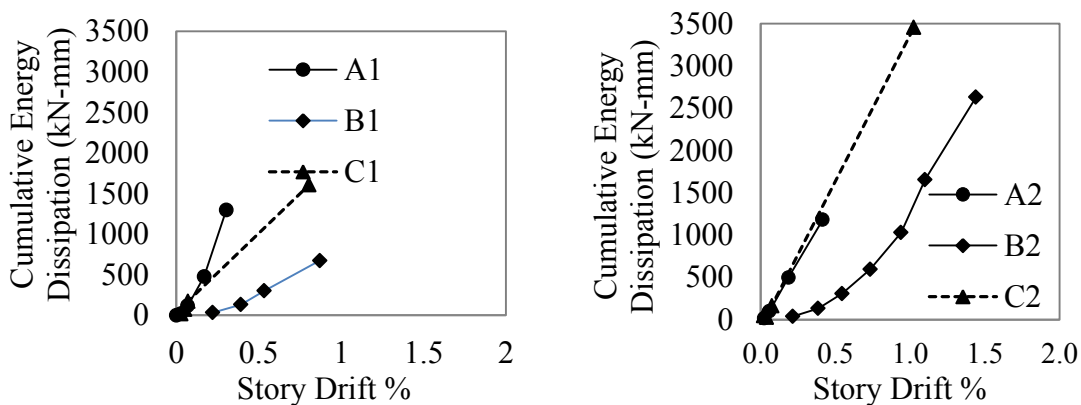


Figure 4.25 (b) Comparative cumulative energy dissipation

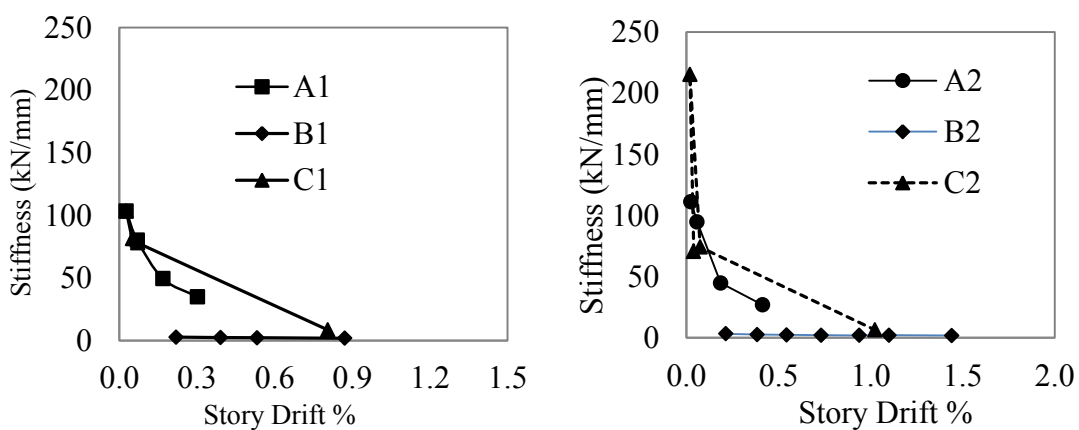


Figure 4.25 (c) Comparative stiffness degradation

#### 4.7 Effectiveness of FC Laminates as a Repair or Retrofitting Material

Effectiveness of FC in contribution of increased shear capacity of damaged brick infilled RC frames, bare RC frames and isolated brick infilled RC frames are illustrated Figure 4.26.

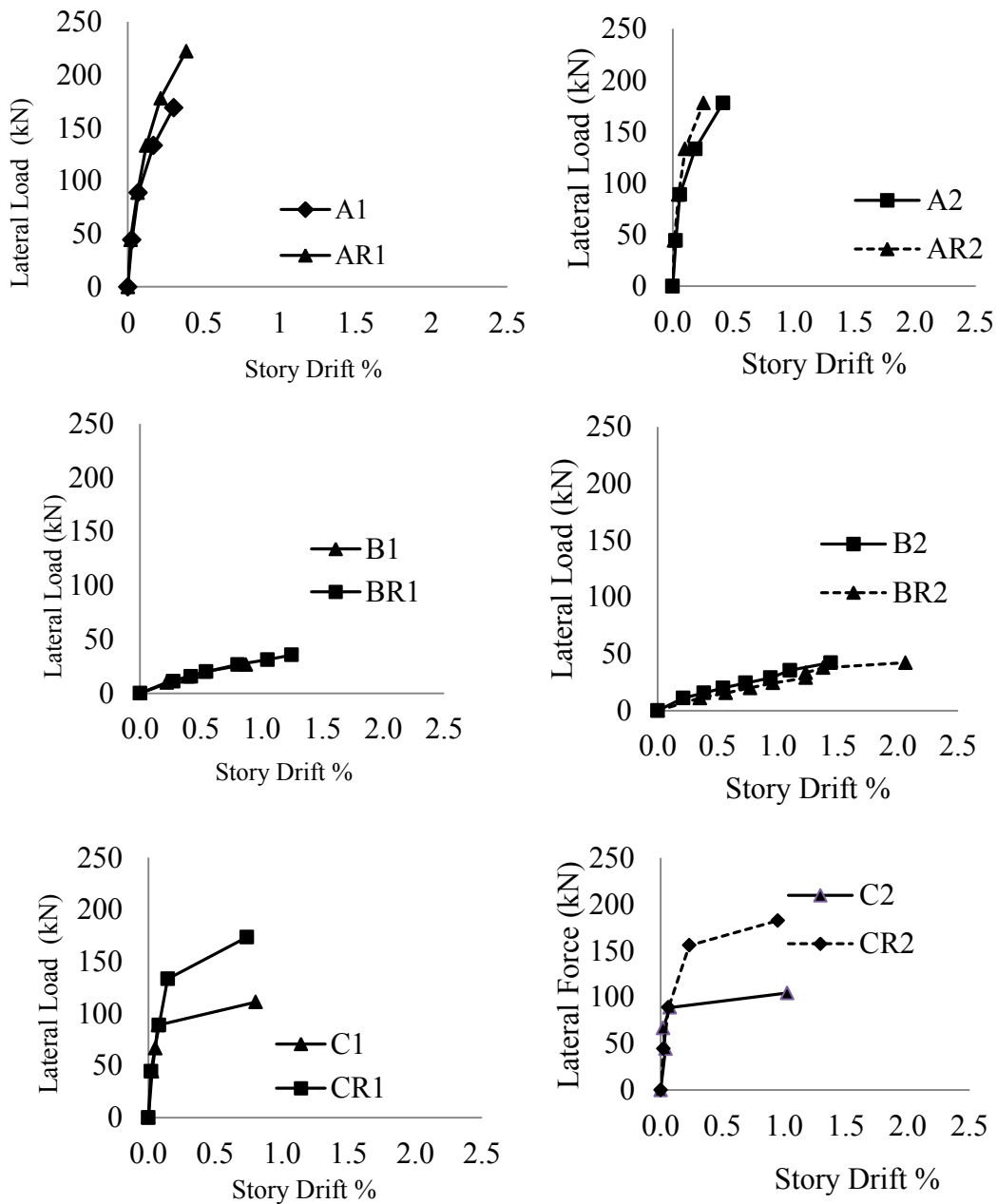


Figure 4.26 Comparative shear capacities of original and FC laminated repaired frames

Effectiveness of FC laminates in reducing stiffness degradation with respect to story drift for brick infilled RC frame, bare RC frames and isolated brick infilled RC frames are depicted in Figure 4.27.

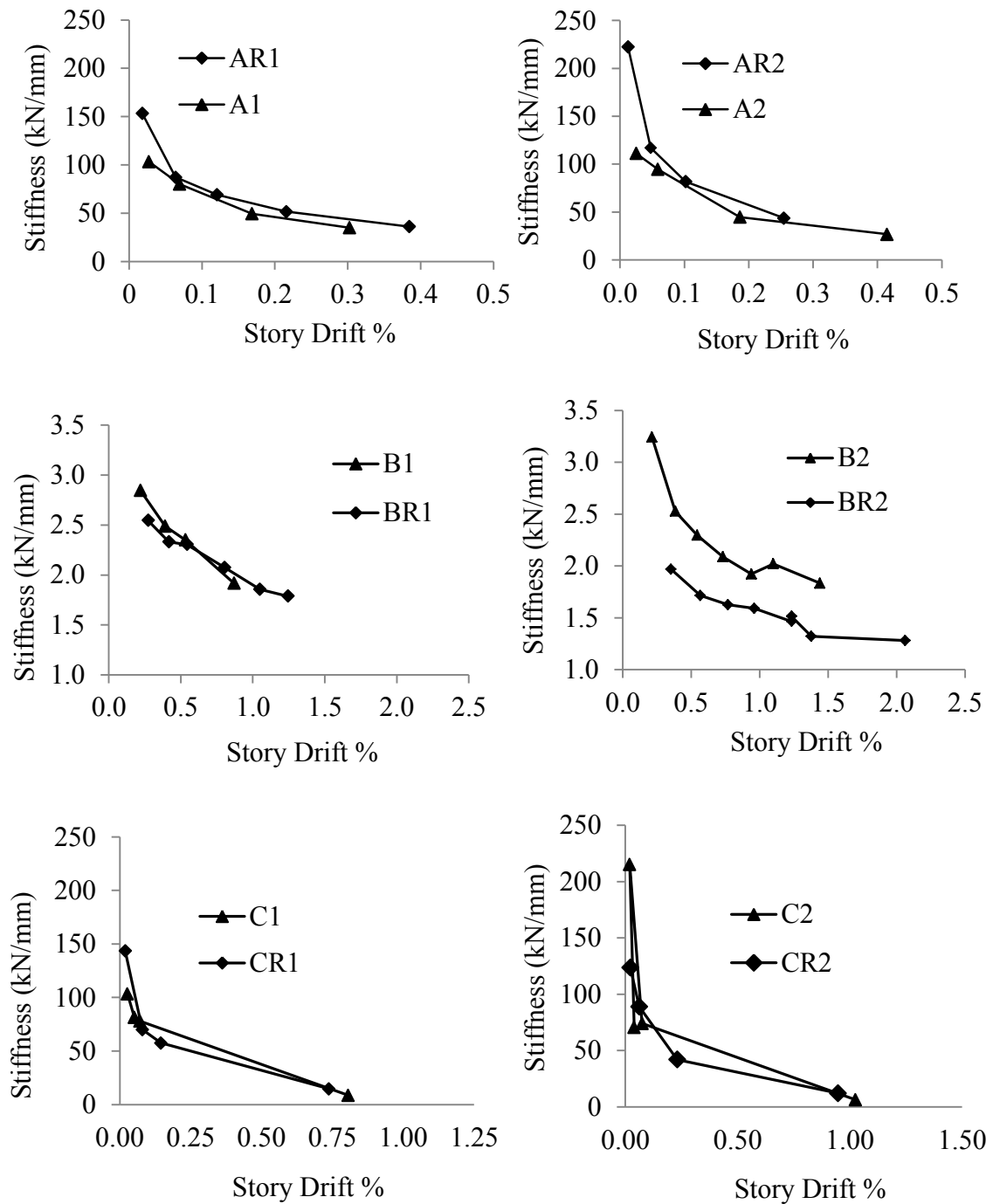


Figure 4.27 Comparative Stiffness Degradation of Original and FC Laminated Repaired Frames



Effectiveness of FC laminates in increasing energy dissipation capacities with respect to story drift for brick infilled RC frame, bare RC frames and isolated brick infilled RC frames are represented in Figure 4.28.

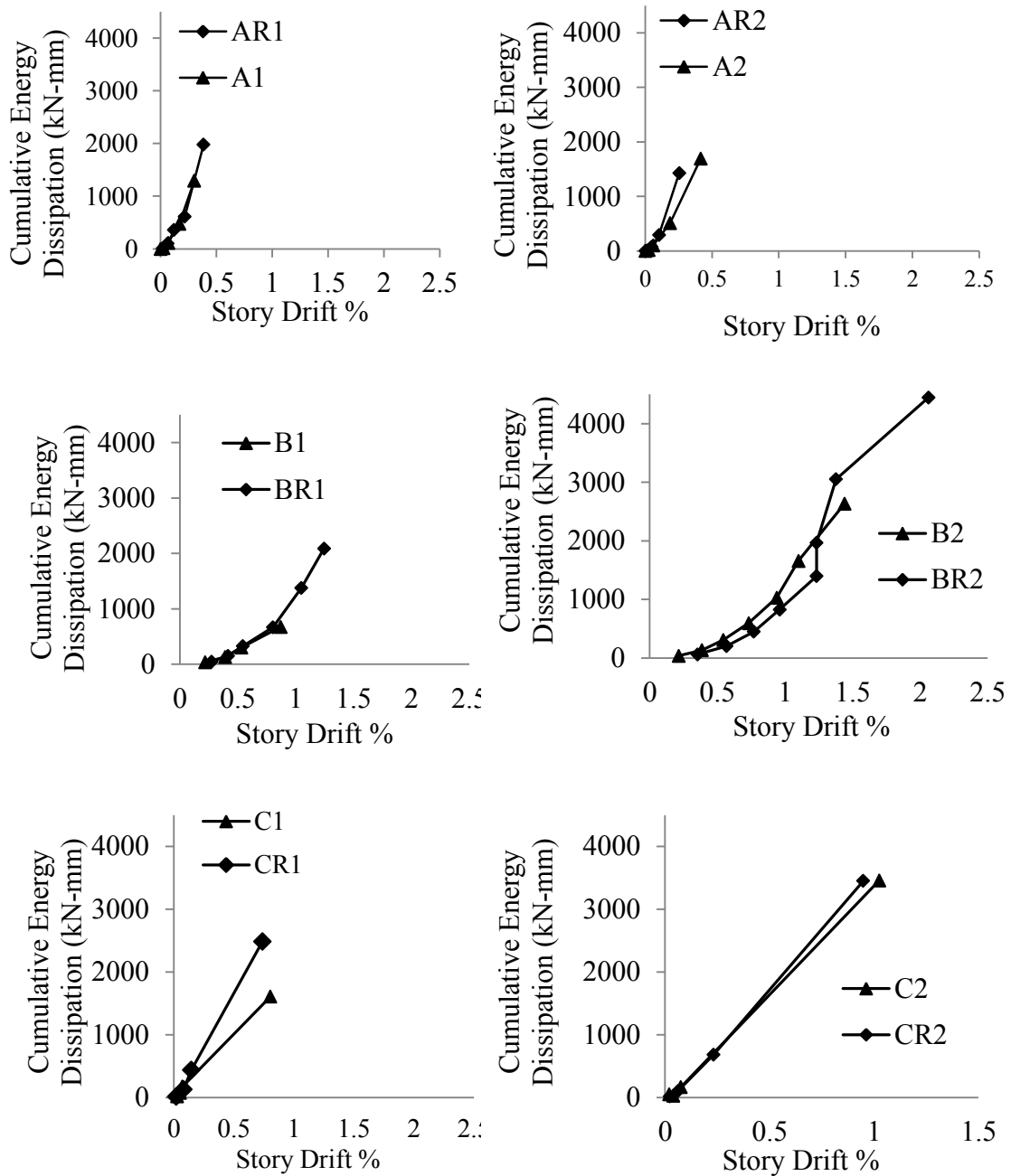


Figure 4.28 Comparative energy dissipation of original and FC laminated repaired frames

**5.1 General**

The present experimental research was conducted to study the comparative in-plane cyclic behavior of brick infilled, isolated brick infilled and bare reinforced concrete (RC) frames and their appropriate repair and retrofit measures against earthquakes. Bangladesh is recognized to be an earthquake prone region where multistoried masonry infilled reinforced concrete framed buildings are commonly seen. Burnt clay bricks are the most common infill materials used as partition walls in those RC frames. Lack of knowledge on the mechanical properties of the local clay brick infills prevents the local structural engineers from idealizing the seismic performances of such buildings in Bangladesh. In this context, present study has focused on the experimental investigation of the comparative in-plane cyclic response of the bare RC frames and the locally available brick infilled RC frames. Moreover, in-plane cyclic behavior of a newly proposed construction method of brick infilled RC frames where the infill is isolated from the surrounding RC frames have also been evaluated and compared with the bare and conventional brick infilled RC frames. Along with, effectiveness of Ferrocement (FC) as a repair and retrofitting material for those frames has also been evaluated. The increasing reverse cyclic in-plane loads were applied on six single bay, single story  $\frac{1}{2}$  scale models comprising two bare RC frames; two brick infilled RC frames and two isolated brick infilled RC frames till their ultimate capacities were reached accompanied by substantial deformation and propagation of cracks. Behaviors of the frames were evaluated through the observed strength and deformation characteristics along with their stiffness degradation, hysteretic energy dissipation capacity and ductility. Later, the damaged specimens were repaired with FC laminates and tested following the same procedures as for the original frames. The experimental results proved the substantially large shear capacity of brick infilled RC frames in comparison to bare RC frames and isolated brick infilled RC frames. While, the isolated brick infilled RC frames exhibited large energy dissipation capacities in comparison to bare and conventional brick infilled RC frames. Furthermore, FC laminating confirmed improved performances of all damaged frames and more than original strengths were achieved.

## **5.2 Findings in Brief**

The findings of the study presented in the previous chapters are summarized below:

### **5.2.1 Comparative in-plane cyclic behavior of brick infilled, bare and isolated brick infilled RC frames**

#### 1) Shear capacity

The maximum shear capacity of the infilled RC frame, the bare RC frame and the isolated infilled RC frame are 178 kN, 42 kN and 111 kN respectively. According to the present investigation, it can be inferred that brick infill can increase the shear capacity of the overall frame around 300%. Whereas, the overall shear capacity of the isolated infilled RC frame is 40% less than the infilled RC frame. Furthermore, the calculated maximum horizontal shear load based on the equation demonstrated by Smith and Coull (1991) regarding diagonal tensile failure of infill showed good agreement with the average maximum shear capacity of the infilled RC frame obtained from the present laboratory investigation.

#### 2) Frame and infill cracking load

The present investigation has confirmed that the frame cracking load of brick infilled RC frame is 40%-50% of its maximum capacity, whereas infill cracking load is 70% of its maximum capacity. On the other hand, the frame cracking load for bare RC frame is 16%-30% of its maximum capacity. Moreover, the frame cracking load for isolated infilled RC frame is 60% of its maximum capacity.

#### 3) Failure mechanism and crack patterns

Brick infilled RC frame exhibited diagonal tensile splitting of brick masonry and partial corner crushing of the infill. Whereas, bare RC frame experienced flexural cracks and yielding of reinforcement in tension zones in the RC frame along with diagonal cracks in beam –column joints. Alternatively, the isolated brick infilled RC frame experienced flexural cracks in columns and beams, shear cracks in columns near beam-column joints along with cracks along the wire mesh attached as horizontal support at the periphery of isolated wall and the surrounding RC frames. In general, there is no crack generated in the isolated

brick infilled wall unless the wire mesh is large enough to contribute in infill-RC frame composite action.

4) Hysteretic behavior and energy dissipation capacity

The comparative hysteretic behavior of brick infilled RC frame, bare RC frame and the isolated infilled RC frame have proved the substantial energy dissipation and energy absorption capacities of the isolated infilled RC frames compared to brick infilled RC frames and bare RC frames.

5) Lateral stiffness and story drift

Isolated infilled RC frame exhibits the substantial lateral deformation similar to bare RC frames after initial stiffening characteristics similar to infilled RC frames until around its ultimate lateral load.

**5.2.2 Effectiveness of ferrocement laminates as a repair or retrofitting techniques for damaged brick infilled, bare and isolated brick infilled RC frames**

1) Failure mechanism and crack patterns

It has been confirmed that two layers of FC laminates sustained equal or even more shear load than respective original bare RC frame, infilled RC frame and isolated infilled RC frame.

2) Shear capacity

In the present investigations, application of ferrocement laminates increased the in-plane shear capacity up to 25% compared to the original infilled frames. Further FC overlay can restore and even increase the in-plane shear capacity of the repaired bare frame up to 33%. Moreover, in-plane shear capacity of the FC laminated isolated brick infilled RC frame can be increased by 55% of the original frame. The capacity of repaired frame depended on the tensile strength of Ferrocement overlay. It can be inferred that the combined shear capacity of the two layers of FC is higher than the masonry.

3) Hysteretic behavior and

FC laminated repaired specimens exhibited better hysteresis behaviors as the more accelerated lateral displacements for similar intensity of lateral loads were

observed in original bare, brick infilled, and the isolated brick infilled RC frame compared to the respective repaired specimens.

4) Energy dissipation capacity

FC laminated repaired frames infilled, bare and isolated infilled RC frames experienced increased energy dissipation and absorption capacities as compared to the respective original frames.

5) Lateral stiffness and story drift

The initial stiffness of the repaired bare frame is around 20-50-% less than the original bare RC frame as the yielding of embedded reinforcement have been occurred already under previous cyclic loading. In case of FC laminated repaired brick infilled and isolated brick infilled RC frame, initial stiffness can be increased in compared to the original frames due to the bonding between infills and the surrounding RC frame.

6) Crack arrest mechanism

In general, the extent of crack openings (width of crack opening) in the FC laminated infill walls and in the RC frames were significantly smaller than those of original frames. This reveals the superior capability of FC in crack arrest mechanism and protecting the damaged structure from large deformation as well as from environmental actions.

### **5.3 Recommendations for Safeguarding Brick Infilled RC Framed Buildings with Soft Ground Floor**

Based on the findings three suggestions have been inferred for safeguarding of masonry infilled RC framed (MIRC) buildings accompanying with/without soft stories are explained as follows:

1) Isolation of infill from the surrounding RC frame

The infills can be deactivated as a structural element by isolating the infills from the surrounding RC frames providing sufficient gap between infill and frame elements. Due to the gap RC frame-brick infill interaction will not occur and the structure will behave like an ordinary sway frame. This may prevent the occurrence of soft story and the assumptions of conventional analysis methods will hold true for the building. However, it must be kept in mind that the wall must be prevented from out of plane collapse during earthquakes. The out of plane failure of the isolated infills can be prevented by applying ferrocement overlay along the surface of infill-RC frame interface.

2) Installation of masonry walls at the open ground floor

Placement of masonry walls between the columns at the open ground floor in an organized manner will increase the stiffness of the storey, on the other hand will be able to offer desired car parking. In this regard, the out of plane failures of the brick infilled must be prevented.

3) Application of ferrocement laminates

The comparative in-plane cyclic behavior of original brick infilled, bare and isolated infilled RC frames and the FC laminated repaired corresponding frames reveals that ferrocement can be utilized as an effective repair and retrofitting material for brick infilled RC framed buildings in Bangladesh due to its improved lateral strength, crack arrest mechanism, energy dissipation capacity, low stiffness degradation against cyclic loads. Moreover, out of plane falling of infill walls can be prevented by FC laminates.

#### **5.4 Scope for Further Study**

Some recommendations are listed below that may be carried out for further advancement of research.

- 1) The experimental results obtained from the present study can deliberately be utilized in establishing the material properties of the infills and the constitutive models for the locally available brick infilled RC frame structures.
- 2) The scope of the present investigation can be expanded by including more stories, bays and spans with different infill materials available in Bangladesh.
- 3) Presence of openings in infill like window or door can be considered in the experimental investigation for in-plane and out-of-plane cyclic response of the infilled RC frames.
- 4) The laboratory experimental investigation can be carried out until total failure with reduction of the ultimate strength to obtain the true ductility factors of the RC frames infilled with different local infill materials
- 5) Further laboratory investigations are needed to be carried out to evaluate the seismic performances of different newly developed repair and retrofitting materials and techniques applicable for the masonry infilled RC framed buildings with soft ground stories or weak stories along the frames.

## REFERENCES

---

- ACI Committee 549, (1993) "State of the Art-Report on Ferrocement", ACI Committee Report ACI 549R-93, November, pp.1-2.
- ACI Committee 224, (2007), Causes, Evaluation, and Repair of Cracks in Concrete Structures, Report 224ACI 224.1R-07.
- AFPS-90, (1990) "Recommendations for the Redaction of Rules Relative to the Structures and Installations Built in Regions Prone to Earthquakes", French Association of Earthquake Engineering, Paris, France.
- Afsaruddin, M. and Hoque, M.F., (1998) "Ferrocement as permanent Formwork for Reinforced Concrete Beams", B.Sc. Engineering Thesis, Department of Civil Engineering, BUET, Dhaka, December, pp.24-30.
- Alam M.M.M., (2003) "Experimental Investigation of Masonry Infilled Reinforced Concrete Frame Retrofitted with Ferrocement", M.Engrg Thesis, Dept. of Civil Engrg., BUET.
- Alcocer,S.M., Ruiz,J., Pinda,J.A., and Zepda,J.A. (1996) "Retrofitting of confined masonry Walls with Welded wire Mesh", Eleventh World Conference on Earthquake Engineering, Paper No.1471, Elsevier Science Ltd.
- Algerian Seismic Code (1988) "Algerian Earthquake Resistant Regulations", Ministry of Town planning and Construction, Algiers, Algeria.
- Amanat, K.M., Alam, M.M.M., Alam M.S.,(2007) "Experimental Investigation of the Use of Ferrocement Laminates for Repairing Masonry Infilled RC Frames", Journal of Civil Engineering, Institution of Engineers, Bangladesh, Vol. 35 (2), pp. 71-80.
- Anwar, A.W., Nimityongskul, P., Pama, R. P. and Robles-Austriaco, L., (1991) "Method of Rehabilitation of Structural beam Elements Using Ferrocement", Journal of Ferrocement, Vol. 21, No.3, pp.229-234.
- Asteris, P.G., (2003) "Lateral stiffness of brick masonry infilled plane frames" Journal of Structural Engineering, ASCE, Vol. 129, No 8, August, pp 1071-1079.
- Asteris, P. G., Cotsovos, D. M., Chrysostomou, C., Mohebkah, & Al-Chaar. (2013) "Mathematical micromodeling of infilled frames: State of the art. Engineering Structures", 56, 1905–1921.
- Buonopane, S. G., and White, R.N., (1999) "Pseudodynamic testing of masonry infilled reinforced concrete frame" Journal of Structural Engineering, ASCE, Vol. 125, No 6, June, pp 578-589.
- Bertero, V., and Brokken, S., (1983) "Infills in Seismic Resistant Building", Journal of the Structural Engineering, ASCE, Vol. 109, No 6, June, pp 1337-1361.
- Binda L., Gambarotta L., Lagomarsino S. & Modena C., (1999) "A multilevel approach to



the damage assessment and seismic improvement of masonry buildings in Italy” on Seismic Damage to Masonry Buildings, Bernarini Ed., Balkema, Rotterdam.

- BNBC, (1993) Housing and Building Research Institute and Bangladesh Standards and Testing Institution, Bangladesh National Building Code.
- BNBC (2014) Housing and Building Research Institute, Dhaka, Bangladesh.
- Costa Rican Seismic Code, (1986) “Seismic Code of Costa Rica”, Federal College of Engineers and Architects of Costa Rica, San Jose, Costa Rica.
- Chowdhury, S.M.M.I and Robles A., L., (1986) “Ferrocement for Repair and Strengthening of Structures” In Proceeding of the Asia-Pacific Concrete Technology Conference, October, pp.13-15.
- Dawe, J. L., and Charalambous, P. D., (1983) “Finite Element Analysis for Wall-Frame Interaction” Proceedings, Eight International Loadbearing Brickwork Symposium, British Ceramic Society, Stoke-on-Trent. UK.
- EERI, (2001) “Annotated Images from the Bhuj, India Earthquake of January 26”, (CD), Earthquake Engineering Research Institute, Oakland, CA.
- Egyptian Seismic Code, (1988) “Regulations for Earthquake Resistant Design of Buildings in Egypt”, Egyptian Society for Earthquake Engineering, Cairo, Egypt.
- El-Gawady, M.A., Lestuzzi, P., Bandoux, M., (2007) “Static Cyclic Response of Masonry Walls Retrofitted with Fiber-Reinforced Polymers”, J. Composite for Construction, ASCE, Vol.11, No.1, February, 50-61.
- Frosch, R. J., Li, W., Jirsa, J., Kreger, M. (1996) “Retrofit of Non-Ductile Moment-Resisting Frames Using Precast Infill Wall Panels”, Earthquake Spectra.
- Gulkan,P., Mayes,R.L. and Clough, R.W., (1979) “Shaking Table Study of Single Story masonry Houses”, Volume 1: Test Structure 1 and 2”, Earthquake Engineering Research Center Report No. UCB-EERC-79-23, University of California, Berkeley, California, September.
- Huang, S., (2005) “Seismic behaviors of reinforced concrete structures with soft Story”, The 3rd International Conference on Structural Stability and Dynamics, June 19-22, Kissimmee, Florida.
- Haque, S. (2007) Behavior of Multistoried RC Framed Buildings with Open Ground Floor Under Seismic Loading, M.Sc. Thesis, Dept. of Civil Engrg., BUET.
- Henderson, R.C., Fricke, K.E., Jones, W. D., Beavers, J. E. and Bennett, R. M., (2003) “Summary of a Large- and Small-Scale Unreinforced Masonry Infill Test Program”, J. Struct. Engrg., ASCE vol.129, No.12, December, 1667-1675.
- Hidalgo,P., mayes, R.L., Mcniven, H.D. and Clough, R.W., (1979) “Cyclic Loading Test of Masonry Single Piers”, Report No. UCE/EERC-79/12, Earthquake Engineering Research Center, University of California, Berkeley, May.

- Holmes, M., (1961) “Steel Frames with Brickwork and Concrete Infilling”, Proc., Inst. Civ. Eng., Struct. Build., 19, 473–478.
- Holmes, M., (1963) “Combined Loading in Infilled Frames”, Proc. Inst. Civ. Eng., Struct. Build., 25(6621), 31–38.
- IS-1893, (2002) Bureau of Indian Standards, Indian Standard Criteria for Earthquake Resistant Design of Structures—Part 1: General Provisions and Buildings (Fifth Revision), New Delhi, India.
- IBC, (2000) Building Officials and Code Administrators International, International Conference of Building Officials and Southern Building, Code Congress International, U.S.A., International Building Code.
- Imran, I., and Aryanto, A. (2009) “Behavior of Reinforced Concrete Frames In-filled with Lightweight Materials Under Seismic Loads”, Civil Engineering Dimension , 11 (2), 69-77.
- Jabarov, M., Kozharinov, S.V. and Lunyov, A.A., (1980) “Strengthening of Damaged Masonry of Reinforced Mortar Layers”, Proceedings, 7<sup>th</sup> WCEE, Istanbul, Vol.4, pp.73.
- Johnston, C.D. and Mattar, S.G., (1976), “Ferrocement Behaviour in Tension and Compression”, Journal of the Structural Engineering, ASCE, Vol. 102, No. ST5, May., pp. 875-889.
- Kadir, M.R.A., Samad, A.A.A., Muda, Z.C. and Ali, A.A.A., (1997) “Flexural Behaviour of Composite Beam with Ferrocement Permanent Formwork”, Journal of Ferrocement, Vil. 27, No.3, July, pp. 209-213.
- Klingner, R. E., and Bertero, V. V., (1978) “Earthquake Resistance of Infilled Frames,” Journal of the Structural Engineering, ASCE, Vol. 104, No. ST6, June, pp. 973-989.
- Kaushik, S. K. and Dubey, A. K., (1994) “Performance Evaluation of RC Ferrocement Composite Beams”, Proceeding of Fifth International Symposium on Ferrocement, UMIST, Manchester, September, pp. 241-255.
- Kolsch H.,(1998) “Carbon fibre cement matrix (CFCM) overlay system for masonry strengthening, Journal for composites for construction, Vol.2, No.2, May 1998,pp.105-109.
- Kwan, K.H., J.Q.Xia, (1995) “Shaking-Table Tests of Large-Scale Shear Wall and Infilled Frame Models”, Proceedings of Institution of the Civil Engineers, Structures and Buildings, Vol.110, pp.66-77.
- Liauw, T. C., and Kwan, K. H., (1983) “Plastic Theory of Non-Integral Infilled Frames”, Proceedings of the Institution of Civil Engineers, Part 2, Vol. 75, pp. 379-396.

- Liauw, T. C. and Kwan, K. H., (1985) "Unified plastic analysis for infilled frames", *Journal of the Structural Engineering, ASCE*, Vol. 120, No.9, 1985, pp. 1861-1876.
- Liauw, T. C., and Lo, C.Q., (1988) "Multi-bay Infilled Frames without Shear Connectors", *ACI Structural Journal*, July-August, pp. 423-428.
- Langenbach, R. (2003) "Crosswalls" Instead of Shearwalls – A Proposed Research Project for the Retrofit of Vulnerable Reinforced Concrete Buildings in Earthquake Areas Based on Traditional "Himis" Construction", *Proc., 5<sup>th</sup> National Conference on Earthquake Engineering*, 26-30 May, Istanbul, Turkey.
- Lourenco, P. B., Brost, R. D. and Rots, J. G. (1997) "A Plane Stress Softening Plasticity Model For Orthotropic Materials", *International Journal For Numerical Methods In Engineering*, Vol. 40, 4033-4057.
- Lu, Y. (2002) "Comparative Study of Seismic Behavior of Multistory Reinforced Concrete Framed Structures", *J. Struct. Engrg., ASCE* vol.128, No.2, February, 169-178.
- Lee, S.I., Raisinghani, M. and Pama, R.P., (1972) "Mechanical Properties of Ferrocement", *FAO Seminar on the Design and Construction of Ferrocement Vessels*, October.
- Lub, K.B., and Van Wanroij, M.C.G., (1988) "Strengthening of Reinforced Concrete Beams with Shotcret Ferrocement" In *Proceeding of Third International Conference on Ferrocement*, Roorkee, University of Roorkee, pp. 477-485.
- Madan, A. Reinhorn, A. M., Mander, J. B., and Valles, R. E.,(1997) "Modeling of Masonry Infill Panels For Structural Analysis", *J. Struct. Engrg., ASCE* Vol. 123, No. 10, October, 1295-1297.
- Mallick, D. V., and Severn, R. T., (1967) "The Behavior of Infilled Frames under Static Loading", *Proceedings of the Institution of Civil Engineers*, Vol. 38, pp. 639-656.
- Mander, J.B., Nair, B., Wojtkowski, K., and Ma, J., (1993) "An Experimental Study on the Seismic Performance of Brick-infilled Steel Frames with and without Retrofit", *Rep. NCEER-93-0001*, State Univ. of New York at Buffalo, N.Y.
- Manzouri, T., Shing, P.B., Amadei, B., (1996) "Analysis of Masonry Structures with Elastic Structures with Elastic/Viscoplastic Models, 1996, "Worldwide Advances in Structural Concrete and Masonry, *Proceedings of the Committee on Concrete and Masonry Symposium, ASCE Structures Congress XIV*, Chicago, Illinois.
- Mehrabi, A. B., Shing, P. B., Schuller, M. P., and Noland, J. N., (1996) "Experimental Evaluation of Masonry-Infilled RC Frames", *Journal of Structural Engineering, ASCE*, Vol. 122, No. 3, March, pp 228-237.
- Mehrabi, A.B., Shing, P.B., (1997) "Finite Element Modeling of Masonry Infilled RC Frames", *ASCE Journal of Structural Division*, Vol.123, No. ST05, pp. 604-613.

- Mezzi, M., (2004) “Architectural and Structural Configurations of Buildings with Innovative Aseismic Systems”, 13th World Conference on Earthquake Engineering, August, (Paper No. 1318), Vancouver, B.C., Canada.
- Meli, R., Hernandez, D. and Padilla, M., (1980) “Strengthening of Adobe Houses for Seismic Actions”, Proceedings, 7<sup>th</sup> WCEE, Istanbul, Vol.4, pp.265.
- Moghaddam, H. A., and Dowling, P. J., (1987) “The State of the Art in Infilled Frames”, Imperial College of Science and Technology, Civil Eng. Department, London, U.K, ESEE Research Report No. 87-2.
- Murty, C. V. R., and Jain, S. K., (2000) “Beneficial influence of masonry infills on seismic performance of RC frame buildings”, Proceedings, 12th World Conference on Earthquake Engineering, New Zealand, Paper No. 1790.
- Negro, P., Verzeletti, G., (1996) “Effect of Infills on the Global Behavior of R/C Frames: Energy Considerations from Pseudo dynamic Response”, Earthquake Engineering and Structural Dynamics.
- NZS-3101, (1995) “Code of Practice for the Design of Concrete Structures”, Part 1, Standards Association of New Zealand, Wellington, New Zealand.
- Naaman, A.E. and Shah, S.P.,(1971) “Tensile Test of Ferrocement” ACI Journal, Vol.68, No. 9, September, pp. 693-698.
- NBC-105, (1995) “Nepal National Building Code for Seismic Design of Buildings in Nepal”, Ministry of Housing and Physical Planning, Department of Buildings, Kathmandu, Nepal.
- NSR-98, (1998) “Colombian Standards for Seismic Resistant Design and Construction”, Bogota, Colombia.
- Pama, R.P., Sutharatanachaiyaporn, C., and Lee, S.L., (1974) “Rigidities and Strength of Ferrocement”, First Australian Conference on Engineering Materials, The University of New South Wales.
- Papia, M., (1998) “Analysis of Infilled Frames Using a Coupled Finite Element and Boundary Element Solution Scheme”, International Journal For Numerical Methods In Engineering, Vol. 26, 731-742.
- Polyakov, S.V., (1956) Masonry Infilled Framed Buildings, G.L. Cairns, (trans), BRS (UK) Publications.
- Rahman, A.K.M.H., (2002) “Strengthening of distressed RC slabs by using ferrocement overlay”, M.Engineering Thesis, Department of Civil Engineering, BUET, Dhaka, August, pp.7-21.
- Rao, A.K., (1969) “A Study of Behaviour of Ferrocement in Direct Compression, Cement and Concrete”, Oct-Dec., pp. 231-237.

- Reinhorn, A.M., Prawel, S.P. and Jia, Zi-He, (1985) "Experimental Study of Ferrocement as a Seismic Retrofit Material for Masonry Walls", *Journal of Ferrocement* Vol. 15, No.3, July, pp. 247-260.
- Pristley, M.J. and Bridgitan, D.O., (1974) "Seismic Resistance of Brick Masonry Walls", *Bulletin of the New Zealand National Society of Earthquake Engineering*, Vol.7, No.4, December.
- Rosenthal, I and Bljucer, F., (1985) "Bending Behavior of Ferrocement - Reinforced Concrete Composite", *Journal of Ferrocement*, Vol. 15, No. 1 January, pp. 15-23.
- Saneinejad, A. and Hobbs, B., (1995) "Inelastic Design of Infilled Frames", *ASCE Journal of Structural Engineering*, Vol. 121, No. 4, April, pp. 634-643.
- Santhi, M.H., Knight, G.M., (2005) "Evaluation of seismic response of soft-storey infilled frames" *Computers and concrete*, Vol. 2, No. 6, December.
- Sathiparan, N., Sakurai, K., Numada, M. And Meguro, K., (2011) "Shaking Table Test on Seismic Response Behaviour of 2-Story Masonry House Model With PP-Band Mesh Retrofitting", *University of Tokyo Bulletin of ERS*, No. 44.
- Smith, B. S. and Coull (1991) "A Infilled-Frame Structures, Tall Building Structures Analysis and Design", John Wiley & Sons, inc. 168-174.
- Smith, B.S., (1962) "Lateral stiffness of infilled frames" *ASCE Journal of Structural Division*, Vol. 88, No. ST6, pp. 183-199.
- Smith, B.S., (1966) "Behavior of the Square Infilled Frames", *J. Struct. Div., ASCE*, 2(1), 381-403.
- Smith, B. S., and Carter, C., (1969) "A Method of Analysis for infilled Frames" *Proceedings of the Inst. of Civil Engineers*, Vol. 44, pp.31-48.
- Singh, K.K., Kaushik, S.K., and Prakash, A., (1976.) "An Investigation of the Ultimate and First Crack Strength of Ferrocement in Flexure", *Indian Concrete Journal*, November, pp. 335-340 & 344.
- Shing, P.B., Restrepo, J., Billington, S., William, K., Mettupalayam, S., (2006) "Seismic Performance Assessment and Retrofit of Non-Ductile RC Frames with Infill Walls", *Project Proposal in NEES Annual Meeting*, July 21-23.
- Silva, P., Myers, J., Belarbi, A., Tumialan, G., El-Domiaty, K. and Nanni, A. (2001) "Performance of Infill URM Wall Systems Retrofitted with FRP Rods and Laminates to Resist In-plane and Out-of-plane Loads", *Structural Faults and Repairs*, London, UK, July 4-6.
- Sharma, S. P., Sharma, P.C, Singh, K.P., and Bhatia, S.S, (1984) "Ferrocement treatment for repairing a 50,000 gallon overhead water tank", *Journal of Ferrocement*, 14(3), pp. 241-248.

- SNIP-II-7-81, (1996) "Building Code on Construction in Seismic Areas", The Ministry for Construction of Russia, Moscow, Russia.
- Schneider,R.R. and Dickey,W.L.,(1980) "Reinforced Masonry Design", Prentice Hall, Englewood Cliffs, New Jersey.
- Sheppard,P. and Tercelli, (1980) "The effect of repair and strengthening method for masonry walls", Proceedings, 7<sup>th</sup> WCEE, Istanbul, 1980, Vol.6, pp.255.
- UBC, (1997) Structural Engineering Design Provisions, International Conference of Building Officials, Uniform Building Code.
- Venezuelan Seismic Code, (1988) Regulations for Earthquake Resistant Buildings, Comision De Normas Industriales, Covenin, Caracas, Venezuela.
- Walkus, B.R., (1975) "The Behaviour of Ferrocement in Bending", Journal of structural Engineering, Roorkee, Vol. 3, No.3, October, pp. 113-125.
- Wood, R.H., (1958) "The Stability of Tall Buildings." Proceedings of the Institution of Civil Engineers, Vol. 11, pp. 69-102.
- Zegarra, L., Bartolomé,A.S., Quiun,D. and Garcia,G.V.,(2000) "Reinforcement of existing adobe houses" in Aridlands newsletter, No. 47, May.

## Appendix-A

### COMPRESSIVE STRENGTH OF CONCRETE CYLINDERS

Properties of Concrete (used in casting of columns and beam)

Coarse aggregate: 12 mm downgraded stone chips

Fine Aggregate: F.M. of Sand=2.5

Mix Proportion (by weight) = C: FA: CA = 1:1.5:3

W/C ratio = 0.45

Table A.1 28 days Compressive Strength of Concrete Cylinder

Name of Model Specimen Frame	Cylinder No	Specimen Area (in <sup>2</sup> )	Maximum Load (ton)	Compressive Strength (psi)	Avg. Comp. Strength (psi)	Avg. Comp. Strength (MPa)
Bare Frame-1	1	13.48	23.29	3870	3698	25.50
	2	13.48	21.22	3526		
Bare Frame-2	1	13.48	21.22	3526	3354	23.13
	2	13.48	19.15	3182		
Infilled Frame-1	1	13.48	19.15	3182	3182	21.94
	2	13.48	19.15	3182		
Infilled Frame-2	1	13.48	20.18	3353	3655	25.21
	2	13.48	23.81	3957		
Isolated Frame-1	1	13.48	20.7	3440	3612	24.91
	2	13.48	22.77	3784		
Isolated Frame-2	1	13.48	22.25	3697	3827	26.39
	2	13.48	23.81	3957		

Table A.2 Compressive Strength of Concrete Cylinders of Respective Frames at the date of Testing

Specimen Name	Cylinder No	Specimen Area (in <sup>2</sup> )	Maximum Load (ton)	Compressive Strength (psi)	Avg. Comp. Strength (psi)	Avg. Comp. Strength (MPa)
Bare Frame-1	Base-1	13.29	31.56	5319	5049	31.30
	Base-2	13.54	31.56	5319		
	Base-3	13.62	27.42	4509		
	Tie beam-1	13.54	27.42	4541	4541	
	Column-1	13.72	19.15	3126	4027	
	Column-2	13.72	23.29	3802		
	Column-3	13.72	31.56	5153		
Bare Frame-2	Base-1	13.47	27.42	4467	4386	32.32
	Base-2	13.75	25.36	4131		
	Base-3	13.47	27.42	4560		
	Tie beam-1	13.24	25.36	4291	4291	
	Column-1	13.7	34.67	5669	5383	
	Column-2	13.54	31.56	5221		
	Column-3	13.44	31.56	5260		
Infilled Frame-1	Base-1	13.75	24.32	3962	3799	27.49
	Base-2	13.64	19.15	3144		
	Base-3	13.24	25.36	4290		
	Tie beam-1	13.75	18.11	2950	2950	
	Column-1	13.72	31.56	5153	5211	
	Column-2	13.54	31.56	5221		
	Column-3	13.44	31.56	5260		



Specimen Name	Cylinder No	Specimen Area (in <sup>2</sup> )	Maximum Load (ton)	Compressive Strength (psi)	Avg. Comp. Strength (psi)	Avg. Comp. Strength (MPa)
Infilled Frame-2	Base-1	13.2	29.5	5006	4823	32.21
	Base-2	13.5	26.4	4380		
	Base-3	13.44	30.5	5083		
	Tie beam-1	13.75	24.3	3959	3959	
	Column-1	13.6	29.5	4859	5228	
	Column-2	13.3	31.5	5305		
	Column-3	13.8	34	5519		
Isolated Frame-1	Base-1	13.6	25.4	4184	3364	31.28
	Base-2	13.5	16.1	2671		
	Base-3	13.24	19.14	3238		
	Tie beam-1	13.62	30.5	5016	5016	
	Column-1	13.6	29.5	4859	5228	
	Column-2	13.3	31.5	5305		
	Column-3	13.8	34	5519		
Isolated Frame-2	Base-1	13.7	25.87	4230	4151	29.62
	Base-2	13.75	30.53	4974		
	Base-3	13.2	19.15	3250		
	Tie beam-1	14.61	26.39	4046	4046	
	Column-1	13.72	27.42	4476	4688	
	Column-2	13.41	26.39	4408		
	Column-3	13.21	30.53	5180		

## Appendix-B

### PROPERTIES OF STEEL EMBEDDED IN THE RC SPECIMEN FRAMES

Table B.1 Properties of Steel

Dia. of Bar (mm)	Sp. No.	Area of Bar (mm <sup>2</sup> )	Yield load (kip)	Yield Strength (MPa)	Yield Strength (psi)	Ultimate load (kip)	Ultimate Strength (MPa)	Ultimate Strength (psi)	Elongation
8	1	65.33	6.26	426.21	61800	7.86	535.15	77597	18%
	2	65.89	6.26	422.59	61275	7.86	530.60	76937	18%
	3	65.82	6.26	423.04	61340	7.86	531.16	77018	18%
12	1	102.50	9.25	401.4	58203	14.82	643.12	93977	13%
	2	101.88	9.74	425.41	61684	14.82	647.03	93819	15%
	3	98.76	9.44	425.16	61648	12.93	582.35	84441	17%
20	1	263.33	18.80	317.58	46049	26.85	453.54	65763	18%
	2	263.20	19.70	332.86	48265	27.30	461.32	66891	22%
	3	257.36	18.58	320.84	46522	26.85	453.54	65763	16%

## Appendix-C

### COMPRESSIVE STRENGTH OF MORTAR CUBES

Properties of Cement Mortar Used in Ferrocement:

Type of Cement	: Ordinary Portland Cement of type 1
Mixing Proportion	: 1: 2.5
Water Cement Ratio	: 0.45
Fineness modulus of Sand	: 2.00

Table C.1 Compressive Strength of Mortar Cubes

Description of Item	Item	Specimen No.	Age (days)	Specimen Area (sq.in)	Max <sup>m</sup> load (lb)	Comp. Strength (psi)	Avg. Comp Strength
Brick Infilled RC Model Specimen Frame	A-1	1	7	4	9049	2262	2304 psi 15.89 MPa
		2	7	4	9349	2337	
		3	7	4	9248	2312	
	A-2	1	7	4	10242	2561	2536 psi 17.49 MPa
		2	7	4	9944	2486	
		3	7	4	10242	2561	
Bare RC Model Specimen Frame	B-1	1	7	4	4276	1069	1003 psi 6.9 MPa
		2	7	4	4474	1119	
		3	7	4	3282	821	
	B-2	1	7	4	3481	870	829 psi 5.7 MPa
		2	7	4	3082	771	
		3	7	4	3381	845	
RC Model Specimen Frame Isolated from Infill Wall	C-1	1	7	4	11933	2983	3025 psi 20.86 MPa
		2	7	4	12430	3108	
		3	7	4	11933	2983	
	C-2	1	7	4	4177	1044	1069 psi 7.37 MPa
		2	7	4	4376	1094	
		3	7	4	4276	1069	

## Appendix-D

### COMPRESSIVE STRENGTH TEST OF BRICK PRISM

Brick Size: 4.5" x 2.75" x 1.75" (115 mm x 70 mm x 45 mm)

Table D.1 Load Parallel to Bed Joint

SP. No.	Size (l x t x h) (in)	Actual cross-section area (in.sq.)	Actual Height (in)	Maximum load (ton)	Compressive Strength (psi)
1	9x2.75x9	26.61	9.5	19.74	1639
2	9x2.75x9	25.34	9.7	21.55	1905
3	9x2.75x9	25.77	9.8	12.18	1059
4	9x2.75x9	25.93	9.8	17.39	1502
5	9x2.75x9	24.18	9.6	12.18	1128
6	9x2.75x9	24.72	9.7	20.51	1859
Mean				17.26	1327 psi (9.15 MPa)

Table D.2 Load Perpendicular to Bed Joint

SP. No.	Size (l x t x h) (in)	Actual cross-section area (in.sq.)	Actual Height (in)	Maximum load (ton)	Compressive Strength (psi)
7	9x2.75x9	27.13	9.0	14.26	1177
8	9x2.75x9	27.66	9.3	10.10	818
9	9x2.75x9	27.43	9.0	8.02	655
10	9x2.75x9	28.01	9.1	17.41	1432
11	9x2.75x9	26.62	9.2	18.95	1595
12	9x2.75x9	29.16	9.1	10.10	776
Mean				13.14	1075 psi (7.41 MPa)

i. Load Parallel to Bed Joint:



Figure D.1 Specimen-1: Maximum Load=19.74 Ton



Figure D.2 Specimen-2: Maximum Load=21.55 Ton



Figure D.3(a) Specimen-3: Maximum Load=12.18 Ton



Figure D.3(b) Specimen-3: Maximum Load=12.18 Ton



Figure D.4(a) Specimen-4: Maximum Load=17.39Ton



Figure D.4(b) Specimen-4: Maximum Load=17.39Ton



Figure D.5(a) Specimen-5: Maximum Load=12.18 Ton



Figure D.5(b) Specimen-5: Maximum Load=12.18 Ton



Figure D.5(c) Specimen-5: Maximum Load=12.18 Ton





Figure D.6(a) Specimen-6: Maximum Load=20.51Ton



Figure D.6(b) Specimen-6: Maximum Load=20.51Ton

ii. Load Perpendicular to Bed Joint:



Figure D.7(a) Specimen-7: Maximum Load=14.26Ton



Figure D.7(b) Specimen-7: Maximum Load=14.26Ton



Figure D.8(a) Specimen-8: Maximum Load=10.10 Ton



Figure D.8(b) Specimen-8: Maximum Load=10.10 Ton



Figure D.9(a) Specimen-9: Maximum Load= 8.02 Ton



Figure D.9(b) Specimen-9: Maximum Load= 8.02 Ton



Figure D.9(c) Specimen-9: Maximum Load= 8.02 Ton



Figure D.10(a) Specimen-10: Maximum Load= 17.41 Ton



Figure D.10(b) Specimen-10: Maximum Load= 17.41 Ton



Figure D.10(c) Specimen-10: Maximum Load= 17.41 Ton



Figure D.11(a) Specimen-11: Maximum Load= 18.95 Ton



Figure D.11(b) Specimen-11: Maximum Load= 18.95 Ton



Figure D.12(a) Specimen-12: Maximum Load= 10.10 Ton



Figure D.12(b) Specimen-12: Maximum Load= 10.10 Ton



Figure D.12(c) Specimen-12: Maximum Load= 10.10 Ton

## Appendix-E CALCULATIONS

1) Diagonal tensile stress at the center of infill at failure:

According Eq. 2.6 in Chapter 2 demonstrated by Smith and Coull (1991),

$$\text{Diagonal tensile stress } \sigma_d = \frac{0.58Q}{Lt}$$

Where,

$Q$  is the horizontal shear load applied by the frame = 173 kN (Average of infilled frames A1 and A2),

$L$  is infill of length=1525 mm, and

$t$  is infill thickness = 75 mm.

Therefore, average diagonal tensile stress  $\sigma_d$  generated at the center of infill at the time of diagonal tension failure can be derived from the equation as 0.88 MPa which can be considered as the ultimate tensile strength of masonry.



2) Calculation of maximum horizontal shear load based on the diagonal tensile failure:

According to Eq. 2.8 in Chapter 2 demonstrated by Smith and Coull (1991), horizontal shear  $Q$ , based on the diagonal tensile failure criterion, is given by

$$Q=1.7Ltf_t$$

Where  $f_t$  = diagonal tensile strength of masonry can be taken as 10% of the compressive strength of masonry.

According to the laboratory investigation results of uniaxial compression test of masonry prisms (Appendix-D), the ultimate compressive strength of masonry corresponding to the uniaxial load parallel to the bed joint is 9.15 MPa and, the ultimate compressive strength of masonry regarding the load perpendicular to the bed joint = 7.14 MPa. The average compressive strength of masonry can be calculated as 8.5 MPa. Considering diagonal tensile strength of masonry as 10% of the compressive strength of masonry,  $f_t=0.85$  MPa.

Accordingly,  $Q= 1.7Ltf_t = 1.7 \times 1525 \times 75 \times 0.85 = 165271.875 \text{ N} = 165.27 \text{ kN}$ .

Therefore, it is confirmed that the variation of the obtained maximum shear capacity (173 kN) with respect to the calculated maximum horizontal shear load (165.27 kN) based on the equation given by Smith and Coull regarding diagonal tensile failure of infill is within 5%.

3) Sample Calculation of Story Drift, Stiffness and Cumulative Energy Dissipation (Infilled Frame A1)

Table E.1 Story Drift, stiffness and cumulative energy dissipation regarding infilled frame A1

Cycle	Lateral load (kN)	Deflection (mm)	Story Drift %	Stiffness (kN/mm)	Cumulative Energy Dissipation (kN-mm)
a	a	b	$(b/h)*100$	a/b	$\Sigma a*b$
1	44	0.43	0.03	103	19
2	89	1.11	0.07	80	118
3	133	2.70	0.17	49	478

Story height, h = 6000 mm